Diplomarbeit zum Thema

Electromagnetic Transition Form Factors of Pseudoscalar and Vector Mesons

vorgelegt dem
Fachbereich 07 der Justus-Liebig-Universität Gießen
von

Carla Terschlüsen

Contents

1 Introduction

In particle and hadron physics, all particles and their interactions can be described at least in principle by the "standard model". This quantum field theory takes the elementary particles quarks, leptons and the force-mediating particles for strong, electromagnetic and weak interaction as degrees of freedom and is so far in agreement with all experimental data (apart from neutrino masses and the absence of dark-matter candidates). One aim of this theory is the description of physical processes by analytic formulas. Unfortunately, these formulas are often given as infinite series which indeed are analytical but cannot be used for numerical calculations. Thus, methods have to be developed to approximate this infinite series by finite sums.

In perturbative quantum field theories, the series are expanded as a Taylor series in terms of the coupling constant of a considered kind of interaction. If the coupling constant is small, the higher the order of a term the less important it will be and the series can be approximated by a finite sum. This is the case for electromagnetic and weak interactions.

In quantum chromodynamics (QCD), the theory of strong interaction, the coupling constant is not small for all energies. Though it is small for high energies, it is not for the lower-energy regime. So, perturbative QCD is only possible in the high-energy region. In the lower-energy region another ansatz has to be used. One possibility is an effective field theory. Instead of expanding in terms of a small coupling constant, the importance of terms is evaluated by comparing scales: A scale describing the region the effective theory should be applicable in has to be determined. This scale should be separated from the scale of the region including degrees of freedom which are not taken into account. E.g., a typical momentum or a typical energy for a given problem is taken as the scale describing the considered region.
Due to the effect of confinement in that lower-energy region of QCD, quarks cannot be treated as unbound. There, hadrons have to be taken as the relevant degrees of freedom instead of quarks and gluons. Thus, developing an effective field theory describing QCD in this energy regime includes the identification of the relevant degrees of freedom, coupling constants and a power counting scheme to order processes by importance. Thereby, the coupling constants can be fixed by comparison with experimental data. Of course, a particular effective field theory is only valid while the conditions via which it is defined are fulfilled and is not valid anymore, at least, when more degrees of freedom than the considered ones become active. So, while developing an effective theory for QCD at lower energies, three questions have to be answered:

- Which hadrons should be taken as the relevant degrees of freedom?
- Which power counting scheme should be taken i.e. how should different processes be ordered?
- For which energy regime is the theory valid?

In the low-energy region of QCD, all dynamics are well-described by the effective field theory called chiral perturbation theory (ChPT). For this theory, the relevant degrees of freedom are the Goldstone bosons — pions, kaons and the η-meson — associated with the spontaneous symmetry breaking of QCD (see chapter 2.2 for an introduction to spontaneous symmetry breaking and Goldstone bosons). These pseudoscalar mesons have low masses compared to other hadrons and, therefore, ChPT is valid for low energies.

The advantage of both a perturbative and an effective quantum field theory is that the approximation of the infinite series can be improved systematically by taking the next higher order in the expansion. Additionally, the influence of the next higher order is smaller than the influence of the already included orders and, therewith, the intrinsic errors of the approach can be controlled. In contrast to this, a phenomenological approach might describe the dynamics of a system successfully but without being able to control the intrinsic errors. A systematic improvement to get a better accuracy is not possible in that case.

Unfortunately, the energy region in which ChPT is valid is not close to the energy region of perturbative QCD. So, the dynamics of hadronic resonances, e.g., the vector mesons ρ^0, ω and ϕ with masses between 0.7 and 1 GeV, and their interactions with the pseudoscalar Goldstone bosons can neither be described with ChPT nor with perturbative QCD. Therefore, both systematic approaches as effective field theories and phenomenological models for this energy region have been developed. In the following, they will be used to explain the differences between these two approaches.
An example for a phenomenological approach is the standard vector meson dominance (VMD) model which will be explained in section 2.4.1. Indeed, the present thesis studies the interactions of hadrons with electromagnetism, i.e. real and virtual photons. Here, the VMD model [Sak69] is the most common approach. The normalised transition form factor for, e.g., the decay of a vector meson into a pseudoscalar meson and a virtual photon with momentum q via a virtual vector meson with mass m is given by

$$F_{\mathrm{VMD}}(q) = \frac{m^2}{m^2 - q^2}\,. \tag{1.1}$$

This model approach has the advantage that calculations can be performed easily. But it does not include a rule how to improve it systematically.
In contrast to this, the most general theory would include all possible powers of q^2 together with coupling constants[1]:

$$F_{\mathrm{general}}(q) = g_0\,\frac{m^2}{m^2 - q^2} + (1 - g_0) + g_1\,\frac{q^2}{m^2} + g_2\,\frac{q^4}{m^4} + \ldots \tag{1.2}$$

[1]The coupling constant for the constant term is equal to one minus the coupling constant for the term of standard VMD type to make sure that the normalised form factor equals 1 at $q^2 = 0$.

As it is an infinite series, it is impossible to fix all parameters. In an effective theory, the coupling constants g_0, $g_1, \ldots$ will be ordered in powers of importance according to a breakdown scale Λ. This breakdown scale denotes the energy scale where new degrees of freedom become important and where the constraints according to which the effective theory was developed are not fulfilled any more. Thus, m/Λ would be small in the case discussed here. As an example, suppose that the coupling constants are ordered as

$$g_1,\, g_2 \in \mathcal{O}(1),\; g_0 \in \mathcal{O}(\frac{m}{\Lambda}) \text{ and } g_i \in \mathcal{O}(\frac{m^{k_i}}{\Lambda^{k_i}}) \text{ for } i \geq 3, k_i \geq 2.$$

With this power ordering, it is possible to perform calculations up to a given order including a finite number of coupling constants[2], e.g., taking in account the terms proportional to g_0, g_1 and g_2 which are of order $\mathcal{O}(\frac{m}{\Lambda})$ and larger. The calculations can be improved systematically by adding the next order $\mathcal{O}(\frac{m^2}{\Lambda^2})$. Furthermore, errors of calculations up to order $\mathcal{O}(\frac{m}{\Lambda})$ can be estimated by the differences between calculations with and without the terms of the order $\mathcal{O}(\frac{m^2}{\Lambda^2})$ as those corrections are smaller than calculations with leading orders.

As the standard VMD model and other hadronic models are approaches without rules for systematic improvements, one aim of recent research is to develop effective field theories for the energy region of the hadronic resonances. The power counting scheme this thesis is based on was recently proposed in [LL08]. It involves both pseudoscalar Goldstone bosons and the nonet of light vector mesons as degrees of freedom and treats them both on equal footing. In section 2.4.2, this scheme will be explained in more detail.

Now, the question is if this counting scheme is able to describe experimental data and if it describes them as good as or even better than the standard phenomenological approaches, in particular the standard VMD model. In [LL08, LL09] radiative decays of light vector and axial-vector mesons and hadronic three-body decays of light vector mesons were considered yielding good agreement with the experimental data. In this thesis, results of calculations based on this new counting scheme are presented and compared to both the standard VMD calculations and the available data for the following types of decays:

- Decays of vector mesons into a pseudoscalar meson and a dilepton[3] (chapter 3),
- decays of pseudoscalar mesons into a dilepton and either a vector meson or a real photon (see chapter 4),
- decays of pseudoscalar mesons into two dileptons (chapter 5).

As an introduction, the relevant theoretical basics are outlined in chapter 2. In chapter 6, a summary and an outlook is presented.

[2] Those constants have to be fixed by comparison with experimental data before.

[3] In this context, dilepton refers to either a dielectron or dimuon as the considered decaying particles are not heavy enough to decay into a ditauon.

2 Theoretical Basics

In this thesis, radiative decays of the light vector mesons ω and ϕ and of the pseudoscalar mesons π^0, η and η' are examined. The decays will be described by effective field theories including among others these mesons as relevant degrees of freedom.

To develop the Lagrangians for those theories describing the considered decays, the QCD Lagrangian involving quarks as degrees of freedom has to be considered first. Its symmetries yield the particle multiplets and allows to identify the pseudoscalar mesons as Goldstone bosons of the spontaneously broken $\mathrm{SU(3)_L} \times \mathrm{SU(3)_R}$ symmetry (sections 2.1, 2.2). In ChPT, these Goldstone bosons are considered as the relevant degrees of freedom for an effective field theory for the low-energy regime (section 2.3). Additionally, the dynamics and interactions of vector mesons with external electromagnetic fields and Goldstone bosons are of interest. For that, both the phenomenological approach VMD and the counting scheme for light vector mesons proposed in [LL08] are explained in section 2.4. On the basis of this counting scheme, the effective leading-order Lagrangian for light vector mesons and their interaction with external electromagnetic fields and the pseudoscalar Goldstone bosons is developed in section 2.5.

For the calculations of transition matrix elements, form factors and decay widths performed in the following chapters, Feynman diagrams and rules are practical tools to simplify calculations. The rules needed for the decays studied in this thesis are listed in section 2.6.

2.1 The QCD Lagrangian and Its Symmetries

In this section, the QCD Lagrangian with quarks as degrees of freedom and its symmetries are considered. It will be used to derive the particle multiplets and to identify the pseudoscalar mesons as Goldstone bosons in the next section 2.2. As we are interested in light pseudoscalar and vector mesons which do consist of the light quarks, up, down and strange, and do not contain the heavy quarks, charm, top and bottom, the QCD Lagrangian will be restricted to the light quarks.

The QCD Lagrangian for the light quarks equals [Sch03]

$$\mathcal{L}_{\mathrm{QCD}} = \sum_{f=u,d,s} \bar{q}_f \left(i\not{D} - m_f \right) q_f - \frac{1}{4} \mathcal{G}_{\mu\nu,a} \mathcal{G}_a^{\mu\nu} = \bar{q} \left(i\not{D} - M \right) q - \frac{1}{4} \mathcal{G}_{\mu\nu,a} \mathcal{G}_a^{\mu\nu} \tag{2.1}$$

with the quark-mass matrix $M = \begin{pmatrix} m_u & 0 & 0 \\ 0 & m_d & 0 \\ 0 & 0 & m_s \end{pmatrix}$. Hereby, the quark field $q = (q_u, q_d, q_s)^T$ also contains indices for colour and spin which are suppressed due to better readability, i.e. for each $f \in \{u, d, s\}$, q_f is a three-component object in colour space. Additionally, the Lagrangian includes the gauge-covariant derivative

$$D_\mu = \partial_\mu - ig \sum_{a=1}^{8} \frac{\lambda_a^C}{2} \mathcal{A}_{\mu,a} \tag{2.2}$$

with eight independent gauge potentials $\mathcal{A}_{\mu,a}$ due to the eight-parameter group SU(3) and the Gell-Mann matrices

$$\begin{aligned}
\lambda_1 &= \begin{pmatrix} 0 & 1 & 0 \\ 1 & 0 & 0 \\ 0 & 0 & 0 \end{pmatrix}, \lambda_2 = \begin{pmatrix} 0 & -i & 0 \\ i & 0 & 0 \\ 0 & 0 & 0 \end{pmatrix}, \lambda_3 = \begin{pmatrix} 1 & 0 & 0 \\ 0 & -1 & 0 \\ 0 & 0 & 0 \end{pmatrix}, \\
\lambda_4 &= \begin{pmatrix} 0 & 0 & 1 \\ 0 & 0 & 0 \\ 1 & 0 & 0 \end{pmatrix}, \lambda_5 = \begin{pmatrix} 0 & 0 & -i \\ 0 & 0 & 0 \\ i & 0 & 0 \end{pmatrix}, \lambda_6 = \begin{pmatrix} 0 & 0 & 0 \\ 0 & 0 & 1 \\ 0 & 1 & 0 \end{pmatrix}, \\
\lambda_7 &= \begin{pmatrix} 0 & 0 & 0 \\ 0 & 0 & -i \\ 0 & i & 0 \end{pmatrix}, \lambda_8 = \frac{1}{\sqrt{3}} \begin{pmatrix} 1 & 0 & 0 \\ 0 & 1 & 0 \\ 0 & 0 & -2 \end{pmatrix}.
\end{aligned} \tag{2.3}$$

The superscript C of the Gell-Mann matrices in Eq. (2.2) denotes that those matrices are acting in colour space.
Furthermore, the field strength tensor is defined as

$$\mathcal{G}_{\mu\nu,a} = \partial_\mu \mathcal{A}_{\nu,a} - \partial_\nu \mathcal{A}_{\mu,a} + g f_{abc} \mathcal{A}_{\mu,b} \mathcal{A}_{\nu,c} \tag{2.4}$$

whereby the last term includes the structure constants f_{abc} of the symmetry group SU(3).

2.1.1 Conserved Currents and Hadron Multiplets

According to "Noether's Theorem", there exists a conserved current for each continuous symmetry transformation that leaves the Lagrangian of a physical system invariant (see [Mos99, Sch03] for more information). So, for all $a = 1, \dots N$ with N being the number of independent symmetry transformations one gets a current $J^{a\mu}$ which fullfils

$$\partial_\mu J^{a\mu} = 0 \tag{2.5}$$

and a corresponding time-independent charge

$$Q^a(t) := \int \mathrm{d}^3x \, J_0^a(\vec{x}, t) \equiv Q^a. \tag{2.6}$$

The QCD Lagrangian (2.1) it invariant under the symmetry group U(1), i.e. for $e^{i\alpha} \in \mathrm{U}(1)$ with $\alpha \in \mathbb{R}$

$$q \mapsto Uq = e^{i\alpha} q, \; \mathcal{G}_{\mu\nu,a} \mapsto \mathcal{G}_{\mu\nu,a}. \tag{2.7}$$

According to Noether's Theorem, this continuous symmetry yields the conserved charge "baryon number",

$$B := \frac{1}{3} \int \mathrm{d}^3x \, q^\dagger q, \tag{2.8}$$

which assigns $\pm 1/3$ to quarks and antiquarks, respectively, $+1$ to baryons and 0 to mesons.
Furthermore, the numbers of quarks of a given flavour,

$$U := + \int \mathrm{d}^3x \, q_u^\dagger q_u, \; D := - \int \mathrm{d}^3x \, q_d^\dagger q_d, \; S := - \int \mathrm{d}^3x \, q_s^\dagger q_s, \tag{2.9}$$

are conserved since the Lagrangian is invariant under the transformation

$$q_f \mapsto e^{i\alpha_f} q_f, \; \alpha_f \in \mathbb{R}, \tag{2.10}$$

for each flavour $f \in \{u, d, s\}$ separately.

In addition to these exact symmetries, the QCD Lagrangian is invariant with respect to the transformation

$$\begin{pmatrix} q_u \\ q_d \end{pmatrix} \mapsto U \begin{pmatrix} q_u \\ q_d \end{pmatrix}, \; U \in \mathrm{SU_f}(2), \tag{2.11}$$

if the difference between the masses of the up and the down quark is neglected, i.e. $m_u \approx m_d$. The conserved charges connected to this symmetry transformation are the so called "isospin operators",

$$\begin{aligned} I_1 &:= \frac{1}{2}\int \mathrm{d}^3x \, \left(q_d^\dagger q_u + q_u^\dagger q_d\right), \\ I_2 &:= \frac{i}{2}\int \mathrm{d}^3x \, \left(q_d^\dagger q_u - q_u^\dagger q_d\right), \\ I_3 &:= \frac{1}{2}\int \mathrm{d}^3x \, \left(q_u^\dagger q_u - q_d^\dagger q_d\right). \end{aligned} \tag{2.12}$$

The squared isospin vector, $I^2 = (I_1, I_2, I_3)^2$, is a conserved quantity, too, with eigen values $I(I+1)$ for $I \in \frac{1}{2}\mathbb{N}_0$. Then, the eigenvalues of I_3 run form $-I$ to $+I$ in unit steps. If the differences between the masses of all three light quarks are neglected, $m_u \approx m_d \approx m_s$, the QCD Lagrangian is even invariant under the transformation

$$q = \begin{pmatrix} u \\ d \\ s \end{pmatrix} \mapsto U \begin{pmatrix} u \\ d \\ s \end{pmatrix}, \; U \in \mathrm{SU_f}(3) \tag{2.13}$$

where the subscript f denotes that the symmetry group is acting in flavour space. It yields eight conserved charges, in particular the "hypercharge",

$$Y := \int \mathrm{d}^3 \left[\frac{1}{3}\left(q_u^\dagger q_u + q_d^\dagger q_d\right) - \frac{2}{3} q_s^\dagger q_s\right] \tag{2.14}$$

which equals $B + S$ in the absence of the heavy quarks. Using the conserved charges of the $\mathrm{SU_f}(3)$ symmetry, particle multiplets can be constructed which consist of particles with the same mass. Thereby, one uses the relation

$$Q = e\left(\frac{1}{2}Y + I_3\right) \tag{2.15}$$

for the electric charge of the particles including the electric charge of the electron, e. The pseudoscalar-, vector-meson and baryon multiplet are shown below. Thereby, the vector-meson state ω_8 is a superposition of the physical state ω- and ϕ-meson. Note, that all particles lying on the same horizontal line belong to an isospin multiplets with $I^2 = \text{const}$. As $\mathrm{SU_f}(3)$ is not exact but only an approximate symmetry which only holds for $m_u = m_d = m_s$, the masses of the particles belonging to the same multiplet are not the same in reality. In Tab. 2.1, the masses of the particles belonging to the multiplets are listed.

- pseudoscalar-meson octet:

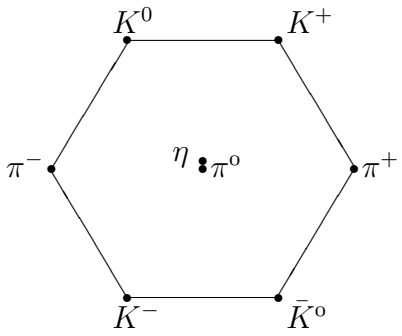

- vector-meson octet:

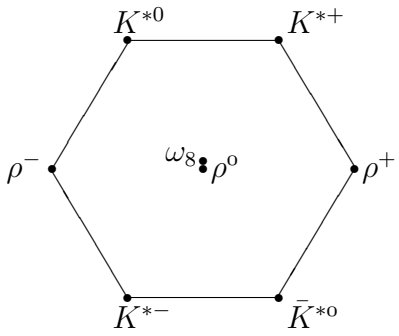

- baryon octet:

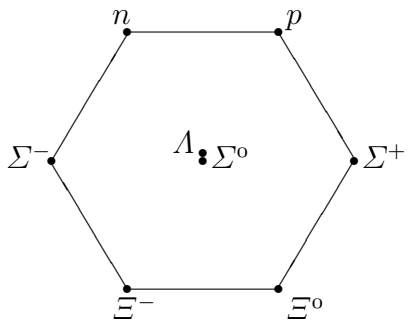

2.1.2 Symmetries in the Chiral Limit

The masses of the light quarks, $m_u \approx 3\,\text{MeV}$, $m_d \approx 6\,\text{MeV}$ and $m_s \approx 123\,\text{MeV}$, are small compared to the masses of the light hadrons (compare Tab. 2.1). Therefore, it seems justified to consider the QCD Lagrangian (2.1) in the chiral limit, $m_u = m_d = m_s = 0$,

$$\mathcal{L}^0_{\text{QCD}} = \bar{q} i \not{D} q - \frac{1}{4} \mathcal{G}_{\mu\nu,a} \mathcal{G}^{\mu\nu}_a \tag{2.16}$$

where the superscript 0 denotes the chiral limit. This Lagrangian exhibits an additional symmetry: It is invariant under the flavour symmetry group $\text{U(3)}_\text{A} \times \text{U(3)}_\text{V}$ whereby the subscript A stands for "axial vector" and V for "vector". This symmetry transforms the quark field according to

$$q \mapsto U_V U_A q = \exp\left[i\theta_a t_a\right] \exp\left[i\tilde{\theta}_a t_a \gamma_5\right],\ U_V \in \text{U(3)}_\text{V},\ U_A \in \text{U(3)}_\text{A} \tag{2.17}$$

including $\gamma_5 := i\gamma^0\gamma^1\gamma^2\gamma^3$. Here, θ_a, $\tilde{\theta}_a \in \mathbb{R}$ and $t_0 = \sqrt{\frac{2}{3}} I_{3\times3}$, $t_a = \lambda_a$ for $a = 1, \ldots, 8$. Moreover, one can show that for all $V \in \text{U(n)}$ with $n \in \mathbb{N}$ there exists $U \in \text{SU(n)}$ so that

$$V = \det(V)^{1/n}\, U.$$

Table 2.1: Masses of the particles in the light pseudoscalar-meson and vector-meson nonet and in the light baryon octet [A+08]. A nonet is a octet plus a singlet. Thereby, the physical states η, η' and ω, ρ^0 are superpositions of the states η_1, η_8 or ω_1, ω_8, respectively.

multiplet	mass [MeV]	multiplet	mass [MeV]
pseudoscalar-meson nonet		vector-meson nonet	
$K^{\pm}$	494	$K^{*\pm}$	892
$K^0, \bar{K}^0$	498	$K^{*0}, \bar{K}^{*0}$	896
$\pi^{\pm}$	140	$\rho^{\pm}, \rho^0$	776
π^0	135	ω	783
η	548	ϕ	1019
η'	958		
baryon octet			
proton p	938		
neutron n	940		
Σ^+	1189		
Σ^0	1193		
Σ^-	1197		
Λ	1116		
Ξ^0	1315		
Ξ^-	1321		

As $\det(V)^{1/n} \in \mathrm{U}(1)$, this yields that for all $n \in \mathbb{N}$

$$\mathrm{U(n)} = \mathrm{U}(1) \times \mathrm{SU(n)}. \tag{2.18}$$

Therewith, the symmetry group $\mathrm{U}(3)_\mathrm{A} \times \mathrm{U}(3)_\mathrm{V}$ can be represented as

$$[\mathrm{U}(1)_\mathrm{A} \times \mathrm{SU}(3)_\mathrm{A}] \times [\mathrm{U}(1)_\mathrm{V} \times \mathrm{SU}(3)_\mathrm{V}] = \mathrm{U}(1)_\mathrm{A} \times \mathrm{U}(1)_\mathrm{V} \times \mathrm{SU}(3)_\mathrm{A} \times \mathrm{SU}(3)_\mathrm{V}. \tag{2.19}$$

QCD as the quantized theory is not invariant under $\mathrm{U}(1)_\mathrm{A}$ anymore. Therefore, the symmetry group is reduced to

$$\mathrm{U}(1)_\mathrm{V} \times \mathrm{SU}(3)_\mathrm{A} \times \mathrm{SU}(3)_\mathrm{V}. \tag{2.20}$$

Thereby, the group $\mathrm{U}(1)_\mathrm{V}$ coincides with the symmetry group U(1) of the full Lagrangian (2.1) which gives rise to baryon number conservation.
Since the matrix t_0 commutes with all other matrices, it is easy to see from (2.17) that the transformation under $\mathrm{SU}(3)_\mathrm{A} \times \mathrm{SU}(3)_\mathrm{V}$ can be expressed as

$$q \mapsto \exp\left[i\theta_a \lambda_a\right] \exp\left[i\tilde{\theta}_a \lambda_a \gamma_5\right] q \tag{2.21}$$

for $\exp\left[i\theta_a\lambda_a\right] \in \mathrm{SU(3)_V}$, $\exp\left[\mathrm{i}\tilde{\theta}_\mathrm{a}\lambda_\mathrm{a}\gamma_5\right] \in \mathrm{SU(3)_A}$ and $\theta_a, \tilde{\theta}_a \in \mathbb{R}$. The group $\mathrm{SU(3)_V}$ coincides with the symmetry group $\mathrm{SU_f(3)}$ introduced in (2.13).

With the projectors

$$P_R = \frac{1}{2}(1+\gamma_5),\ P_L = \frac{1}{2}(1-\gamma_5) \tag{2.22}$$

the QCD Lagrangian (2.16) can be split into a term describing "right-handed quarks", $q_R := P_R q$, and one describing "left-handed quarks", $q_L := P_L q$, yielding

$$\mathcal{L}^0_{\mathrm{QCD}} = \bar{q}_R i\not{D} q_R + \bar{q}_L i\not{D} q_L - \frac{1}{4}\mathcal{G}_{\mu\nu,a}\mathcal{G}^{\mu\nu}_a. \tag{2.23}$$

By using $(\gamma_5)^2 = 1$, the transformation of the right- and left-handed quarks transform under $\mathrm{SU(3)_A} \times \mathrm{SU(3)_V}$ is given as

$$\begin{aligned} q_R &\mapsto \exp\left[i\theta_a\lambda_a\right] \exp\left[+i\tilde{\theta}_a\lambda_a\right] q_R, \\ q_L &\mapsto \exp\left[i\theta_a\lambda_a\right] \exp\left[-i\tilde{\theta}_a\lambda_a\right] q_L. \end{aligned} \tag{2.24}$$

In addition, the transformation of left- and right-handed quarks under the group $\mathrm{SU(3)_L} \times \mathrm{SU(3)_R}$ is defined as

$$q_L \overset{\mathrm{SU(3)_L}}{\mapsto} \exp\left[i\theta_{La}\frac{\lambda_a}{2}\right] q_L,\ q_R \overset{\mathrm{SU(3)_L}}{\mapsto} q_R, \tag{2.25}$$

$$q_R \overset{\mathrm{SU(3)_R}}{\mapsto} \exp\left[i\theta_{Ra}\frac{\lambda_a}{2}\right] q_R,\ q_L \overset{\mathrm{SU(3)_R}}{\mapsto} q_L. \tag{2.26}$$

This transformation is equivalent to the transformation under $\mathrm{SU(3)_A} \times \mathrm{SU(3)_V}$ as one sees by setting $\theta_{La} = 2(\theta_a - \tilde{\theta}_a)$ and $\theta_{Ra} = 2(\theta_a + \tilde{\theta}_a)$. Therewith, the QCD Lagrangian in the chiral limit (2.23) is invariant under the symmetry group

$$\mathrm{U(1)_V} \times \mathrm{SU(3)_L} \times \mathrm{SU(3)_R}. \tag{2.27}$$

The conserved currents associated with the $\mathrm{SU(3)_L} \times \mathrm{SU(3)_R}$ symmetry according to Noether's Theorem are

$$L^{\mu,a} = \bar{q}_L\,\gamma^\mu\,\frac{\lambda_a}{2}\,q_L, \tag{2.28}$$

$$R^{\mu,a} = \bar{q}_R\,\gamma^\mu\,\frac{\lambda_a}{2}\,q_R. \tag{2.29}$$

Then, the linear combinations of these currents

$$V^{\mu,a} := R^{\mu,a} + L^{\mu,a} = \bar{q}\,\gamma^\mu\,\frac{\lambda_a}{2}\,q, \tag{2.30}$$

$$A^{\mu,a} := R^{\mu,a} - L^{\mu,a} = \bar{q}\,\gamma^\mu\,\gamma_5\,\frac{\lambda_a}{2}\,q \tag{2.31}$$

act as vector and axial-vector currents, respectively. I.e., including the definition

$$q\left(\vec{x},t\right) \overset{\text{parity}}{\mapsto} \gamma_0 q\left(\vec{x},t\right) \tag{2.32}$$

they transform under parity operation into + or − themselves:

$$V^{\mu,a}(\vec{x},t) \overset{\text{parity}}{\mapsto} PV^{\mu,a}(\vec{x},t)P^{-1} = +V^a_\mu(-\vec{x},t), \tag{2.33}$$

$$A^{\mu,a}(\vec{x},t) \overset{\text{parity}}{\mapsto} PA^{\mu,a}(\vec{x},t)P^{-1} = -A^a_\mu(-\vec{x},t). \tag{2.34}$$

The corresponding time-independent charges equal

$$Q^a_V := \int \mathrm{d}^3x\, V^a_0(\vec{x},t), \quad Q^a_A := \int \mathrm{d}^3x\, A^a_0(\vec{x},t) \tag{2.35}$$

for $a = 1,\ldots,8$. The charges Q^a_V are the eight conserved charges already mentioned after (2.13). In particular, the charges Q^3_V and Q^8_V commute with each other and correspond up to normalisations to I_3 and Y as introduced in (2.12) and (2.14), respectively. They lead to the multiplet assignments discussed above. Naively one would expect that the corresponding charges Q^3_A and Q^8_A extend the multiplets with (approximately) degenerate masses by adding states with opposite parity. However, these "parity partners" do not exist in the hadron spectrum. The non-degeneracy of hadrons with opposite parity is explained by the effect of spontaneous symmetry breaking of $\mathrm{SU(3)_A}$ (see section 2.2).

2.2 Goldstone Bosons in QCD

Chiral perturbation theory (ChPT) is an effective field theory describing QCD for low energies and particles with small masses (see introduction). In this section, these particles are identified by applying "Goldstone's Theorem" following the explanations in [Mos99, Sch03]. An introduction to that theorem which proves that a "spontaneously broken" or "hidden" symmetry of a theory yields the existence of massless particles will be given in subsection 2.2.1. Thereby, a symmetry is spontaneously broken, if the ground state $|0\rangle$ is not invariant under the full symmetry group of the Hamiltonian. In the second subsection, the pseudoscalar mesons will be identified as the Goldstone bosons of QCD associated with the spontaneous symmetry breaking of the symmetry group $\mathrm{SU}(3)_\mathrm{L} \times \mathrm{SU}(3)_\mathrm{R}$.

2.2.1 Goldstone's Theorem

In this subsection, an introduction to the proof of Goldstone's Theorem will be given. For that purpose, let $\mathcal{L}$ be a Lagrangian with a continuous symmetry and the conserved current J^μ and time-independent charge operator $Q = \int \mathrm{d}^3x\, J_0(x)$ according to Noether's Theorem (see subsection 2.1.1) and let this symmetry be spontaneously broken, i.e. in the case discussed:

$$Q|0\rangle \neq 0. \tag{2.36}$$

Since Q is a symmetry of the Lagrangian, it commutes with the Hamiltonian $\hat{H}$. With E_min denoting the energy of the ground state this yields

$$\hat{H}Q|0\rangle = Q\hat{H}|0\rangle = E_\mathrm{min} \cdot Q|0\rangle. \tag{2.37}$$

So, $Q|0\rangle$ can also be taken as the ground state of the system (as the ground state is defined as being the state which minimizes the energy) and thus the system has a degenerate ground state.

For the further argumentation, an arbitrary field operator F coupling to one-particle states $|k\rangle$ is considered that is not invariant under the symmetry operation generated by Q:

$$[J_0(x), F(y)] \neq 0. \tag{2.38}$$

Using $\partial_\mu J^\mu = 0$ and Gauss' law one can show that

$$\int \mathrm{d}^3x \,\langle 0|\,[J_0(x), F(y)]\,|0\rangle \tag{2.39}$$

is time-independent and not equal to zero. By inserting a complete set of eigenstates $|n\rangle$[1] of the Hamiltonian with eigenvalues $E_n + E_{\min}$ and representing

$$J_0(x) = e^{iPx} J_0(0) e^{-iPx} \tag{2.40}$$

including the operator P of total four-momentum of QCD, this integral can be evaluated as

$$\begin{aligned}
&\int \mathrm{d}^3x \sum_n \left(\langle 0|J_0(x)|n\rangle\langle n|F(y)|0\rangle - \langle 0|F(y)|n\rangle\langle n|J_0(x)|0\rangle\right) \\
&= (2\pi)^3 \sum_n \delta^{(3)}(\vec{p}_n) \left(\langle 0|J_0(0)|n\rangle\langle n|F(y)|0\rangle e^{-iE_n x_0} - \langle 0|F(y)|n\rangle\langle n|J_0(0)|0\rangle e^{+iE_n x_0}\right).
\end{aligned} \tag{2.41}$$

Due to the δ-function the only allowed states $|n\rangle$ are those with $\vec{p}_n = 0$ and thus $E_n = m_n$. Additionally, the whole expression should be time independent and, therefore, all exponential functions have to be equal to 1. As $E_n = m_n$, only states $|n\rangle$ with $m_n = 0$ yield $e^{\pm iE_n x_0} = 1$. Therefore, $\langle 0|J_0(0)|n\rangle = 0$ for all states $|n\rangle$ with $m_n \neq 0$. Furthermore, the whole expression is not equal to zero, so there has to exist at least one state $|n_0\rangle$ with $m_{n_0} = 0$ and

$$\langle 0|J_0(0)|n_0\rangle\langle n_0|F(y)|0\rangle \neq 0. \tag{2.42}$$

Thus, the spontaneous symmetry breaking of the ground state has generated a massless particle $|n_0\rangle$. This particle has to carry the quantum numbers of the generator in question to exclude $\langle 0|J_0(0)|n_0\rangle = 0$. As the considered current J^μ is either a vector or an axial-vector current, the particle has to be a boson with mass zero called "Goldstone boson".

This procedure can be repeated for all charge operators $Q_1, \ldots, Q_n$ of the spontaneously broken symmetry of the Lagrangian $\mathcal{L}$ fulfilling

$$Q_i|0\rangle \neq 0,\ i \in \{1, \ldots, n\}. \tag{2.43}$$

Then, each of these operators will generate a massless Goldstone boson. The number of all Goldstone bosons associated with a spontaneous symmetry breaking of a symmetry group is given by the difference between the number of generators of the full symmetry group and the number of generators of the symmetry group of the ground state.

After expanding the fields around a preselected ground state and writing the Lagrangian in terms of those new fields, the following statements hold:

- The new fields will represent the massless Goldstone bosons and the massive particles of the theory.
- Represented in the new fields, the full symmetry of the Lagrangian is not obvious anymore, it is "hidden" in the new definition of the fields.

[1] As the operator F only acts on one-particle states, the remaining m-particle states of the complete set of eigenstates, $m \in \mathbb{N}_0 \setminus \{1\}$, do not need to be considered.

2.2.2 Spontaneous Symmetry Breaking in QCD

In this subsection, we will show indications that the QCD symmetry group $\mathrm{SU}(3)_\mathrm{L} \times \mathrm{SU}(3)_\mathrm{R}$ is spontaneously broken. Therefor, let $|i,+\rangle$ be an eigenstate of the QCD Hamiltonian H^0_QCD in the chiral limit with eigenvalue E_i and positive parity:

$$H^0_\mathrm{QCD}|i,+\rangle = E_i|i,+\rangle,\ P|i,+\rangle = +|i,+\rangle. \tag{2.44}$$

Consider the state $|\Phi\rangle := Q^a_A|i,+\rangle$ with the axial-vector charge Q^a_A (2.35) defined in subsection 2.1.2. As the axial-vector charge and the Hamiltonian commute, $|\Phi\rangle$ is also an eigenvector with eigenvalue E_i but with negative parity:

$$P|\Phi\rangle = PQ^a_AP^{-1}P|i,+\rangle = -Q^a_A|i,+\rangle = -|\Phi\rangle. \tag{2.45}$$

Furthermore, let the states $|i,+\rangle$ and $|j,-\rangle$ be members of a basis of an irreducible representation of the symmetry group $\mathrm{SU}(3)_\mathrm{L}\times\mathrm{SU}(3)_\mathrm{R}$ with positive and negative parity, respectively, and $a^\dagger_i$ and $b^\dagger_j$ the corresponding creation operators. Then, the commutator between the axial-vector charge and the creation operator for states with positive parity can be expressed as

$$\left[Q^a_A, a^\dagger_i\right] = -t^a_{ij}b^\dagger_j. \tag{2.46}$$

Hence, the state $|\Phi\rangle$ is equal to

$$Q^a_A|i,+\rangle = Q^a_Aa^\dagger_i|0\rangle = \left(\left[Q^a_A, a^\dagger_i\right] + a^\dagger_iQ^a_A\right)|0\rangle = -t^a_{ij}|j,-\rangle + a^\dagger_iQ^a_A|0\rangle. \tag{2.47}$$

There are two possibilities:

1. $Q^a_A|0\rangle = 0$:

   In this case, $|\Phi\rangle = Q^a_A|i,+\rangle = -t^a_{ij}|j,-\rangle$. Thus, a degenerate state of negative parity for every state of positive parity is expected. As no negative-parity states have been observed which are degenerate, e.g., with the ground state baryon octet, this hypothesis is experimentally disproven. Instead of this, the assumption is that

2. $Q^a_A|0\rangle \neq 0$:

   Then, there would be a spontaneous symmetry breaking in QCD yielding massless Goldstone bosons with spin zero corresponding to the axial-vector charges Q^a_A. The whole symmetry group of the Lagrangian $\mathcal{L}^0_{QCD}$ is $G = \mathrm{SU}(3)_\mathrm{L} \times \mathrm{SU}(3)_\mathrm{R}$ and the ground state is still invariant under the subgroup $H = \mathrm{SU}(3)_\mathrm{V}$, since this leads to the multiplets observed in nature as discussed in subsection 2.1.1. Therefore, there should exist

   $$n = n_G - n_H = 2(3^2-1) - (3^2-1) = 8 \tag{2.48}$$

   Goldstone bosons ϕ_a. They must have the same transformation behaviour as the axial-vector charges and thus

- are pseudoscalar bosons since $Q_A^a \overset{\text{parity}}{\mapsto} -Q_A^a$,
- transform under H as an octet, i.e. $\left[Q_V^a, \phi^b(x)\right] = i f_{abc}\phi^c$.

This assumption is experimentally supported by the octet of pseudoscalar mesons which have small masses in comparison to the corresponding 1^- vector mesons and all other hadrons. In reality, their masses are unequal to zero (but small) due to the explicit symmetry breaking of QCD: Since the masses of the light quarks are non-vanishing, a term including the quark-mass matrix $M = \text{diag}\,(m_u, m_d, m_s)$,

$$\mathcal{L}_{\text{mass}} = -\bar{q}Mq = -\left[\bar{q}_R M q_L + \bar{q}_L M q_R\right], \tag{2.49}$$

has to be added to the QCD Lagrangian $\mathcal{L}^0_{\text{QCD}}$ in order to get the original Lagrangian (2.1). This additional term is not invariant under the symmetry group G anymore. Take, e.g., the simple case that both q_R and q_L transform as

$$q_{R/L} \overset{g\in G}{\mapsto} (1 - i\theta_a\lambda_a)\, q_{R/L} + \mathcal{O}(\theta_a^2) \tag{2.50}$$

with $\theta_a \in \mathbb{R}$ small. Then,

$$\mathcal{L}_{\text{mass}} \overset{g\in G}{\mapsto} -\bar{q}\,(1 + i\theta_a\lambda_a)\, M\, (1 - i\theta_a\lambda_a) = \mathcal{L}_{\text{mass}} + i\theta_a[M, \lambda_a]_- + \mathcal{O}(\theta_a^2). \tag{2.51}$$

As the mass matrix does not commute with the Gell-Mann matrices, the mass term is not invariant under the symmetry group G of the QCD Lagrangian in the chiral limit. This mass term yields non-vanishing masses of the QCD-Goldstone bosons. As the masses of the light quarks are small, the masses of the pseudoscalar Goldstone bosons are also small in comparison to other hadrons. For a derivation of their masses, see section 4.3.

The eight Goldstone-boson fields ϕ_a are continuous real functions on the Minkowski space. As it is explained in section A.1 in the appendix, they can be collected in a Hermitian and traceless matrix

$$\Phi = \phi_a\lambda_a = \begin{pmatrix} \phi_3 + \frac{1}{\sqrt{3}}\phi_8 & \phi_1 - i\phi_2 & \phi_4 - i\phi_5 \\ \phi_1 + i\phi_2 & -\phi_3 + \frac{1}{\sqrt{3}}\phi_8 & \phi_6 - i\phi_7 \\ \phi_4 + i\phi_5 & \phi_6 + i\phi_7 & -\frac{2}{\sqrt{3}}\phi_8 \end{pmatrix} =: \begin{pmatrix} \pi^0 + \frac{1}{\sqrt{3}}\eta & \sqrt{2}\pi^+ & \sqrt{2}K^+ \\ \sqrt{2}\pi^- & -\pi^0 + \frac{1}{\sqrt{3}}\eta & \sqrt{2}K^0 \\ \sqrt{2}K^- & \sqrt{2}\bar{K}^0 & -\frac{2}{\sqrt{3}}\eta \end{pmatrix} \tag{2.52}$$

with the fields $\pi^{0/\pm}$, η and $K^{0/\pm}$ describing the (physical) pseudoscalar mesons. Actually, the η state does not match the physical state. The physical η-meson is a combination of the Goldstone-boson state and the singlet η_1. For the decay of vector mesons into pseudoscalar mesons (chapter 3) the physical η-meson is approximated by the Goldstone boson, yet for the decay of pseudoscalar mesons (chapters 4, 5) this mixing has to be taken into account (see section 4.3 for details).

2.3 The Effective Leading-Order Lagrangian for Goldstone Bosons

2.3.1 The Leading-Order Chiral Lagrangian for Goldstone Bosons and External Fields

The aim of this subsection is to give a short summary of how to construct a general theory describing the dynamics of the pseudoscalar Goldstone bosons associated with the spontaneous symmetry breakdown in QCD and their interactions with external fields (for further and more detailed information see, e.g., [Sch03], chapter 4). This theory was first suggested by Weinberg [Wei79] and further developed by Gasser and Leutwyler [GL84, GL85a].
The constructed Lagrangian $\mathcal{L}_{\text{eff}}$ has to fulfill the following properties:

- It has to be invariant under the group $\mathrm{U(1)_V} \times \mathrm{SU(3)_L} \times \mathrm{SU(3)_R}$ in the chiral limit where the masses of the light quarks up, down and strange are set to zero. As the Goldstone bosons have baryon number zero, they transform as

$$\Phi \overset{\mathrm{U(1)_V}}{\mapsto} \Phi \tag{2.53}$$

  under $\mathrm{U(1)_V}$ and, thus, this symmetry will be fulfilled automatically.

- $\mathcal{L}_{\text{eff}}$ should contain exactly eight pseudoscalar degrees of freedom which describe the eight Goldstone bosons and transform as an octet under the subgroup $\mathrm{SU(3)_V}$. They are collected in the field

$$U(x) := \exp\left(i\,\frac{\lambda_a \phi_a(x)}{f}\right) \tag{2.54}$$

  with the eight real-valued Goldstone-boson fields $\phi_a(x)$ and the Gell-Mann matrices λ_a. f denotes the pion-decay constant in the chiral limit which is determined by the weak decay of a pion into a muon and a neutrino and further theoretical considerations (see, e.g., [LL08]). The field U transforms under $\mathrm{SU(3)_L} \times \mathrm{SU(3)_R}$ as

$$U \mapsto U' = V_R U V_L^\dagger \tag{2.55}$$

  with space-time dependent SU(3)-matrices V_R and V_L.

- Due to the spontaneous symmetry breaking of QCD the ground state of the theory should only be invariant under $\mathrm{SU(3)_V} \times \mathrm{U(1)_V}$.

As a first step, the QCD Lagrangian for quarks and

- the external vector fields $v^\mu(x)$ and $v^\mu_{(\mathrm{s})}(x)$,

- the external axial-vector fields $a^\mu(x)$,
- the external scalar field $s(x)$ and
- the external pseudoscalar field $p(x)$

is considered with $\operatorname{tr} v^\mu = \operatorname{tr} a^\mu = 0$. All external fields are colour-neutral, Hermitian 3×3 matrices that act in flavour space. The Lagrangian describing the dynamics of the light quarks and their interactions with those external fields equals

$$\mathcal{L} = \mathcal{L}^0_{\mathrm{QCD}} + \mathcal{L}_{\mathrm{ext}} = \mathcal{L}^0_{\mathrm{QCD}} + \bar{q}\gamma_\mu \left(v^\mu + \frac{1}{3} v^\mu_{(\mathrm{s})} + \gamma_5 a^\mu \right) q - \bar{q}\,(s - i\gamma_5 p)\, q \tag{2.56}$$

whereby one obtains the QCD Lagrangian $\mathcal{L}_{\mathrm{QCD}}$ by the replacement $s \to M$ and dropping all other external fields. By splitting the quark field into its left-handed part q_L and its right-handed part q_R and defining the left- and right-handed external field

$$l_\mu := v_\mu - a_\mu, \; r_\mu := v_\mu + a_\mu, \tag{2.57}$$

this Lagrangian can be rearranged as

$$\begin{aligned} \mathcal{L} = \mathcal{L}^0_{\mathrm{QCD}} &+ \bar{q}_L \gamma^\mu \left(l_\mu + \frac{1}{3} v^{(\mathrm{s})}_\mu \right) q_L + \bar{q}_R \gamma^\mu \left(r_\mu + \frac{1}{3} v^{(\mathrm{s})}_\mu \right) q_R \\ &- \bar{q}_R\,(s + ip)\, q_L - \bar{q}_L\,(s - ip)\, q_R. \end{aligned} \tag{2.58}$$

It is invariant under the symmetry group $\mathrm{U(1)_V} \times \mathrm{SU(3)_L} \times \mathrm{SU(3)_R}$, i.e. under the local transformation

$$q_R \mapsto \exp\left(-i\, \frac{\Theta(x)}{3} \right) V_R(x) q_R, \tag{2.59}$$

$$q_L \mapsto \exp\left(-i\, \frac{\Theta(x)}{3} \right) V_L(x) q_L \tag{2.60}$$

with independent space-time dependent SU(3)-matrices $V_L(x)$ and $V_R(x)$ and $\Theta(x) \in \mathbb{R}$ as defined in subsection 2.1.2 provided that the external fields transform as

$$l_\mu \mapsto V_L l_\mu V_L^\dagger + i V_L \partial_\mu V_L^\dagger, \tag{2.61}$$

$$r_\mu \mapsto V_R r_\mu V_R^\dagger + i V_R \partial_\mu V_R^\dagger, \tag{2.62}$$

$$v^{(s)}_\mu \mapsto v^{(s)}_\mu - \partial_\mu \Theta, \tag{2.63}$$

$$s + ip \mapsto V_R (s + ip) V_L^\dagger, \tag{2.64}$$

$$s - ip \mapsto V_L (s - ip) V_R^\dagger. \tag{2.65}$$

On the basis of the Lagrangian (2.56) for light quarks and external fields, the Lagrangian describing the interactions of the pseudoscalar Goldstone bosons with themselves and

these external fields is constructed. Therefore, a covariant derivative D_μ involving the left- and right-handed fields l_μ and r_μ is defined for all objects X transforming as $X' = V_R X V_L^\dagger$. It is defined as having the same transformation behaviour as the object it acts on and hence equals

$$D_\mu X := \partial_\mu X - i r_\mu X + i X l_\mu \mapsto D'_\mu X' = V_R (D_\mu X) V_L^\dagger. \tag{2.66}$$

The right- and left-handed fields are collected in the field strength tensors

$$f_{\mu\nu}^R := \partial_\mu r_\nu - \partial_\nu r_\mu - i[r_\mu, r_\nu], \tag{2.67}$$
$$f_{\mu\nu}^L := \partial_\mu l_\nu - \partial_\nu l_\mu - i[l_\mu, l_\nu]. \tag{2.68}$$

It holds $\mathrm{tr}\{f_{\mu\nu}^R\} = \mathrm{tr}\{f_{\mu\nu}^L\} = 0$ as $\mathrm{tr}\{r_\mu\} = \mathrm{tr}\{l_\mu\} = 0$.
The scalar and the pseudoscalar external field are combined in

$$\chi = 2B_0(s + ip). \tag{2.69}$$

with a so far arbitrary constant B_0 which has dimension mass.

All objects introduced so far should be combined to invariant terms. Taking objects A and B transforming as $A' = V_R A V_L^\dagger$ and $B' = V_R B V_L^\dagger$ the trace of the product $AB^\dagger$ is always invariant. Hence, invariant terms can be built by traces of such products. For the leading-order Lagrangian, the only considered terms are those up to the order Q^2 for a typical momentum Q. In the counting scheme of chiral perturbation theory, the single building blocks are of the order

$$U \in \mathcal{O}(Q^0),\ D_\mu \in \mathcal{O}(Q),\ \chi \in \mathcal{O}(Q^2). \tag{2.70}$$

In particular, χ will be connected to the squared Goldstone boson masses (see section 4.3 for more details). Furthermore, the external field v_μ will be associated with the external electromagnetic field A_μ. It holds

$$r_\mu,\ l_\mu \in \mathcal{O}(Q),\ f_{\mu\nu}^{R/L} \in \mathcal{O}(Q^2). \tag{2.71}$$

Therewith, there exist the following invariants up to order Q^2 which are not constant (especially not zero):

$$\begin{aligned} &\mathrm{tr}\{D_\nu U (D_\mu U)^\dagger\},\ -\mathrm{tr}\{(D_\mu D_\nu U) U^\dagger\},\ -\mathrm{tr}\{U (D_\nu D_\mu U)^\dagger\}, \\ &\mathrm{tr}\{\chi U^\dagger\},\ \mathrm{tr}\{U \chi^\dagger\}. \end{aligned} \tag{2.72}$$

Hereby, the first three terms are equal up to a total derivative. As the parity of the Lagrangian should be +1 and $PUP^{-1} = U^\dagger$, $P(D_\mu U)P^{-1} = (D_\mu U)^\dagger$ and $P\chi P^{-1} = \chi^\dagger$, the term $\mathrm{tr}\{\chi U^\dagger - U\chi^\dagger\}$ has the wrong parity. Using in addition that, due to Lorentz

invariance of the Lagrangian, Lorentz indices have to be contracted, the most general, locally invariant, effective Lagrangian at lowest chiral order equals

$$\mathcal{L}_2 = \frac{1}{4} f^2 \,\mathrm{tr}\{D_\mu U (D^\mu U)^\dagger\} + \frac{1}{4} f^2 \,\mathrm{tr}\{\chi U^\dagger + U \chi^\dagger\}. \tag{2.73}$$

This Lagrangian includes two free parameters, the pion-decay constant f and the parameter B_0 hidden in χ. At lowest order both parameters can be connected to the chiral quark condensate $\langle \bar{q} q \rangle$ (see [Sch03], section 4.3) by

$$3 f^2 B_0 = -\langle \bar{q} q \rangle. \tag{2.74}$$

In this thesis, external electromagnetic fields are considered. From (2.56) and the Lagrangian of quantum electrodynamic (QED) one can see that the coupling of quarks to an external electromagnetic field A_μ is given by

$$v_\mu = -e\, Q A_\mu \tag{2.75}$$

including the quark charge matrix

$$Q = \begin{pmatrix} \frac{2}{3} & 0 & 0 \\ 0 & -\frac{1}{3} & 0 \\ 0 & 0 & -\frac{1}{3} \end{pmatrix}. \tag{2.76}$$

The leading-order interaction of Goldstone bosons with such fields is given by the first term of the Lagrangian $\mathcal{L}_2$ involving the covariant derivative

$$D_\mu X = \partial_\mu X + ieA_\mu [Q, X]_- \tag{2.77}$$

which emerges from the general formula (2.56) by setting all other external fields to zero. In this case, the field strength tensors equal

$$f^R_{\mu\nu} = f^L_{\mu\nu} = -eQ\left(\partial_\mu A_\nu - \partial_\nu A_\mu\right) =: -eQF_{\mu\nu}\,. \tag{2.78}$$

Taking $p = 0$ and $s = M = \mathrm{diag}(m_u, m_d, m_s)$ with the masses of the light quarks, m_u, m_d and m_s, the combination of pseudoscalar and scalar field χ equals

$$2B_0 M =: \chi_0\,. \tag{2.79}$$

Hence, the second term of the Lagrangian (2.73) which includes $\chi = \chi_0 = \chi^\dagger$ gives rise to the explicit symmetry breaking caused by the non-vanishing quark masses.

2.3.2 The Effective Wess-Zumino-Witten Action

The lowest-order Lagrangian $\mathcal{L}_2$ developed in the previous subsection as well as the next-to-leading-order Lagrangian $\mathcal{L}_4$ as it is given in section 4.7 in [Sch03] are more symmetric than QCD is in reality. Both Lagrangians are even in the number of Goldstone bosons. Thus, reactions which are odd in the number of Goldstone bosons cannot be described with these Lagrangians. E.g., the following reactions are not describable:

- In the case of no external fields except the scalar one $s = M$ yielding $\chi_0 = 2B_0M$, the reaction $K^+K^- \to \pi^+\pi^-\pi^0$ is not described.
- If there is an external electromagnetic field, the decay $\pi^0 \to \gamma\gamma$ will not be described.

This is connected to the "$\mathrm{U(1)_A}$ anomaly" of QCD: As mentioned in subsection 2.1.2, the quantized theory of QCD is not invariant under $\mathrm{U(1)_A}$ anymore. However, let $\exp\left[i\tilde{\theta}\gamma_5\right]$ with $\tilde{\theta} \in \mathbb{R}$ be a typical element of $\mathrm{U(1)_A}$. Since $(\gamma_5)^2 = 1$, it equals

$$\cos\tilde{\theta} + i\sin\tilde{\theta}\gamma_5. \tag{2.80}$$

Therewith, left- and right-handed quarks transform as

$$\begin{aligned} q_{R/L} &\mapsto \left(\cos\tilde{\theta} + i\sin\tilde{\theta}\gamma_5\right)\frac{1}{2}\left(1 \pm \gamma_5\right) q_{R/L} = \frac{1}{2}\left[\cos\tilde{\theta} \pm i\sin\tilde{\theta} \pm \left(\cos\tilde{\theta} \pm i\sin\tilde{\theta}\right)\gamma_5\right] q_{R/L} \\ &= e^{\pm i\tilde{\theta}}\frac{1}{2}\left(1 \pm \gamma_5\right) q_{R/L} = e^{\pm i\tilde{\theta}} q_{R/L}\,. \end{aligned} \tag{2.81}$$

Consider now the case $\tilde{\theta} = \pi/2$. Then,

$$q_R \overset{\tilde{\theta}=\pi/2}{\mapsto} iq_R,\; q_L \overset{\tilde{\theta}=\pi/2}{\mapsto} -iq_L\,. \tag{2.82}$$

Thus, a general pseudoscalar-meson current transforms as

$$\overline{q_f}\,\gamma_5\, q_g = \overline{q_{fL}}\, q_{gR} - \overline{q_{fR}}\, q_{gL} \overset{\tilde{\theta}=\pi/2}{\mapsto} -\overline{q_{fL}}\, g_{gR} + \overline{q_{fR}}\, q_{gL} = -\overline{q_f}\,\gamma_5\, q_g\,. \tag{2.83}$$

Hence, $\mathcal{L}_2$ and $\mathcal{L}_4$ which are even in the number of Goldstone bosons are invariant under this special $\mathrm{U(1)_A}$ transformation which is a contradiction to the quantized theory QCD not being $\mathrm{U(1)_A}$ invariant anymore. Therefore, terms in addition to $\mathcal{L}_2 + \mathcal{L}_4$ are needed which explicitly break the $\mathrm{U(1)_A}$ symmetry, i.e. which include an odd number of Goldstone boson fields. Following the construction done by Wess, Zumino and Witten (for details, see [Sch03], section 4.8), in the presence of an external electromagnetic field $v_\mu = -e\,Q A_\mu$ the additional term of the Lagrangian which contains photon fields equals

$$\begin{aligned} \mathcal{L}_{\mathrm{WZW}} = &- enA_\mu J^\mu + i\frac{ne^2}{48\pi^2}\,\varepsilon^{\mu\nu\alpha\beta}\,\partial_\nu A_\alpha\, A_\beta\,\mathrm{tr}\left\{2Q^2\left(U\partial_\mu U^\dagger - U^\dagger\partial_\mu U\right)\right. \\ &\left. -QU^\dagger Q\partial_\mu U + QUQ\partial_\mu U^\dagger\right\} \end{aligned} \tag{2.84}$$

with the current

$$J^\mu = \frac{1}{48\pi^2}\,\varepsilon^{\mu\nu\alpha\beta}\,\mathrm{tr}\left\{Q\,\partial_\nu U\,U^\dagger\,\partial_\alpha U\,U^\dagger\,\partial_\beta U\,U^\dagger + Q\,U^\dagger\,\partial_\nu U\,U^\dagger\,\partial_\alpha U\,U^\dagger\,\partial_\beta U\right\}. \tag{2.85}$$

$\varepsilon^{\mu\nu\alpha\beta}$ denotes the Levi-Civita tensor in the representation

$$\varepsilon^{\mu\nu\alpha\beta} = \begin{cases} +1, & \text{for all even permutations of } (\mu,\nu,\alpha,\beta) = (0,1,2,3) \\ -1, & \text{for all odd permutations of } (\mu,\nu,\alpha,\beta) = (0,1,2,3) \\ 0, & \text{otherwise} \end{cases}. \tag{2.86}$$

Obviously, the Wess-Zumino-Witten term $\mathcal{L}_{\mathrm{WZW}}$ is of the order Q^4 and hence it is not leading order but a next-to-leading-order term of the Lagrangian.

The constant n can be restricted to integers by topological arguments. Matching to QCD it can be shown that its modulus is equal to the number of colours. Calculating further the partial decay width for, e.g. the decay $\pi^0 \to \gamma\gamma$ and comparing the result to the experimental value given in [A+09] yields

$$|n| = 3 \tag{2.87}$$

which is equal to the generally assumed number of colours[2]. As only the squared transition matrix element which can be calculated with the Lagrangian (2.84) and, thus, n^2 is contained in any observables, the absolute sign of this number is not fixed at this moment. That is caused by the freedom to choose whether the field Φ represents Goldstone bosons or its negative, $-\Phi$. In section 2.5, the Lagrangian describing dynamics of light vector mesons will be introduced whose absolute sign cannot be fixed by comparing to experimental values, either. But if the overall sign for one of the Lagrangians is fixed, the sign for the other one can be fixed by comparing to experimental data as, e.g., the transition form factors for the transition of a pseudoscalar meson into a real photon. To simplify calculations in this thesis, the overall signs for both Lagrangians were fixed in advance yielding a not yet fixed relative sign between both Lagrangians, i.e. whether the Lagrangians have to be added or subtracted. Due to historical reasons, n is set to $+3$ and the prefactor h_A included in the Lagrangian describing vector mesons will be set to a positive value. It will turn out that the relative sign between the two Lagrangians will be determined as negative by comparing the calculations to experimental data for the $\eta \to \gamma$ transition form factor (see section 4.5).

[2]The result $|n| = 3$ will only be derived if the electric charges of the up quark and of the down and the strange quark are fixed as $+(2/3)e$ and $-(1/3)e$, respectively. As in the standard model the quark charges generally scale with $1/N_c$ for the number N_c of colours, the decay of $\pi^0 \to \gamma\gamma$ will not yield any information about N_c if the charges are not fixed in advance. See [BW01] for more information.

2.4 Vector Meson Dominance and Power Counting Schemes

2.4.1 Standard Vector Meson Dominance

The calculations presented in this subsection are based on the vector-meson-dominance model (VMD) [Sak69]. In this model, all interactions of hadrons with photons are mediated by intermediate vector mesons.

Standard VMD is a phenomenological approach to describe the energy regime where light vector mesons appear as relevant degrees of freedom. It yields a normalised form factor for the transition of a vector or pseudoscalar meson A into either a pseudoscalar meson, a vector meson or a photon B in the standard VMD representation[3]:

$$F_{AB}(q^2) = \left(\sum_{V=\rho^0,\omega,\phi} g_{ABV}\, g_{V\gamma} \right)^{-1} \sum_{V=\rho^0,\omega,\phi} g_{ABV}\, g_{V\gamma}\, \frac{m^2(V)}{m^2(V) - q^2}\,. \tag{2.88}$$

Here, g_{ABV} denotes the coupling constant for the decay $A \to BV$ with the intermediate vector meson V and $g_{V\gamma}$ the one for the decay of this vector meson into a photon. It is common practice to describe the standard VMD form factor in the "pole approximation"

$$F_{AB}(q^2) = \frac{1}{1 - \Lambda^{-2} q^2} \tag{2.89}$$

with the characteristic pole mass

$$\Lambda^{-2} = \left. \frac{\mathrm{d}F_{AB}}{\mathrm{d}q^2} \right|_{q^2=0} = \left(\sum_{V=\rho^0,\omega,\phi} g_{ABV}\, g_{V\gamma} \right)^{-1} \sum_{V=\rho^0,\omega,\phi} \frac{g_{ABV}\, g_{V\gamma}}{m^2(V)}\,. \tag{2.90}$$

The success of standard VMD is ambivalent. For some processes experimental data are well described by standard VMD but for others it fails to described the data. Examples are the decays $\eta \to \gamma\mu^+\mu^-$ and $\omega \to \pi^0\mu^+\mu^-$, respectively, where data taken by the NA60 collaboration are available [A+09]. The decay of the η-meson is well described by the standard VMD form factor while it fails to describe the decay of the ω-meson. In Fig. 2.1 the form factors for both decays calculated with the standard VMD model are plotted in comparison to the experimental data.

[3] See subsections 3.1.2 and 4.1.3 for the definition of the transition form factor.

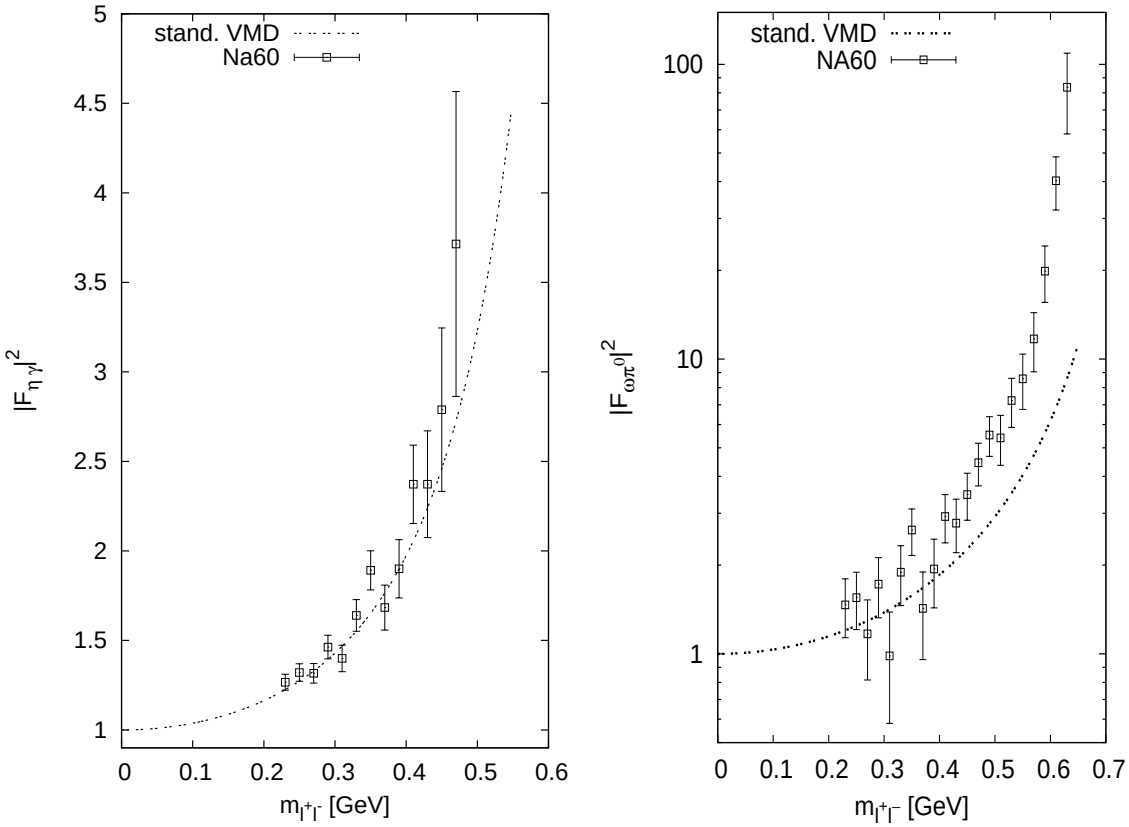

Figure 2.1: Form factors calculated with the standard VMD model (dot-dashed line) in comparison to the experimental data taken by the NA60 collaboration [A+09] for the decay $\eta \to \gamma\mu^+\mu^-$ on the left-hand side and for the decay $\omega \to \pi^0\mu^+\mu^-$ on the right-hand side.

2.4.2 The Novel Counting Scheme

In this thesis, a recently proposed power counting scheme [LL08] is used. In contrast to the standard counting scheme of ChPT, both the pseudoscalar Goldstone bosons P and the light vector mesons V are treated on equal footing. Thus, the masses of both are treated as soft, i.e. they are of the order of a typical momentum Q:

$$m(V),\, m(P) \in \mathcal{O}(Q). \tag{C1}$$

So, within the framework of this counting scheme masses up to the mass of the ϕ-meson, $m_\phi \approx 1.02\,\text{GeV}$, are soft. Additionally, this thesis is limited to decays of either light vector or pseudoscalar mesons. Hence, all involved momenta are smaller than the mass

of the decaying particle and the corresponding derivatives are also of the order of Q

$$\partial_\mu \in \mathcal{O}(Q). \tag{C2}$$

The restriction to pseudoscalar and light vector mesons as the only relevant degrees of freedom can be justified by the hadrogenesis conjecture [LK04]. It suggests that all other low-lying mesons are dynamically generated by the interactions between the light pseudoscalar and vector mesons. Therewith, there is a reasonably large gap to other mesons which otherwise would have to be included as additional degrees of freedom. Below in subsection 2.5.2 it will be argued that the power counting scheme (C1), (C2) is at least applicable well below the threshold of two vector mesons which equals about 1.5 GeV. For such high energies, additional degrees of freedom might become important anyway (like the excited pseudoscalar or vector meson states at approximately 1.3 to 1.4 GeV [A+08]).

As this counting yields a systematic ordering of processes, the leading-order Lagrangian and thus the leading-order form factors can be different from the standard VMD ones[4]. E.g., the form factor calculated with the standard VMD model for the $\omega \to \pi^0$ transition equals

$$F_{\omega\pi^0}^{\text{VMD}}(q) = \frac{m_\rho^2}{m_\rho^2 - q^2} \tag{2.91}$$

with the mass m_ρ of the ρ^0-meson. In contrast, the form factor calculated with the Lagrangian based on the power counting scheme (C1), (C2) has a term of standard VMD type plus additional terms which are not of VMD type[5]

$$F_{\omega\pi^0}(q) = \tilde{g}_0 \frac{m_\rho^2}{m_\rho^2 - q^2} + (1 - \tilde{g}_0 - \tilde{g}_1) + \tilde{g}_1 \left(1 + \frac{q^2}{m_\omega^2}\right) \frac{m_\rho^2}{m_\rho^2 - q^2} \tag{2.92}$$

with the mass m_ω of the ω-meson and real constants $\tilde{g}_0$ and $\tilde{g}_1$. With the representation

$$\begin{aligned}
&\tilde{g}_0 \frac{m_\rho^2}{m_\rho^2 - q^2} + (1 - \tilde{g}_0 - \tilde{g}_1) + \tilde{g}_1 \frac{m_\rho^2}{m_\rho^2 - q^2} + \tilde{g}_1 \frac{m_\rho^2}{m_\omega^2} \frac{q^2 - m_\rho^2 + m_\rho^2}{m_\rho^2 - q^2} \\
&= \left[\tilde{g}_0 + \tilde{g}_1 \left(1 + \frac{m_\rho^2}{m_\omega^2}\right)\right] \frac{m_\rho^2}{m_\rho^2 - q^2} + \left[1 - \tilde{g}_0 - \tilde{g}_1 \left(1 + \frac{m_\rho^2}{m_\omega^2}\right)\right] \\
&=: g_0 \frac{m_\rho^2}{m_\rho^2 - q^2} + (1 - g_0),
\end{aligned} \tag{2.93}$$

this form factor is in agreement with the first two terms of the general form factor (1.2). Thus, in the effective field theory used in this thesis all g_i of (1.2) with $i \geq 1$ are subleading. Still, the expression (2.93) is more general than the VMD result (2.91). Only for $g_0 = 1$ one recovers (2.91). It will turn out that g_0 is very different from 1.

[4] The leading-order Lagrangian is developed in section 2.5 and the form factors in the parts after this one.

[5] See subsection 3.2.1 for the derivation of the $\omega \to \pi^0$ transition form factor.

2.5 Interactions with Vector Mesons

In this section a leading-order Lagrangian will be developed which describes interactions of vector mesons with themselves, with Goldstone bosons and with external electromagnetic fields. Thereby, the order of a term is identified in accordance with the counting scheme (C1), (C2) given in the last section.

2.5.1 The Free Lagrangian for Vector Mesons

In this thesis, the light vector mesons are described by antisymmetric tensor fields $W_{\mu\nu} = -W_{\nu\mu}$ collected in the matrix [LL08]

$$V_{\mu\nu} = \begin{pmatrix} \rho^0_{\mu\nu} + \omega_{\mu\nu} & \sqrt{2}\rho^+_{\mu\nu} & \sqrt{2}K^+_{\mu\nu} \\ \sqrt{2}\rho^-_{\mu\nu} & -\rho^0_{\mu\nu} + \omega_{\mu\nu} & \sqrt{2}K^0_{\mu\nu} \\ \sqrt{2}K^-_{\mu\nu} & \sqrt{2}\bar{K}^0_{\mu\nu} & \sqrt{2}\Phi_{\mu\nu} \end{pmatrix} \tag{2.94}$$

which is an especially convenient representation if interactions with external fields as, e.g., electromagnetic fields are considered since electromagnetic gauge invariance is easy to ensure (see [LL08, LS08]).
The most general free Lagrangian for an antisymmetric tensor field $W^{\mu\nu}$ equals

$$\mathcal{L} = a\,\partial^\mu W_{\mu\nu}\,\partial_\rho W^{\rho\nu} + b\,\partial^\rho W_{\mu\nu}\,\partial_\rho W^{\mu\nu} + c\,W_{\mu\nu}W^{\mu\nu} \tag{2.95}$$

with arbitrary constants a, b and c. As vector mesons are massive spin-1 particles, they contain three degrees of freedom. Hence, the six degrees of freedom of a general antisymmetric tensor field have to be reduced by the choice of the constants. Choosing e.g. $b = 0$ the three fields W^{ij} for $i, j = 1, \ldots, 3$ are frozen (see appendix in [GL84]). With $a = -\frac{1}{2}$ and $c = \frac{1}{4}m_W^2$ the free Lagrangian for a vector meson with mass m_W equals

$$\mathcal{L} = -\frac{1}{2}\,\partial^\mu W_{\mu\nu}\,\partial_\rho W^{\rho\nu} + \frac{1}{4}\,m_W^2 W_{\mu\nu}W^{\mu\nu}. \tag{2.96}$$

2.5.2 The Leading-Order Lagrangian

The vector meson matrix $V_{\mu\nu}$ transforms as an octet under the symmetry group $\mathrm{SU(3)_V}$, i.e. for all $A \in \mathrm{SU(3)_V}$ it transforms as

$$V^{\mu\nu} \overset{A}{\mapsto} AV^{\mu\nu}A^\dagger. \tag{2.97}$$

In order to get the same transformation property for the Goldstone bosons, they have to be collected in

$$U_\mu = \frac{1}{2} u^\dagger \left(D_\mu U\right) u^\dagger = \frac{1}{2} u^\dagger \left(\left(\partial_\mu e^{i\frac{\Phi}{f}}\right) + ieA_\mu \left[Q, e^{i\frac{\Phi}{f}}\right]_- \right) u^\dagger \tag{2.98}$$

instead of the collection in the field U defined in section 2.3.1. The field U_μ includes the square root [Sch03]

$$u = \sqrt{U} = \exp\left(\frac{i\Phi}{2f}\right) \tag{2.99}$$

of the primary field U. Due to the new transformation properties a new covariant derivative

$$D_\mu X = \partial_\mu X + \left[\Gamma_\mu, X\right]_- + ieA_\mu \left[Q, X\right]_- \tag{2.100}$$

acting on the vector meson field $V_{\mu\nu}$ and the collection of the Goldstone fields U_μ has to be defined including

$$\Gamma_\mu = \frac{1}{2}\left(u^\dagger \partial_\mu u + u\, \partial_\mu u^\dagger\right). \tag{2.101}$$

According to the counting scheme (2.70), (2.71) of ChPT proposed in the section 2.3.1 and the counting scheme for vector mesons (C1), (C2), the formal chiral powers

$$\begin{aligned} &V_{\mu\nu} \in \mathcal{O}(Q^0),\ U_\mu \in \mathcal{O}(Q),\ D_\mu \in \mathcal{O}(Q), \\ &\chi_\pm := \frac{1}{2} u \chi_0 u \pm \frac{1}{2} u^\dagger \chi_0 u^\dagger \in \mathcal{O}(Q^2) \end{aligned} \tag{2.102}$$

are assigned. For the case of interest in this thesis, the leading-order Lagrangian for the hadronic reactions up to the order Q^2 concerning the formal chiral powers given above reads [LL08]

$$\begin{aligned} \mathcal{L} \;=\; & i\frac{m_V h_V}{4} \operatorname{tr}\left\{V_{\alpha\mu} V^{\mu\nu} V^{\alpha}{}_{\nu}\right\} + i\frac{\tilde{h}_V}{4m_V} \operatorname{tr}\left\{\left(D^\alpha V_{\alpha\mu}\right) V_{\mu\nu} \left(D^\beta V_{\beta\nu}\right)\right\} \\ & + i\frac{h_A}{8} \varepsilon^{\mu\nu\alpha\beta} \operatorname{tr}\left\{\left(V_{\mu\nu}\left(D^\tau V_{\tau\alpha}\right) + \left(D^\tau V_{\tau\alpha}\right) V_{\mu\nu}\right) U_\beta\right\} \\ & + i\frac{m_V h_P}{2} \operatorname{tr}\left\{U_\mu V^{\mu\nu} U_\nu\right\} + i\frac{b_A}{8} \varepsilon^{\mu\nu\alpha\beta} \operatorname{tr}\left\{\left[V_{\mu\nu}, V_{\alpha\beta}\right]_+ \chi_-\right\}, \end{aligned} \tag{2.103}$$

whereby the terms are ordered according to their formal chiral powers.
All terms and therewith the Lagrangian have positive parity due to the Levi-Civita tensor $\varepsilon^{\mu\nu\alpha\beta}$. So, the terms including a Levi-Civita tensor are those corresponding to the Wess-Zumino-Witten term and the chiral anomaly.

Additional electromagnetic interaction vertices are constructed with the field-strength tensor for the photon field A_μ,

$$F_{\mu\nu} = \partial_\mu A_\nu - \partial_\nu A_\mu. \tag{2.104}$$

It is combined with the Goldstone boson field to the building block

$$f^{\pm}_{\mu\nu} = \frac{1}{2}\left(uQu^\dagger \pm u^\dagger Q u\right) F_{\mu\nu} \tag{2.105}$$

which has the same chiral transformation properties as the vector meson field $V_{\mu\nu}$ and as the collection of the Goldstone bosons U_μ. It is counted as Q^2. Using these building blocks, the leading-order Lagrangian describing the interaction of light vector mesons with electromagnetic fields is equal to

$$\mathcal{L}_{e.m.} = -\frac{e_V m_V}{8}\,\mathrm{tr}\left\{V^{\mu\nu} f^+_{\mu\nu}\right\} - i\frac{e_M}{4}\,\mathrm{tr}\left\{\left[V_\mu{}^\alpha, V^{\mu\beta}\right]_- f^+_{\alpha\beta}\right\}. \tag{2.106}$$

Since the Lagrangian constructed in this section is of leading order, the influence of the next-to-leading order is of interest in order to get information about the intrinsic error of the calculations. As a very rough estimate, one particular next-to-leading-order term

$$\mathcal{L} = i\,\frac{e_A}{4m_V}\,\varepsilon^{\mu\nu\alpha\beta}\;\mathrm{tr}\left\{\left(f^+_{\mu\nu}\left(D^\tau V_{\tau\alpha}\right) + \left(D^\tau V_{\tau\alpha}\right) f^+_{\mu\nu}\right) U_\beta\right\} \tag{2.107}$$

is taken into account which describes the direct decay of a vector meson into a pseudoscalar meson and a photon. Therewith, the intrinsic error is estimated as the difference between the leading-order calculation and the calculation involving this particular next-to-leading-order term. Keep in mind that this is of course not the whole next-to-leading-order Lagrangian, not even for the decays studied in this thesis. The full next-to-leading-order Lagrangian would also contain loops and is beyond the scope of this thesis. Take, e.g., the next-to-leading order processes for the decay of an ω-meson into a neutral pion and a dilepton l^+l^-. One of these processes is the direct decay described by the Lagrangian (2.107) (diagram on the left-hand side of Fig. 2.2) but there are also loop diagrams contributing, e.g., with a $\rho\pi\pi$ loop or a K^*KK loop (diagrams in the middle and on the right-hand side of Fig. 2.2, respectively).

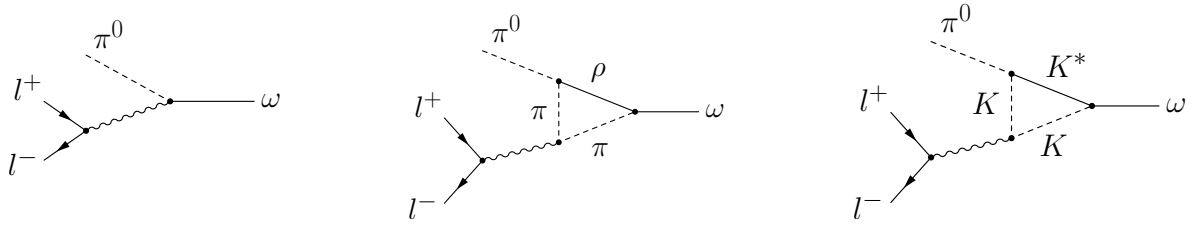

Figure 2.2: Selection of next-to-leading order processes for the decay $\omega \to \pi^0 l^+ l^-$.

For a complete error estimate at given energy and momentum a full next-to-leading-order calculation would be necessary. Additionally, the accuracy does not only depend on typical energies and momenta but also on the reaction one considers. In general, it is not possible to predict for given energy and momentum the accuracy of a leading-order calculation of an arbitrary reaction. This problem already occurs in ChPT. Here, processes as, e.g., the majority of the pion reactions can be described for which the effects of next-to-leading-order calculations are small [GL84] but there are also processes describable for which the next-to-leading-order results are much more important than the leading-order ones. An example for such processes is the decay of an η-meson into three pions [GL85b].

The Lagrangians (2.103), (2.106) and (2.107) presented above can be used to calculate radiative and hadronic decays of light vector mesons depending on the parameters m_V, h_V, $\tilde{h}_V$, h_A, h_P, b_A, e_V, e_M and e_A. Additionally, the matrix U_μ describing the Goldstone bosons and χ_0 contain the free parameters f and B_0, respectively. Three of these parameters are fixed independently of decays of vector mesons:

- The pion decay constant $f = 90\,\text{MeV}$ in the chiral limit is determined through the decay $\pi^+ \to \mu^+\nu_\mu$ and further theoretical considerations [LL08],
- $B_0 M$ is defined by the averaged Goldstone boson masses $\bar{m}_\pi \approx 138\,\text{MeV}$ and $\bar{m}_K = 496\,\text{MeV}$ via the identity $\chi_0 = 2B_0M = \begin{pmatrix} \bar{m}_\pi^2 & 0 & 0 \\ 0 & \bar{m}_\pi^2 & 0 \\ 0 & 0 & 2\bar{m}_K^2 - \bar{m}_\pi^2 \end{pmatrix}$ (see chapter 4.3 for a derivation of the value B_0M) and
- $m_V := 776\,\text{MeV}$ is introduced in order that the other parameters are dimensionless.

Furthermore, the value of the electric charge needed for QED is determined as [LL08]

$$e = \sqrt{4\pi\alpha} = 0.303\,. \tag{2.108}$$

The remaining parameters can be fixed by fitting to experimental data (for more details, see [LL08]). E.g., the value e_V is fixed by comparing the calculated partial decay widths for the decays of the neutral light vector mesons ρ^0-, ω- and ϕ-meson into dielectrons and equals

$$e_V = 0.22\,. \tag{2.109}$$

The parameters e_A, h_A and b_A are related to the decays of a vector meson into a Goldstone boson and a photon. They can be fitted to the decays with real photons (for details see subsection 3.1 below).
For leading-order calculations, the term (2.107) proportional to e_A should not be considered. This is realised by setting $e_A = 0$ and therewith fixing the parameter set

$$e_A = 0,\ h_A = 2.32,\ b_A = 0.27 \tag{P1}$$

for the leading-order calculation[6]. As discussed in subsection 2.3.2, the determination of h_A as positive is not concluded by comparison to experimental values but set by definition. What matters are the relative signs between the constants e_A, h_A and b_A. To get a rough error estimate, a second parameter set with $e_A \neq 0$ is established[7]:

$$e_A = 0.015,\ h_A = 2.10,\ b_A = 0.19\,. \tag{P2}$$

In table 2.2, the values for the partial decay widths of the decays $\omega \to \pi^0\gamma$, $\omega \to \eta\gamma$ and $\phi \to \eta\gamma$ calculated with both parameter set (P1) and (P2) are listed in comparison to the experimental data given in [A+08]. For the calculations Eq. (3.24) and the form factors which will be given in the subsections 3.2.1, 3.3.1 and 3.4.1 are used. Both calculations agree well with the experimental values and do not differ much from each other. This legitimates treating the results taken with parameter set (P2) as a very rough estimate of the intrinsic errors of the leading-order calculation.

Table 2.2: Partial decay width calculated with parameter set (P1) and parameter set (P2), respectively, compared to the experimental values as collected in [A+08].

	experimental value	param. set (P1)	param. set (P2)
$\Gamma_{\omega\to\pi^0\gamma}$	$(7.03 \pm 0.30) \cdot 10^{-4}$ GeV	$7.14 \cdot 10^{-4}$ GeV	$7.34 \cdot 10^{-4}$ GeV
$\Gamma_{\omega\to\eta\gamma}$	$(3.91 \pm 0.38) \cdot 10^{-6}$ GeV	$3.71 \cdot 10^{-6}$ GeV	$3.83 \cdot 10^{-6}$ GeV
$\Gamma_{\phi\to\eta\gamma}$	$(5.58 \pm 0.15) \cdot 10^{-5}$ GeV	$5.38 \cdot 10^{-5}$ GeV	$5.12 \cdot 10^{-5}$ GeV

In [LL08, LL09], radiative decays of light vector mesons and hadronic three-body decays of light vector mesons were calculated based on the counting scheme (C1), (C2) and the Lagrangians given in this subsection. All calculations agreed well with the available experimental data. This suggests that the proposed approach including the power counting scheme can provide reliable answers. Nevertheless, some problems might occur within this framework. They will be discussed in the next subsection.

2.5.3 Problems

The first term $i\,\frac{m_V h_V}{4}\,\mathrm{tr}\,\{V_{\alpha\mu}V^{\mu\nu}V^{\alpha}{}_{\nu}\}$ in the Lagrangian (2.103) is of the order Q^0 and could cause problems within the framework of the counting scheme (C1), (C2) used in this thesis. As an illustration, consider the annihilation and production of two pseudoscalar Goldstone bosons via one virtual vector meson without loops. In Fig. 2.3, this process is represented by a "Feynman diagram" which can be used as a graphical way to calculate the corresponding transition matrix element. Feynman diagrams and rules are explained in section 2.6.

[6] All other parameters are not necessary for the calculations presented in this thesis and hence are not listed here. Their values are given in [LL08].

[7] The values differ from those given in [LL08] because of better experimental data.

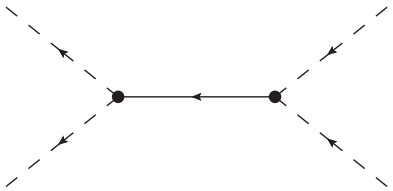

Figure 2.3: Tree-level diagram for the process $P + P \to V^* \to P + P$.

The term proportional to h_P in the Lagrangian (2.103) yields that the vertices for two Goldstone bosons and one vector meson are always of the order Q^2. As the vector mesons are counted as soft, i.e. the mass is of the order of Q, the propagator is proportional to

$$\frac{1}{m_V^2 - Q^2} \in \mathcal{O}\left(\frac{1}{Q^2}\right). \tag{2.110}$$

Thus, the process $P + P \to V^* \to P + P$ without loops is of the order

$$Q^2 \frac{1}{Q^2} Q^2 = Q^2. \tag{2.111}$$

The order of the process including any loops should be higher so that diagrams containing loops are less important than tree-level diagrams. Take, e.g., the process with a loop consisting of two vector mesons and a Goldstone boson (Fig. 2.4, left-hand side). The loop itself counts as Q^4 [Sch03] and the propagators for the three involved particles count as Q^{-2} each. The vertices for two Goldstone bosons and one vector meson count again as Q^2 and the three-vector meson vertex counts as Q^0. Thus, the whole diagram counts as

$$Q^2 \frac{1}{Q^2} Q^0 \frac{1}{Q^2} Q^2 \frac{1}{Q^2} Q^2 \frac{1}{Q^2} Q^4 = Q^2 \tag{2.112}$$

and hence is of the same order as the tree-level diagram. Taking into account an additional three-vector-meson loop (Fig. 2.4, right-hand side) the order of the diagram is even lower than the order of the tree-level diagram:

$$Q^2 \frac{1}{Q^2} Q^0 \frac{1}{Q^2} Q^0 \frac{1}{Q^2} Q^0 \frac{1}{Q^2} Q^4 \frac{1}{Q^2} Q^2 \frac{1}{Q^2} Q^2 \frac{1}{Q^2} Q^4 = Q^0. \tag{2.113}$$

Thus, it is possible to construct loop diagrams with orders less or equal to the order of the tree-level diagram. Hence, one would have to calculate infinitely many loop diagrams for a leading-order calculation. For that reason, the question arises how to reconcile the formal Q^0 term with a power counting scheme which is of practical use. Two lines of reasoning can be brought forward which essentially end at the same conclusion:

Figure 2.4: Diagrams including one loop (left-hand side) and including two loops (right-hand side) for the process $P + P \to V^* \to P + P$.

On the one hand, the problem can be solved by observing that the incriminated term in (2.103) proportional to h_V involves the appearance of at least two vector mesons at the same time. The connected inelasticity starts at an energy of about 1.5 GeV. In contrast, the energy regime considered here is at one vector-meson mass and below. In between, new active degrees of freedom might appear like the excited pseudoscalar or vector states with masses of 1.3 GeV or higher [A+08]. As a conservative approach it is reasonable to restrict the range of applicability to energies well below the threshold of two vector mesons. Thus, treating all vector mesons as soft is not reasonable anymore. If two appear at the same time, one vector meson has to be treated as hard, i.e. the mass is formally much larger than Q. Then the propagator for this vector meson is proportional to

$$\frac{1}{m_V^2 - Q^2} \approx \frac{1}{m_V^2} \in \mathcal{O}(Q^0). \tag{2.114}$$

Therewith, the diagrams with one and two loops given in Fig. 2.4 count as Q^4 and Q^6, respectively. Hence, they are suppressed compared to the tree-level diagram which is counted as Q^2.
On the other hand, arguments for a large number, N_c, of colours can be applied [LL08]. According to large-N_c rules, vertices with n mesons count as $N_c^{1-n/2}$. Therewith, the term proportional to $\mathrm{tr}\,\{V_{\alpha\mu}V^{\mu\nu}V^{\alpha}{}_{\nu}\}$ would be suppressed by $\frac{1}{\sqrt{N_c}}$. This is introduced in the counting scheme by identifying $Q \sim N_c^{-1/2}$ and assigning an additional factor Q^{n_V-2} to all interactions involving $n_V \geq 2$ vector-meson fields. Both diagrams in Fig. 2.4 would then count as Q^3, i.e. are subleading. This is sufficient for the leading-order calculations presented in this thesis.
Both lines of reasoning lead to the fact that for the calculations of vector-meson decays in leading order in the power counting one has to consider only tree-level diagrams with the interaction terms given in (2.103) and (2.106). For decays of pseudoscalar mesons, the issue is more involved as will be discussed next.

2.5.4 Decays of Pseudoscalar Mesons

As the vector-meson Lagrangians given in subsection 2.5.2 include both vector and pseudoscalar mesons, they describe some of the necessary terms for the decay of a pseudoscalar meson into a vector meson and a (real or virtual) photon or into two photons via virtual vector mesons. Consider, e.g., the decay of a vector meson into a pseudoscalar meson and a photon via a virtual vector meson (Fig. 2.5, left-hand side). If this process is mirrored, one sees the connection to the decay of a pseudoscalar meson into two photons via two virtual vector mesons (Fig. 2.5, right-hand side).

Figure 2.5: Decays $V \to V^*P \to \gamma P$ (left-hand side) and $P \to V^*V^* \to \gamma\gamma$ (right-hand side).

In ChPT, the leading-order Lagrangian for the decay of a pseudoscalar meson into two photons is given by the WZW Lagrangian (2.84) which describes the direct decay into two photons and is of order Q^4. As the process $P \to V^*V^* \to \gamma\gamma$ includes two vector mesons at the same time, one of them has to be treated as hard in the approach used in this thesis due to the arguments given in the previous subsection. Therefore, this process is also counted as Q^4. Thus, for a leading-order calculation of a decay of a pseudoscalar meson into two photons both possibilities, the direct decay and the decay via two virtual vector mesons, have to be considered. Additionally, there are further contributing processes as, e.g., the decay via one intermediate vector meson described by the Lagrangian (2.107) but also loop diagrams. In this thesis, the calculations are restricted to those processes described by the WZW Lagrangian (2.84) and by the vector-meson Lagrangians (2.103), (2.106) and (2.107) and it is studied whether they are able to describe the available data (see chapters 4 and 5). Furthermore, the influence of the WZW term in comparison to the decay via one or two virtual vector mesons is analysed. The remaining terms of the Lagrangian describing the decay of a pseudoscalar meson are not developed in this thesis. Also the calculation of loop diagrams is beyond the scope of this thesis. Note that these considerations only concern the pseudoscalar decays (chapters 4 and 5). For the vector-meson decays (chapter 3), a complete leading-order calculation is presented.

2.6 Feynman Diagrams and Rules

In particle physics, one is interested in scatterings and decays of particles. An important quantity for the study of such processes is the probability of one or more initial particles, described by an initial state $\{\vec{k}_i\}$, to scatter or decay and become a finial state $\{\vec{p}_f\}$,

$$|\,{}_{\text{out}}\langle\{\vec{p}_f\}|\{\vec{k}_i\}\rangle_{\text{in}}\,|^2, \tag{2.115}$$

which defines the "invariant transition matrix element" $\mathcal{M}(\{k_i\} \to \{p_f\})$ by

$${}_{\text{out}}\langle\{\vec{p}_f\}|\{\vec{k}_i\}\rangle_{\text{in}} =: (2\pi)^4\delta^{(4)}\left(\sum k_i - \sum p_f\right) i\mathcal{M}(\{k_i\} \to \{p_f\}). \tag{2.116}$$

To calculate this probability, all possible processes in which the initial state $\{\vec{k}_i\}$ becomes the final state $\{\vec{p}_f\}$ have to be considered and summed up. To simplify the identification of all possible processes, "Feynman diagrams" are introduced. They yield a graphical way to describe processes of interest and a "simple" formula for the transition matrix element so that it can be read off from the diagrams directly.
The derivation of this simple formula is exemplary done for the case of the ϕ^4 theory described by the Lagrangian

$$\mathcal{L} = \frac{1}{2}\left(\partial_\mu\phi\right)^2 - \frac{1}{2}m^2\phi^2 - \frac{\lambda}{4!}\phi^4 \tag{2.117}$$

in section A.2 in the appendix following the explanations given in [PS95].

Under the assumption that all particles do not interact during their formation and their detection, the probability (2.115) can be calculated by replacing the eigenstates $\langle\{\vec{p}_f\}|$ and $|\{\vec{k}_i\}\rangle$ of the full Hamiltonian H by eigenstates of the Hamiltonian H_0 of the free theory. Then it is possible to show that

$$\begin{aligned}{}_{\text{out}}\langle\{\vec{p}_f\}|\{\vec{k}_i\}\rangle_{\text{in}} &= \lim_{t_f\to\infty(1-i\varepsilon)}\left(\left\langle\{(\vec{p}_f)_0\}\left|T\left\{\exp\left[-i\int_{-t_f}^{+t_f}\mathrm{d}t\, H_I(t)\right]\right\}\right|\{(\vec{k}_i)_0\}\right\rangle\right) \\ &= \begin{pmatrix}\text{sum over all connected,}\\ \text{amputated Feynman diagrams}\end{pmatrix}.\end{aligned} \tag{2.118}$$

Here, the operator T denotes the time ordering of a product. Furthermore:

- "Connected" diagrams are fully connected diagrams where all external lines are connected to each other and no "vacuum bubbles" are left.
- To amputate a diagram start from the tip of each leg. Cut the diagram at the last point at which the leg can be separated from the rest of the diagram by removing a single propagator.

In momentum space, the transition matrix element defined by Eq. (2.116) can be expressed as the sum over the Feynman diagrams due to the overall δ-function describing the momentum conservation which cancels the one in the definition of the scattering probability:

$$i\mathcal{M}(\{\vec{k}_i\} \to \{\vec{p}_f\}) = \begin{pmatrix}\text{sum over all connected,}\\ \text{amputated diagrams}\end{pmatrix}. \tag{2.119}$$

2.6.1 Feynman Rules for Interactions with Vector Mesons and QED

In this thesis, decays of vector mesons and pseudoscalar mesons into dileptons and either pseudoscalar mesons, vector mesons or real photons are considered. Therefore, both a Lagrangian which describes the decay into a virtual photon and the QED Lagrangian which describes the decay of the virtual photon into a dilepton are needed. To calculate the observable quantities as transition form factors and partial decay widths, the Feynman diagrams describing the alternative ways for the decay have to be sketched. Each Feynman diagram has a value which is the product of all analytical expressions associated with the different parts of the diagram. According to the introduction of this section, the transition matrix element can be calculated as the sum over the values of all possible Feynman diagrams. The Feynman rules that define the analytical expressions associated with a particular part of a Feynman diagram are given in this subsection.

Each particle in the Lagrangians given in this thesis is defined as an incoming particle or, equivalently, as an outgoing antiparticle. If the particle is given with a derivative, there is a factor $-i \cdot$(momentum of the particle) associated with the Feynman diagram. Of course, this momentum is always the momentum of an incoming particle, an outgoing antiparticle causes a factor $-i \cdot (-\text{momentum}) = +i \cdot (\text{momentum})$.
Each vertex in the Feynman diagram associated with a term including a coupling constant g in the Lagrangian yields an additional factor $+ig$.

The Feynman rules for QED needed to describe an external photon or the decay of an virtual photon into a dilepton are the following [PS95]:

- Photon propagator for a photon with momentum p: $\frac{-ig_{\mu\nu}}{p^2+i\varepsilon}$.
- QED vertex for dileptons: $-ie\gamma^\mu$.
- Outgoing external photons with momentum p and polarisation λ: $\varepsilon^*_\mu(p,\lambda)$.
  Outgoing external fermions with momentum p and spin s: $\bar{u}^s(p)$.
  Outgoing external antifermions with momentum p and spin s: $v^s(p)$.

Hereby, $\varepsilon_\mu(p,\lambda)$ denotes the polarisation vector of a photon and the spinors $u^s(p)$ and $v^s(p)$ describe the plane wave solutions of the Dirac equation

$$(i\partial\!\!\!/ - m)\psi = 0 \tag{2.120}$$

with positive frequency, $\psi(x) = u^s(p)e^{-ipx}$, and with negative frequency, $\psi(x) = v^s(p)e^{+ipx}$, respectively.

The rules for external vector mesons $\langle 0|V(0)|V(p,\lambda)\rangle$ and the propagators $\langle 0|TV(x)V(y)|0\rangle$ including the mass m of the vector meson and the momenta p of the external particle and q of the virtual vector meson are the following [GL84, LS08]:

- $\langle 0|V_{\mu\nu}(0)|V(p,\lambda)\rangle = \varepsilon_{\mu\nu}(p,\lambda) = \dfrac{i}{m}\left[p_\mu\varepsilon_\nu(p,\lambda) - p_\nu\varepsilon_\mu(p,\lambda)\right],$
- $\langle 0|TV_{\mu\nu}(x)V_{\alpha\beta}(y)|0\rangle = -\dfrac{i}{m^2}\displaystyle\int \frac{\mathrm{d}^4q}{(2\pi)^4}e^{-iq(x-y)}S(q^2)\Big[(m^2-q^2)g_{\mu\alpha}g_{\nu\beta} + g_{\mu\alpha}q_\nu q_\beta - g_{\mu\beta}q_\nu q_\alpha - (\mu\to\nu)\Big].$

By taking derivatives of these expressions one gets

- $\langle 0|\partial^\mu V_{\mu\nu}|V(p,\lambda)\rangle = m\varepsilon_\nu(p,\lambda),$
- $\langle 0|TV_{\mu\nu}(x)\partial^\alpha V_{\alpha\beta}(y)|0\rangle = \displaystyle\int \frac{\mathrm{d}^4q}{(2\pi)^4}e^{-iq(x-y)}S(q^2)\left[q_\mu g_{\nu\beta} - q_\nu g_{\mu\beta}\right],$
- $\langle 0|T\partial^\mu V_{\mu\nu}(x)V_{\alpha\beta}(y)|0\rangle = -\displaystyle\int \frac{\mathrm{d}^4q}{(2\pi)^4}e^{-iq(x-y)}S(q^2)\left[q_\alpha g_{\nu\beta} - q_\beta g_{\nu\alpha}\right],$
- $\langle 0|T\partial^\mu V_{\mu\nu}(x)\partial^\alpha V_{\alpha\beta}(y)|0\rangle = -i\displaystyle\int \frac{\mathrm{d}^4q}{(2\pi)^4}e^{-iq(x-y)}S(q^2)\Big[q^2 g_{\nu\beta} - q_\nu q_\beta\Big].$

$S(q^2)$ is the scalar propagator describing a structureless vector meson. It is defined as

$$S(q^2) = \frac{1}{q^2 - m^2} \tag{2.121}$$

with the mass m of the virtual vector meson. As vector mesons are not stable particles but resonances, the propagator has to be extended according to their finite life time, i.e. the inverse of their energy-dependent width:

$$S_{\text{width}}(q^2) = \frac{1}{q^2 - m^2 + i\sqrt{q^2}\,\Gamma(q^2)}\,. \tag{2.122}$$

In this thesis, the energy-dependent widths for the neutral vector mesons ρ^0, ω and ϕ are needed. For the ρ^0- and ϕ-meson which decay dominantly into two Goldstone bosons the width is given by [LL09]

$$\Gamma(q^2) = \Gamma_0\left[\frac{p_{\text{cm}}(q^2)}{p_{\text{cm}}(m^2)}\right]^3\frac{m^2}{q^2} \tag{2.123}$$

including the on-shell widths [A+08]

$$\Gamma_{0,\rho^0} = (149.1 \pm 0.8)\,\text{MeV},\ \Gamma_{0,\phi} = (4.26 \pm 0.04)\,\text{MeV} \tag{2.124}$$

of the mesons and the center-of-mass momentum of the decay particles according to the decay branch with the dominant branching ratio, i.e.

$$p_{\text{cm},\rho^0}(q^2) = \frac{1}{2}\sqrt{q^2 - 4\bar{m}_\pi^2},\ p_{\text{cm},\phi}(q^2) = \frac{1}{2}\sqrt{q^2 - 4m_{K^\pm}^2}\,. \tag{2.125}$$

The energy-dependence of the width of the ω-meson is not relevant and $\Gamma_\omega(q^2)$ is approximated by $\Gamma_{0,\omega} = (8.49 \pm 0.08)\,\text{MeV}$.

For most of the decays presented in this thesis, the differences between the calculations with the energy-dependent width and without width are negligible so that the calculations could be done with the approximative propagator $S_{\text{width}}(q^2) \approx S(q^2)$.

3 Radiative Two- and Three-Body Decays of Vector Mesons

In this chapter, electromagnetic transitions of vector mesons A into pseudoscalar mesons B are considered, i.e. the processes $A \to B\gamma^{(\star)}$ with a real or virtual photon.
The relevant leading-order Lagrangian and the formulas for the transition form factor and the partial decay width are derived in section 3.1. In the subsequent sections 3.2, 3.3 and 3.4, the transitions $\omega \to \pi^0$, $\omega \to \eta$ and $\phi \to \eta$ are considered. The results of this chapter are published in [TL10].

As explained in section 2.5, the calculations presented in this and in the subsequent chapters 4 and 5 are leading-order calculations according to the counting scheme C1, C2. These calculations are done with the parameter set (P1). Additionally, a particular next-to-leading order term (2.107) is used to estimate the intrinsic error very roughly. Therefore, further calculations are done with the parameter set (P2). In this parameter set, the parameter e_A of the particular next-to-leading-order term is non-zero.

3.1 Leading-Order Lagrangian, Transition Form Factor and Partial Decay Width

3.1.1 The Relevant Leading-Order Lagrangian

The leading-order chiral Lagrangian according to the power counting scheme (C1), (C2) is given in (2.103) and (2.106). As

$$f_{\mu\nu}^{+} = QF_{\mu\nu} + \mathcal{O}\left(\Phi^2\right) = Q\left(\partial_\mu A_\nu - \partial_\nu A_\mu\right) + \mathcal{O}\left(\Phi^2\right) \tag{3.1}$$

this Lagrangian does neither describe a direct transition of a pseudoscalar meson into a photon nor a transition decay of a vector meson into a pseudoscalar meson. Therefore, this leading-order Lagrangian only describes the decay of vector meson A into a pseudoscalar meson B and a (real or virtual) photon via a virtual vector meson V which transforms into the photon. This is shown in Fig. 2.5, left-hand side. The parts of the Lagrangians (2.103) and (2.106) which are relevant for the decay of a vector meson into a pseudoscalar meson and a photon are the following:

1. Decay $A \to BV$:

$$\begin{aligned}
\mathcal{L}_{11} &= i\frac{h_A}{8}\,\varepsilon^{\mu\nu\alpha\beta}\,\mathrm{tr}\left\{\left(V_{\mu\nu}\left(D^\tau V_{\tau\alpha}\right) + \left(D^\tau V_{\tau\alpha}\right)V_{\mu\nu}\right)\,U_\beta\right\} \\
&\approx i\frac{h_A}{8}\,\varepsilon^{\mu\nu\alpha\beta}\,\mathrm{tr}\left\{\left(V_{\mu\nu}\left(\partial^\tau V_{\tau\alpha}\right) + \left(\partial^\tau V_{\tau\alpha}\right)V_{\mu\nu}\right)\,\frac{i}{2f}\partial_\beta\Phi\right\} \\
&= -\frac{h_A}{16f}\,\varepsilon^{\mu\nu\alpha\beta}\,\mathrm{tr}\left\{\left(V_{\mu\nu}\left(\partial^\tau V_{\tau\alpha}\right) + \left(\partial^\tau V_{\tau\alpha}\right)V_{\mu\nu}\right)\,\partial_\beta\Phi\right\}, \qquad (3.2) \\
\mathcal{L}_{12} &= i\frac{b_A}{8}\,\varepsilon^{\mu\nu\alpha\beta}\,\mathrm{tr}\left\{\left[V_{\mu\nu}, V_{\alpha\beta}\right]_+\chi_-\right\} \\
&\approx -\frac{b_A}{16f}\,\varepsilon^{\mu\nu\alpha\beta}\,\mathrm{tr}\left\{\left[V_{\mu\nu}, V_{\alpha\beta}\right]_+\left[\Phi, \chi_0\right]_+\right\} \\
&= -\frac{b_A}{8f}\,\varepsilon^{\mu\nu\alpha\beta}\,\mathrm{tr}\left\{V_{\mu\nu}V_{\alpha\beta}\left[\Phi, \chi_0\right]_+\right\}. \qquad (3.3)
\end{aligned}$$

2. Transition $V \to \gamma$:

$$\begin{aligned}
\mathcal{L}_2 &= -\frac{e_V\, m_V}{8}\,\mathrm{tr}\left\{V^{\mu\nu}\, f_{\mu\nu}^{+}\right\} \\
&\approx -\frac{e_V\, m_V}{8}\,\mathrm{tr}\left\{V^{\mu\nu}\, Q\left(\partial_\mu A_\nu - \partial_\nu A_\mu\right)\right\} \\
&= -\frac{e_V\, m_V}{8}\,\mathrm{tr}\left\{V^{\mu\nu}\, Q\,\partial_\mu A_\nu + V^{\nu\mu}\, Q\,\partial_\nu A_\mu\right\} \\
&= -\frac{e_V\, m_V}{4}\,\mathrm{tr}\left\{V^{\mu\nu}\, Q\right\}\,\partial_\mu A_\nu\,. \qquad (3.4)
\end{aligned}$$

Due to charge and strangeness conservation, only the neutral vector mesons ρ^0, ω and ϕ can transform into a photon. Thus, the Lagrangian above describing the $V \to \gamma$ transition contains only the fields describing these mesons and reduces to

$$\mathcal{L}_2 = -\frac{e_V m_V}{12}\left[3\left(\rho^0\right)^{\mu\nu} - \sqrt{2}\,\phi^{\mu\nu} + \omega^{\mu\nu}\right]\partial_\mu A_\nu\,. \tag{3.5}$$

Therewith, the relevant leading-order Lagrangian for the decay of a vector meson A into a pseudoscalar meson B and a photon γ equals

$$\begin{aligned}
\mathcal{L}^{(1)}_{A\to B\gamma} &= \mathcal{L}_{11} + \mathcal{L}_{12} + \mathcal{L}_2 \\
&= -\frac{h_A}{16f}\,\varepsilon^{\mu\nu\alpha\beta}\,\mathrm{tr}\left\{\left(V_{\mu\nu}\left(\partial^\tau V_{\tau\alpha}\right) + \left(\partial^\tau V_{\tau\alpha}\right)V_{\mu\nu}\right)\partial_\beta\Phi\right\} \\
&\quad -\frac{b_A}{8f}\,\varepsilon^{\mu\nu\alpha\beta}\,\mathrm{tr}\left\{V_{\mu\nu}V_{\alpha\beta}\left[\Phi,\chi_0\right]_+\right\} \\
&\quad -\frac{e_V\,m_V}{4}\,\mathrm{tr}\left\{V^{\mu\nu}\,Q\right\}\,\partial_\mu A_\nu\,.
\end{aligned} \tag{3.6}$$

Additionally, the particular next-to-leading order term given in Eq. (2.107) describes the direct decay of the vector meson A into the pseudoscalar meson B and the photon:

$$\begin{aligned}
\mathcal{L}^{(2)}_{A\to B\gamma} &= i\,\frac{e_A}{4m_V}\,\varepsilon^{\mu\nu\alpha\beta}\,\mathrm{tr}\left\{\left(f^+_{\mu\nu}\left(D^\tau V_{\tau\alpha}\right) + \left(D^\tau V_{\tau\alpha}\right)f^+_{\mu\nu}\right)U_\beta\right\} \\
&\approx -\frac{e_A}{8f\,m_V}\,\varepsilon^{\mu\nu\alpha\beta}\,\mathrm{tr}\left\{\left(Q\left(\partial^\tau V_{\tau\alpha}\right) + \left(\partial^\tau V_{\tau\alpha}\right)Q\right)\partial_\beta\Phi\right\}\,F^{\mu\nu} \\
&= -\frac{e_A}{4f\,m_V}\,\varepsilon^{\mu\nu\alpha\beta}\,\mathrm{tr}\left\{\left(Q\left(\partial^\tau V_{\tau\alpha}\right) + \left(\partial^\tau V_{\tau\alpha}\right)Q\right)\partial_\beta\Phi\right\}\,\partial_\mu A_\nu.
\end{aligned} \tag{3.7}$$

As already explained in section 2.5.2, this term can be used to estimate the intrinsic errors very roughly. This intrinsic errors are produced from the restriction to leading-order calculations. The result will be given as the leading-order calculation plus the difference between this calculation and the one including the term proportional to e_A as an error. Therefore, the general Lagrangian

$$\mathcal{L}_{A\to B\gamma} = \mathcal{L}^{(1)}_{A\to B\gamma} + \mathcal{L}^{(2)}_{A\to B\gamma} \tag{3.8}$$

is used with two parameter sets (P1), (P2) for the open parameters e_A, h_A and b_A.

3.1.2 Transition Form Factor and Partial Decay Width for the Decays of Vector Mesons

Taking the Lagrangian (3.8) and the Feynman rules given in subsection 2.6.1, the transition matrix element for a decay of a vector meson A into a pseudoscalar meson B and

either a real photon or a dilepton can be calculated. As already mentioned, the decay of a virtual photon into a dilepton is thereby described by usual QED.

The matrix element for the decay of a vector meson A into a pseudoscalar meson B and a real photon can be expressed as

$$\mathcal{M}_{A\to B\gamma} = -e\, f_{AB}(0)\, \varepsilon^{\mu\nu\alpha\beta}\, p_\mu q_\nu\, \varepsilon_\alpha(p,\lambda_A)\, \varepsilon^*_\beta(q,\lambda_\gamma) \tag{3.9}$$

and the one for the decay into a pseudoscalar meson and a dilepton l as

$$\mathcal{M}_{A\to Bl^+l^-} = e^2\, f_{AB}\left(\sqrt{q^2}\right)\, \varepsilon^{\mu\nu\alpha\beta}\, p_\mu q_\nu\, \varepsilon_\alpha(p,\lambda_A)\, \frac{1}{q^2}\, \bar{u}_s(q_1)\gamma_\beta v_{s'}(q_2). \tag{3.10}$$

Here, $f_{AB}\left(\sqrt{q^2}\right)$ is the form factor for the $A \to B$ transition, p and q are the four-momenta of the incoming particle A and the (virtual) photon, respectively, q_1 and q_2 those of lepton and anti-lepton and $\varepsilon(p,\lambda_A)$ and $\varepsilon(q,\lambda_\gamma)$ are the polarization four-vectors of the particle A and the photon. In order to shorten calculations, the definitions

$$l_\rho(q) := -\varepsilon^*_\rho(q,\lambda_\gamma) \tag{3.11}$$

for the decay into a real photon and

$$l_\rho(q = q_1 + q_2) := \frac{e}{(q_1+q_2)^2}\, \bar{u}_s(q_1)\gamma_\rho v_{s'}(q_2) \tag{3.12}$$

for the decay into a dilepton will be used. Therewith, the general matrix elements for the considered decays of a vector meson A into either a photon or a dilepton are both equal to

$$\mathcal{M}_{A\to B\gamma/Bl^+l^-} = e\, f_{AB}\left(\sqrt{q^2}\right)\, \varepsilon^{\mu\nu\alpha\beta}\, p_\mu q_\nu\, \varepsilon_\alpha(p,\lambda_A)\, l_\beta(q). \tag{3.13}$$

Note that this general matrix element has to be evaluated at $q^2 = 0$ for the decay into a real photon.
Furthermore, the transition form factor will be normalized as

$$F_{AB}\left(\sqrt{q^2}\right) := \frac{f_{AB}\left(\sqrt{q^2}\right)}{f_{AB}(0)} \tag{3.14}$$

so that $F_{AB}(0) = 1$. Additionally, $\sqrt{q^2}$ will be abbreviated with q.

For further calculations, the averaged squared matrix element $\overline{|\mathcal{M}|^2}$ will be needed. Therefore, the average over all possible incoming states and sum over all possible final states has to be taken. As all vector mesons have spin 1, one gets an additional factor $\frac{1}{3}$

after taking the average over the incoming states. The sum over all possible spin states s and s' of lepton and anti-lepton, respectively, yields

$$\begin{aligned}&\sum_{s,s'} \bar{u}_s\left(q_1\right)\, \gamma_\beta\, v_{s'}\left(q_2\right)\, \bar{v}_{s'}\left(q_2\right)\, \gamma_{\bar{\beta}}\, u_s\left(q_1\right)\\ &\quad = \sum_{s,s'} \left(\bar{u}_s\left(q_1\right)\right)_a\, \left(\gamma_\beta\right)_{ab}\, \left(v_{s'}\left(q_2\right)\right)_b\, \left(\bar{v}_{s'}\left(q_2\right)\right)_c\, \left(\gamma_{\bar{\beta}}\right)_{cd}\, \left(u_s\left(q_1\right)\right)_d .\end{aligned} \tag{3.15}$$

Using $\sum_s u_s\left(q_1\right) \bar{u}_s\left(q_1\right) = \not{q}_1 + m_l$ and $\sum_{s'} v_{s'}\left(q_2\right) \bar{v}_{s'}\left(q_2\right) = \not{q}_2 - m_l$ with the lepton mass m_l, this equals

$$\begin{aligned}\left(\not{q}_1 + m_l\right)_{da} \left(\gamma_\beta\right)_{ab} \left(\not{q}_2 - m_l\right)_{bc} \left(\gamma_{\bar{\beta}}\right)_{cd} &= \operatorname{tr}\left\{\left(\not{q}_1 + m_l\right) \gamma_\beta \left(\not{q}_2 - m_l\right) \gamma_{\bar{\beta}}\right\}\\ &= 4\left[\left(q_1\right)_\beta \left(q_2\right)_{\bar{\beta}} + \left(q_1\right)_{\bar{\beta}} \left(q_2\right)_\beta - g_{\beta\bar{\beta}} \left(q_1 \cdot q_2 + m_l^2\right)\right].\end{aligned} \tag{3.16}$$

Additionally, one uses that

$$\sum_{\lambda_A} \varepsilon_{\bar{\alpha}}\left(p, \lambda_A\right) \varepsilon_\alpha^*\left(p, \lambda_A\right) = -g_{\alpha\bar{\alpha}} + \frac{p_\alpha p_{\bar{\alpha}}}{m_A^2}, \tag{3.17}$$

$$\sum_{\lambda_\gamma} \varepsilon_{\bar{\beta}}\left(q, \lambda_\gamma\right) \varepsilon_\beta^*\left(q, \lambda_\gamma\right) = -g_{\beta\bar{\beta}} \tag{3.18}$$

with the mass m_A of the vector meson. Note that due to $\varepsilon^{\mu\nu\alpha\beta} p_\mu p_\alpha = 0$ the second term in (3.17) never contributes to the squared matrix element.

With the calculations done above the averaged transition matrix element equals

$$\overline{\left|\mathcal{M}_{A\to B\gamma}\right|^2} = \frac{2}{3} e^2 f_{AB}^2\left(q\right) \left(p \cdot q\right)^2 \tag{3.19}$$

for the decay into a real photon and

$$\begin{aligned}\overline{\left|\mathcal{M}_{A\to Bl^+l^-}\right|^2} \;=\; &\frac{1}{3} e^4 \left|f_{AB}\right|^2\left(q\right) \Bigg[q^2 + 2\left(m_{23}^2 - m_B^2 - m_A^2\right) + \Bigg(2m_l^4 + m_B^4 + m_A^4\\ &- 2m_l^2\left(m_B^2 + m_A^2\right) - 2\left(2m_l^2 + m_B^2 + m_A^2\right) m_{23}^2 + 2m_{23}^4\Bigg) \frac{1}{q^2}\\ &- 2m_l^2\left(m_A^2 - m_B^2\right)^2 \frac{1}{q^4}\Bigg]\end{aligned} \tag{3.20}$$

for the decay into a dilepton including the mass m_B of the pseudoscalar particle and the invariant mass

$$m_{23}^2 = \left(q_2 + k\right)^2 \tag{3.21}$$

of antilepton and pseudoscalar meson.

According to [A+08], the differential partial decay width for the decay $A \to B\gamma$ equals

$$\frac{\mathrm{d}\Gamma_{A\to B\gamma}}{\mathrm{d}\Omega} = \frac{1}{32\pi^2}\,\overline{|\mathcal{M}_{A\to B\gamma}|^2}\,\frac{\left|\vec{k}\right|}{m_A^2}\,. \tag{3.22}$$

Here, $\left|\vec{k}\right|$ is the momentum of the pseudoscalar meson B given as

$$\left|\vec{k}\right| = \frac{m_A^2 - m_B^2}{2m_A} \tag{3.23}$$

and $\mathrm{d}\Omega$ its solid angle in the rest frame of the decaying vector meson. Integrating over $\mathrm{d}\Omega$ yields the full partial decay width

$$\Gamma_{A\to B\gamma} = \frac{1}{8\pi\, m_A^2}\,\overline{|\mathcal{M}_{A\to B\gamma}|^2}\,\left|\vec{k}\right| = \frac{m_A^2 - m_B^2}{16\pi\, m_A^3}\,\overline{|\mathcal{M}_{A\to B\gamma}|^2} = \frac{\left(m_A^2 - m_B^2\right)^3 e^2}{96\pi m_A^3}\,\left|f_{AB}\,(0)\right|^2\,. \tag{3.24}$$

Including the definition $m_{23}^2 = (q_2 + k)^2$, the double-differential decay width for the decay $A \to Bl^+l^-$ is given as [A+08]

$$\frac{\mathrm{d}\Gamma_{A\to Bl^+l^-}}{\mathrm{d}q^2\,\mathrm{d}m_{23}^2} = \frac{1}{2\pi^3}\,\frac{1}{32m_A^3}\,\overline{|\mathcal{M}_{A\to Bl^+l^-}|^2}\,. \tag{3.25}$$

Here, q^2 runs from $4m_l^2$ to $(m_A - m_B)^2$ and

$$(m_{23})^2_{\min} = (E_2^* + E_3^*)^2 - \left(\sqrt{E_2^{*2} - m_l^2} + \sqrt{E_3^{*2} - m_B^2}\right)^2, \tag{3.26}$$

$$(m_{23})^2_{\max} = (E_2^* + E_3^*)^2 - \left(\sqrt{E_2^{*2} - m_l^2} - \sqrt{E_3^{*2} - m_B^2}\right)^2 \tag{3.27}$$

with the energies

$$E_2^* = \frac{1}{2}\sqrt{q^2}, \tag{3.28}$$

$$E_3^* = \frac{m_A^2 - m_B^2 - q^2}{2\sqrt{q^2}} \tag{3.29}$$

of antilepton and pseudoscalar meson, respectively, in the $\sqrt{q^2}$ rest frame. By integrating over $\mathrm{d}m_{23}^2$ one gets the single-differential decay width [Lan85]

$$\begin{aligned}\frac{\mathrm{d}\Gamma_{A\to Bl^+l^-}}{\mathrm{d}q^2\,\Gamma_{A\to B\gamma}} &= \frac{e^2}{12\pi^2}\sqrt{1 - \frac{4m_l^2}{q^2}}\left(1 + \frac{2m_l^2}{q^2}\right)\frac{1}{q^2}\left[\left(1 + \frac{q^2}{m_A^2 - m_B^2}\right)^2 - \frac{4m_A^2 q^2}{\left(m_A^2 - m_B^2\right)^2}\right]^{3/2}\left|F_{AB}\,(q)\right|^2 \\ &= X_{\mathrm{QED}}\cdot\left|F_{AB}\,(q)\right|^2\end{aligned} \tag{3.30}$$

with X_{QED} denoting the single-differential decay width of pure QED.

3.2 Decay $\omega \to \pi^0 l^+ l^-$

3.2.1 Form Factor for the $\omega \to \pi^0$ Transition

For the decay of an ω-meson into a neutral pion and a real or virtual photon the Lagrangian (3.8) becomes

$$\mathcal{L}_{\omega\pi} = \mathcal{L}_{\omega\pi}^{\text{dir}} + \mathcal{L}_{\omega\pi}^{\text{indir}} \tag{3.31}$$

with one term describing the direct decay into the pion and the photon,

$$\mathcal{L}_{\omega\pi}^{\text{dir}} = -\frac{e_A}{2f\, m_V}\, \varepsilon^{\mu\nu\alpha\beta}\, \left(\partial^\tau \omega_{\tau\alpha}\right)\, \partial_\beta \pi^0\, \partial_\mu A_\nu\,, \tag{3.32}$$

and the other one describing the decay via a virtual vector meson,

$$\begin{aligned}\mathcal{L}_{\omega\pi}^{\text{indir}} = &-\frac{h_A}{4f}\, \varepsilon^{\mu\nu\alpha\beta}\, \left[\rho^0_{\mu\nu}\, (\partial^\tau w_{\tau\alpha})\, \partial_\beta \pi^0 + \left(\partial^\tau \rho^0_{\tau\alpha}\right) \omega_{\mu\nu} \partial_\beta \pi^0\right] \\ &- \frac{\bar{m}_\pi^2 b_A}{f}\, \varepsilon^{\mu\nu\alpha\beta}\, \omega_{\mu\nu}\, \rho^0_{\alpha\beta}\, \pi^0 \\ &- \frac{e_V\, m_V}{4}\, \rho^0_{\mu\nu}\, \partial_\mu A_\nu\,. \end{aligned} \tag{3.33}$$

In the last part $\mathcal{L}_{\omega\pi}^{\text{indir}}$, the first two terms describe the decay of the ω-meson into the pion and a virtual ρ^0-meson and the last one the decay of the virtual ρ^0-meson into a, real or virtual, photon.

The Lagrangian yields that the ω-meson can only decay via a virtual ρ^0-meson into a neutral pion and a photon. This is in accordance with isospin conservation: As the ω-meson has isospin 0 and the neutral pion isospin 1, the virtual vector meson has to have isospin 1 so that its isospin and the isospin of the pion can again couple to isospin 0. Since the ϕ-meson has isospin 0, the only possible virtual vector meson is the ρ^0-meson which has isospin 1[1].

The transition matrix element can again be calculated as the sum over all possible kinds of decays given in the Lagrangian (3.31) by the terms proportional to e_A, h_A and b_A. Furthermore, the Feynman rules given in section 2.6.1 have to be used. Then, the matrix element consists of the following terms:

[1] Of course, the virtual vector meson has to have electromagnetic charge zero due to charge conservation.

1). Direct decay:

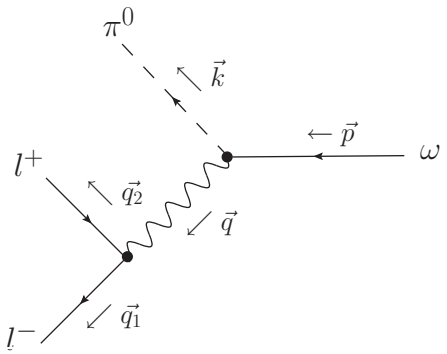

Figure 3.1: Direct decay of the ω-meson into a neutral pion and a dilepton l.

$$\begin{aligned} i\mathcal{M}^1_{\omega\pi} &= m_\omega \varepsilon_\alpha(p,\lambda_\omega) \left(-i\,\frac{e_A}{2f\,m_V}\,\varepsilon^{\mu\nu\alpha\beta}\right)(+ik_\beta)\,(+iq_\mu)\,(-l_\nu(q)) \\ &= -\,i\,\frac{e_A m_\omega}{2f m_V}\,\varepsilon^{\mu\nu\alpha\beta}\,k_\beta q_\mu\,\varepsilon_\alpha(p,\lambda_\omega)\,l_\nu(q). \end{aligned} \tag{3.34}$$

With $k = p - q$ and $\varepsilon^{\mu\nu\alpha\beta} q_\beta q_\mu = 0$ this term of the matrix element equals

$$i\mathcal{M}^1_{\omega\pi} = -\,i\,\frac{e_A\,m_\omega}{2f\,m_V}\,\varepsilon^{\mu\nu\alpha\beta}\,p_\mu q_\nu\,\varepsilon_\alpha(p,\lambda_\omega)\,l_\beta(q). \tag{3.35}$$

2). Indirect decay:

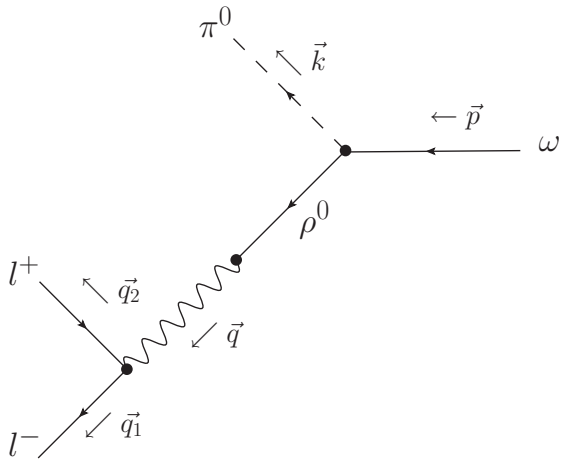

Figure 3.2: Indirect decay of the ω-meson into a neutral pion and a dilepton l via a virtual ρ^0-meson.

- Decay via $-\frac{h_A}{4f}\,\varepsilon^{\mu\nu\alpha\beta}\,\rho^0_{\mu\nu}\,(\partial^\tau w_{\tau\alpha})\,\partial_\beta\pi^0 - \frac{e_V\,m_V}{4}\,\rho^0_{\mu\nu}\,\partial_\mu A_\nu$:

$$\begin{aligned} i\mathcal{M}^2_{\omega\pi} &= m_\omega\varepsilon_\alpha(p,\lambda_\omega)\,\left(-\frac{2i}{m_\rho^2}S_\rho\left(q^2\right)\right)\,\left[\left(m_\rho^2-q^2\right)g_{\mu\rho}g_{\nu\sigma}+g_{\mu\rho}q_\nu q_\sigma-g_{\mu\sigma}q_\nu q_\rho\right] \\ &\quad\cdot\left(-i\,\frac{h_A}{4f}\,\varepsilon^{\mu\nu\alpha\beta}\right)\,(+ik_\beta)\,(+iq_\rho)\,\left(-i\frac{e_V m_V}{4}\right)(-l_\sigma(q)) \\ &= +\,i\,\frac{h_A e_V m_V m_\omega}{8fm_\rho^2}\,S_\rho\left(q^2\right)\,\varepsilon^{\mu\nu\alpha\beta}\,k_\beta\,\varepsilon_\alpha(p,\lambda_\omega) \\ &\quad\cdot\left[\left(m_\rho^2-q^2\right)q_\mu g_{\nu\sigma}+q_\mu q_\nu q_\sigma-q^2q_\nu g_{\mu\sigma}\right]\,l_\sigma(q). \end{aligned} \tag{3.36}$$

With $\varepsilon^{\mu\nu\alpha\beta}q_\mu q_\nu = 0$ and $-\varepsilon^{\mu\nu\alpha\beta}q^2q_\mu g_{\nu\sigma} = +\varepsilon^{\mu\nu\alpha\beta}q^2q_\nu g_{\mu\sigma}$ this is equal to

$$\begin{aligned} i\mathcal{M}^2_{\omega\pi} &= +\,i\,\frac{h_A e_V m_V m_\omega}{8f}\,S_\rho\left(q^2\right)\,\varepsilon^{\mu\nu\alpha\beta}\,k_\beta q_\mu\,\varepsilon_\alpha(p,\lambda_\omega)\,l_\nu(q) \\ &= +\,i\,\frac{h_A e_V m_V m_\omega}{8f}\,S_\rho\left(q^2\right)\,\varepsilon^{\mu\nu\alpha\beta}\,p_\mu q_\nu\,\varepsilon_\alpha(p,\lambda_\omega)\,l_\beta(q). \end{aligned} \tag{3.37}$$

- Decay via $-\frac{h_A}{4f}\,\varepsilon^{\mu\nu\alpha\beta}\,(\partial^\tau\rho^0_{\tau\alpha})\,\omega_{\mu\nu}\partial_\beta\pi^0 - \frac{e_V\,m_V}{4}\,\rho^0_{\mu\nu}\,\partial_\mu A_\nu$:

$$\begin{aligned} i\mathcal{M}^3_{\omega\pi} &= \varepsilon_{\mu\nu}(p,\lambda_\omega)\,\left(-S_\rho\left(q^2\right)\right)\,[-q_\rho g_{\alpha\sigma}+q_\sigma g_{\alpha\rho}]\,\left(-i\frac{h_A}{4f}\,\varepsilon^{\mu\nu\alpha\beta}\right)(+ik_\beta)\,(+iq_\rho) \\ &\quad\cdot\left(-i\,\frac{e_V m_V}{4}\right)(-l_\sigma(q)) \\ &= +\frac{h_A e_V m_V}{16f}\,S_\rho\left(q^2\right)\varepsilon^{\mu\nu\alpha\beta}\,\frac{i}{m_\omega}\,[p_\mu\varepsilon_\nu(p,\lambda_\omega)-p_\nu\varepsilon_\mu(p,\lambda_\omega)]\,k_\beta\left[-q^2g_{\alpha\sigma}+q_\alpha q_\sigma\right]l_\sigma(q) \\ &= +i\,\frac{h_A e_V m_V}{8fm_\omega}\,S_\rho\left(q^2\right)\varepsilon^{\mu\nu\alpha\beta}\,p_\mu k_\beta\,\varepsilon_\nu(p,\lambda_\omega)\,\left[-q^2g_{\alpha\sigma}+q_\alpha q_\sigma\right]\,l_\sigma(q). \end{aligned} \tag{3.38}$$

Using $\varepsilon^{\mu\nu\alpha\beta}p_\mu k_\beta q_\alpha = 0$ and $\varepsilon^{\mu\nu\alpha\beta}\,p_\mu k_\beta\,\varepsilon_\nu(p,\lambda_\omega)\,l_\alpha(q) = \varepsilon^{\mu\nu\alpha\beta}p_\mu q_\beta\,\varepsilon_\alpha(p,\lambda_\omega)\,l_\beta(q)$, one gets

$$i\mathcal{M}^3_{\omega\pi} = +\,i\,\frac{h_A\,e_V\,m_V}{8f\,m_\omega}\,S_\rho\left(q^2\right)\,q^2\,\varepsilon^{\mu\nu\alpha\beta}\,p_\mu q_\nu\,\varepsilon_\alpha(p,\lambda_\omega)\,l_\beta(q). \tag{3.39}$$

- Decay via $-\frac{\bar{m}_\pi^2 b_A}{f}\,\varepsilon^{\mu\nu\alpha\beta}\,\omega_{\mu\nu}\,\rho^0_{\alpha\beta}\,\pi^0 - \frac{e_V\,m_V}{4}\,\rho^0_{\mu\nu}\,\partial_\mu A_\nu$:

$$\begin{aligned} i\mathcal{M}^4_{\omega\pi} =& \varepsilon_{\mu\nu}(p,\lambda_\omega)\,\left(-i\,\frac{\bar{m}_\pi^2\,b_A}{f}\,\varepsilon^{\mu\nu\alpha\beta}\right)\left(-\frac{2i}{m_\rho^2}\,S_\rho\left(q^2\right)\right)\left[\left(m_\rho^2-q^2\right)g_{\alpha\rho}g_{\beta\sigma}+g_{\alpha\rho}q_\beta q_\rho\right. \\ &\left.-\,g_{\alpha\sigma}q_\beta q_\rho\right]\cdot 1\cdot(+iq_\rho)\,\left(-i\,\frac{e_V m_V}{4}\right)(-l_\sigma(q)) \\ =& -\,i\,\frac{b_A\bar{m}_\pi^2 e_V m_V}{fm_\omega}\,S_\rho\left(q^2\right)\,\varepsilon^{\mu\nu\alpha\beta}\,p_\mu q_\nu\,\varepsilon_\alpha(p,\lambda_\omega)\,l_\beta(q). \end{aligned} \tag{3.40}$$

Thus, the transition matrix element equals

$$\begin{aligned}\mathcal{M}_{\omega\to\pi^0\gamma/\pi^0 l^+ l^-} &= \mathcal{M}^1_{\omega\pi} + \mathcal{M}^2_{\omega\pi} + \mathcal{M}^3_{\omega\pi} + \mathcal{M}^4_{\omega\pi} \\ &= e\, f_{\omega\pi}(q)\, \varepsilon^{\mu\nu\alpha\beta}\, p_\mu q_\nu\, \varepsilon_\alpha(p,\lambda_\omega)\, l_\beta(q)\end{aligned} \tag{3.41}$$

with the transition form factor

$$f_{\omega\pi}(q) = \frac{m_\omega}{2 f m_V e}\left[-e_A + \frac{1}{4} h_A e_V m_V^2\, S_\rho\left(q^2\right)\left(1 + \frac{q^2}{m_\omega^2}\right) - 2 b_A e_V m_V^2\, \frac{\bar{m}_\pi^2}{m_\omega^2}\, S_\rho\left(q^2\right)\right]. \tag{3.42}$$

Recall that for the decay into a real photon q^2 has to be zero. For that case, $S_\rho(0) = -\frac{1}{m_\rho^2}$ and the matrix element equals

$$\mathcal{M}_{\omega\to\pi^0\gamma} = \frac{m_\omega}{2 f m_V}\left[e_A + \frac{1}{4} h_A e_V\, \frac{m_V^2}{m_\rho^2} - 2 b_A e_V\, \frac{m_V^2}{m_\rho^2}\, \frac{\bar{m}_\pi^2}{m_\omega^2}\right] \varepsilon^{\mu\nu\alpha\beta}\, p_\mu q_\nu\, \varepsilon_\alpha(p,\lambda_\omega)\, \varepsilon^*_\beta(q,\lambda_\gamma). \tag{3.43}$$

Since the only possible virtual vector meson is a ρ^0-meson, the standard VMD form factor (2.88) simplifies to

$$F_{\mathrm{VMD}}(q) = \frac{m^2_{\mathrm{virtual}}}{m^2_{\mathrm{virtual}} - q^2} \tag{3.44}$$

with $m_{\mathrm{virtual}} = m_\rho$. Though the b_A term is of VMD type, the whole form factor (3.42) is not of VMD type. The e_A term is constant in q and the h_A term is of mixed type. Neglecting the energy-dependent width yields $S_\rho\left(q^2\right) \approx \left(q^2 - m_\rho^2\right)^{-1}$ and the normalised form factor $F_{\omega\pi}(q)$ consists of the first two terms of the general form factor (1.2) (compare subsection 2.4.2)

$$F_{\omega\pi}(q) \approx g_0\, \frac{m_\rho^2}{m_\rho^2 - q^2} + (1 - g_0) = \frac{b\left(1 + \frac{m_\rho^2}{m_\omega^2}\right) + c}{a + b + c}\, \frac{m_\rho^2}{m_\rho^2 - q^2} + \frac{a - b\frac{m_\rho^2}{m_\omega^2}}{a + b + c} \tag{3.45}$$

with the coefficients[2]

$$a = -e_A,\; b = -\frac{1}{4} h_A e_V,\; c = 2 b_A e_V\, \frac{\bar{m}_\pi^2}{m_\omega^2}. \tag{3.46}$$

Thereby, $g_0 = 2.00 \pm 0.23$.
To estimate the qualitative difference between the standard VMD form factor and form factor (3.42) roughly, the terms of minor importance, those proportional to e_A and b_A, and therewith the coefficients a and c are set to zero. If additionally the difference

[2]Here, the relation $m_V = 776\,\mathrm{MeV} = m_\rho$ was used.

between the mass of the ω- and the ρ-meson is neglected, the normalised form factor (3.45) will be approximately equal to

$$F_{\omega\pi}(q) \approx 2\,\frac{m_\rho^2}{m_\rho^2 - q^2} - 1 = \frac{m_\rho^2 + q^2}{m_\rho^2 - q^2}\,. \tag{3.47}$$

This predicts a q dependent shift of the standard VMD form factor. In particular, the slope at $q^2 = 0$ (cf. (2.90)),

$$\frac{\mathrm{d}F_{\omega\pi}}{\mathrm{d}q^2}\,|_{q^2=0} \approx \frac{2}{m_\rho^2}, \tag{3.48}$$

is much larger than the slope of standard VMD,

$$\frac{\mathrm{d}F_{\mathrm{VMD}}}{\mathrm{d}q^2}\,|_{q^2=0} = \frac{1}{m_\rho^2}. \tag{3.49}$$

In Fig. 3.3, our calculations (done without the energy-dependent width) are compared to both the standard VMD form factor (3.44) and the experimental dimuon data taken by the NA60 collaboration [A$^+$09]. The calculations with parameter set (P1) and (P2) (solid and dotted line, respectively) do not differ much from each other which supports the leading-order calculation to be quite accurate. Both calculations fit the experimental data very well while the standard VMD form factor (dot-dashed line) fails to describe the data. The only data points which cannot be well described with our calculations are the last two which are close to the upper kinematic boundary, $\sqrt{q^2} < m_\omega - m_\pi$.

3.2.2 Single-Differential and Full Partial Decay Widths for the Decays into Dimuon and Dielectron

According to Eq. (3.42), the form factor for the $\omega \to \pi^0$ transition contains the ρ^0-meson propagator which includes the energy-dependent width according to (2.122). Analogical, the transition form factors for the decays considered hereafter will include energy-dependent widths of vector mesons. However, the partial decays widths with and without these width for the decays of vector mesons considered in this thesis differ by less than 1%. This would be a better accuracy than the leading-order calculation and the determination of the parameters (P1), (P2) provide. Therefore, energy-dependent widths are neglected in the calculations for decaying vector mesons. In these cases the vector-meson propagator equals

$$S_V\left(q^2\right) = \frac{1}{q^2 - m(V)^2}. \tag{3.50}$$

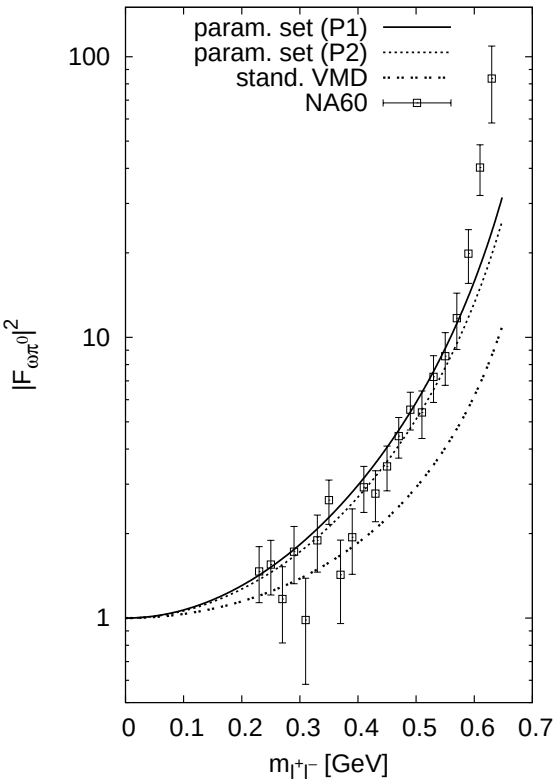

Figure 3.3: Form factor of the decay $\omega \to \pi^0 l^+ l^-$ compared to dimuon data taken by the NA60 collaboration [A+09]. The solid line describes the form factor calculated with parameter set (P1) and the dotted line the one calculated with parameter set (P2). The dot-dashed line is calculated with the VMD model (3.44) using the mass of the ρ-meson, $m_{\text{virtual}} = m_\rho$.

The same holds for radiative two- and three-body decays of neutral pions and η-mesons. Due to the relatively high mass of the η'-meson, $m_{\eta'} = 958\,\text{GeV}$, and the zero mass of the photon, the allowed phase space for decays of η'-mesons (see sections 4.6 and 5.5) contains singularities of the simplified vector-meson propagator (3.50). Thus, the energy-dependent widths have to be taken into account. Additionally, the decays of neutral pions and η-mesons into two dileptons are calculated with energy-dependent widths (see sections 5.3 and 5.4).

In Fig. 3.4, the single-differential decay width defined in Eq. (3.30) for the decay $\omega \to \pi^0 \mu^+ \mu^-$ is plotted. Again, the calculations with our approach (solid and dotted) are compared to those with the VMD model (dot-dashed) and the experimental data taken by the NA60 collaboration. Hereby, for the VMD model and to translate the NA60 form-factor data into single-differential decay widths data the experimental value $\Gamma^{\text{exp}}_{\omega\to\pi^0\gamma}$ given in [A+08] is inserted in Eq. (3.30). The two data points close to the

upper kinematic boundary, which could not be described by the form factor given in (3.42), are of less importance in the single-differential decay width. Thus, they will not contribute much to the full partial decay width which is determined by integrating the single-differential decay width. Therefore, the value for the full partial decay width

$$\Gamma_{\omega\to\pi^0\mu^+\mu^-} = (9.85 \pm 0.58) \cdot 10^{-7}\,\text{GeV} \tag{3.51}$$

calculated with the form factor (3.42) and the parameter sets (P1) and (P2) by integrating (3.30) over the interval $\left[4m_\mu^2\,,\,(m_\omega - m_{\pi^0})^2\right]$ agrees very well with the experimental partial decay widths given in [A+08],

$$\Gamma^{\text{exp}}_{\omega\to\pi^0\mu^+\mu^-} = (8.15 \pm 2.13) \cdot 10^{-7}\,\text{GeV}.$$

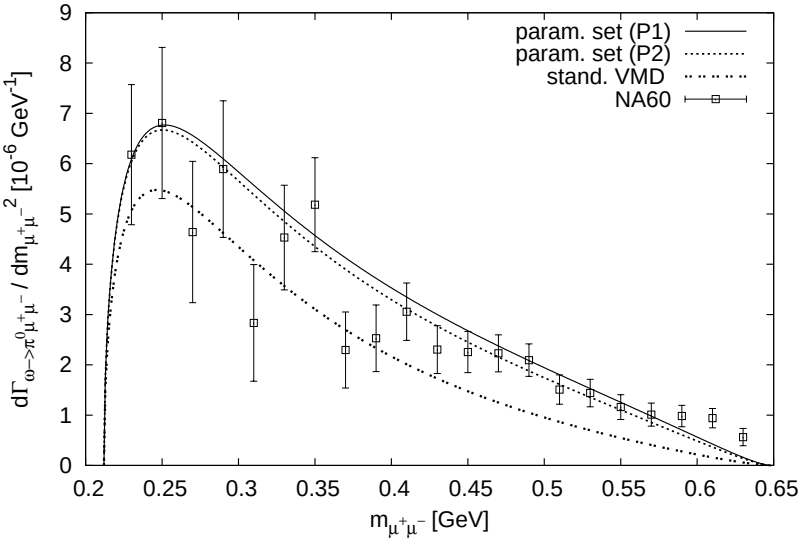

Figure 3.4: Single-differential decay width of the decay $\omega \to \pi^0\mu^+\mu^-$ compared to the experimental data calculated with Eq. (3.30) and the form factor data taken at the NA60 experiment [A+09]. The solid/dashed line is calculated with the parameter set (P1)/(P2), the dot-dashed one with the VMD model.

The single-differential decay width of the decay $\omega \to \pi^0 e^+ e^-$ is plotted in Fig. 3.5. As one can see, it is largely dominated by the low-energy region. Comparing with Fig. 3.3 which shows the normalised form factor yields that in this region the deviation from QED is irrelevant, i.e. the normalised form factor is approximately one. Therefore, it is interesting for experiments to compare the results of the decay of the ω-meson into a neutral pion and a dielectron to those of the decay into a dimuon. The relevant part of the single-differential decay width of the decay into a dielectron, the part above $m_{e^+e^-} = 2m_\mu$, is plotted in Fig. 3.6. In this plot, the obvious differences between the approach used in this thesis and the VMD model are well visible.

Again, the result for the partial decay width

$$\Gamma_{\omega\to\pi^0 e^+e^-} = (6.93 \pm 0.09) \cdot 10^{-6}\,\text{GeV} \tag{3.52}$$

agrees very well with the experimental value [A+08]

$$\Gamma^{\text{exp}}_{\omega\to\pi^0 e^+e^-} = (6.54 \pm 0.54) \cdot 10^{-6}\,\text{GeV}.$$

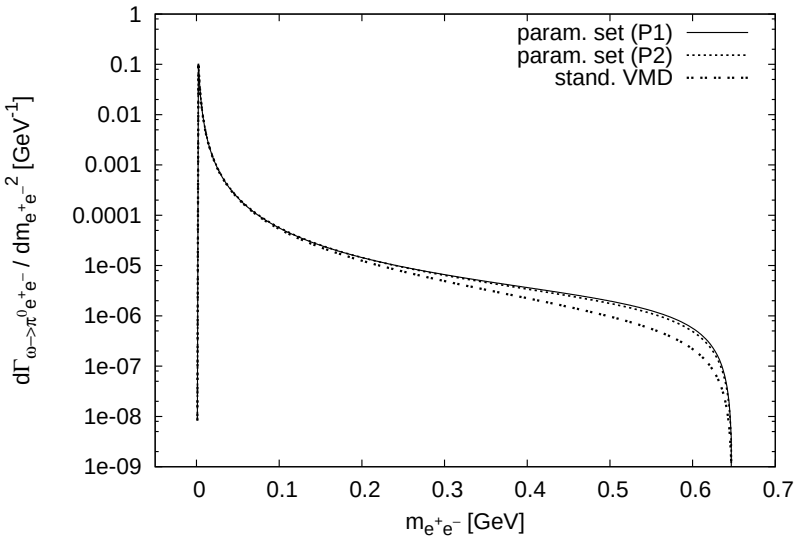

Figure 3.5: Single-differential decay width of the decay $\omega \to \pi^0 e^+ e^-$ calculated with parameter set (P1) and (P2) (solid and dashed, respectively) and the VMD model (dot-dashed).

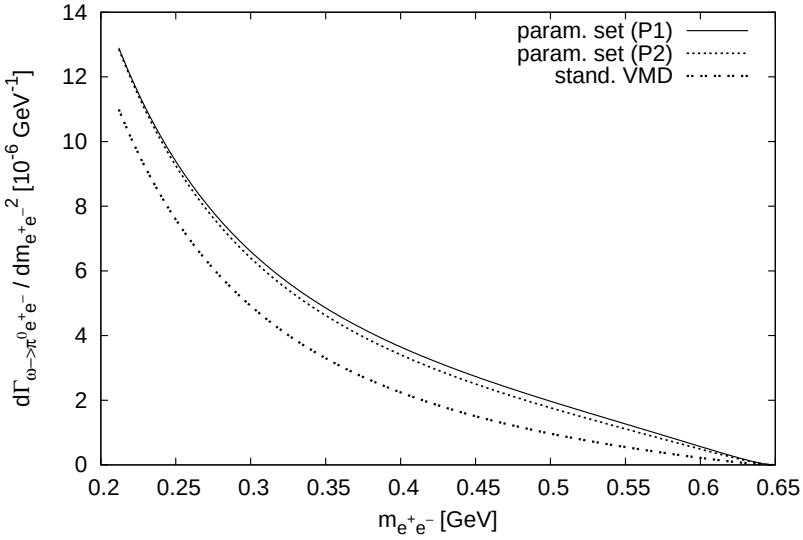

Figure 3.6: The same as in Fig. 3.5 for $m_{e^+e^-} \geq 2m_\mu$.

3.3 Decay $\omega \to \eta l^+ l^-$

3.3.1 Form Factor for the $\omega \to \eta$ Transition

Evaluating the Lagrangian 3.8 yields that the ω-meson can either decay directly into an η-meson and a, real or virtual, photon or via a virtual ω-meson. The relevant Lagrangian equals $\mathcal{L}_{\omega\eta} = \mathcal{L}_{\omega\eta}^{\text{dir}} + \mathcal{L}_{\omega\eta}^{\text{indir}}$ with the direct decay being described by

$$\mathcal{L}_{\omega\eta}^{\text{direct}} = -\frac{e_A}{6\sqrt{3}fm_V}\,\varepsilon^{\mu\nu\alpha\beta}\,(\partial^\tau\omega_{\tau\alpha})\,\partial_\beta\eta\,\partial_\mu A_\nu \tag{3.53}$$

and the indirect decay by

$$\begin{aligned}\mathcal{L}_{\omega\eta}^{\text{indir}} = &-\frac{h_A}{4\sqrt{3}f}\,\varepsilon^{\mu\nu\alpha\beta}\,\omega_{\mu\nu}\,(\partial^\tau\omega_{\tau\alpha})\,\partial_\beta\eta \\ &-\frac{b_A\bar{m}_\pi^2}{2\sqrt{3}f}\,\varepsilon^{\mu\nu\alpha\beta}\,\omega_{\mu\nu}\,\omega_{\alpha\beta}\,\eta \\ &-\frac{e_V m_V}{12}\,\omega^{\mu\nu}\,\partial_\mu A_\nu\,.\end{aligned} \tag{3.54}$$

According to isospin conservation, the ω-meson could either decay indirectly via an intermediate ω- or an intermediate ϕ-meson into an η-meson and a photon. The decay via a ϕ-meson is suppressed by the Okubo-Zweig-Iizuka (OZI) rule [Oku63, Zwe64, Iiz66] which claims that processes with disconnected quark lines are suppressed. The quark structures of the involved mesons are equal to

$$\omega_\mu \sim \bar{u}\gamma_\mu u + \bar{d}\gamma_\mu d,\ \phi_\mu \sim \bar{s}\gamma_\mu s,\ \eta \sim \bar{u}\gamma_5 u + \bar{d}\gamma_5 d - 2\bar{s}\gamma_5 s \tag{3.55}$$

with the fields u, d and s for the light quarks up, down and strange, respectively. As the ω-meson has no strange-quark part, the decay into an η- and a ϕ-meson yields a diagram with disconnected quark lines and, thus, this decay is suppressed (see Fig. 3.7). The Lagrangian (2.103) is constructed such that it respects the OZI rule.

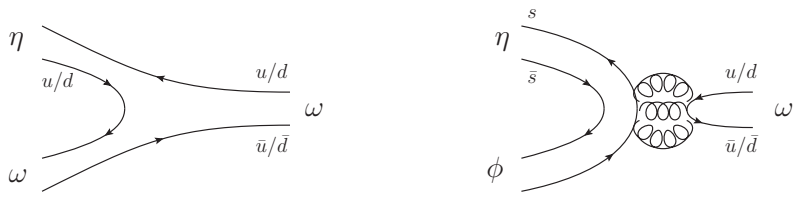

Figure 3.7: Decay of an ω-meson into an η-meson and an ω-meson on the left-hand side and into a ϕ-meson on the right-hand side. As the decay into a ϕ-meson contains disconnected quark lines, it is suppressed according to the OZI rule.

Analogical to the calculations performed in subsection 3.2.1, the form factor for the $\omega \to \eta$ transition can be calculated from the Lagrangian $\mathcal{L}_{\omega\eta}$ by using the Feynman rules given in section 2.6.1. Therewith, the following form factor for the $\omega \to \eta$ transition is calculated:

$$f_{\omega\eta}(q) = \frac{m_\omega}{6\sqrt{3} f m_V e} \left[-e_A + \frac{1}{4} e_V \, h_A \, m_V^2 \left(1 + \frac{q^2}{m_\omega^2}\right) S_\omega\left(q^2\right) - 2 b_A \, e_V \, m_V^2 \, \frac{\bar{m}_\pi^2}{m_\omega^2} \, S_\omega\left(q^2\right) \right]. \tag{3.56}$$

The normalised form factor $F_{\omega\eta}(q) = f_{\omega\eta}(q)/f_{\omega\eta}(0)$ is plotted in Fig. 3.8. As for the form factor for the $\omega \to \pi^0$ transition, the calculations with the two different parameter sets (P1) and (P2) do not differ much from each other. Both disagree with the standard VMD calculation (3.44) for $m_{\text{virtual}} = m_\omega$.

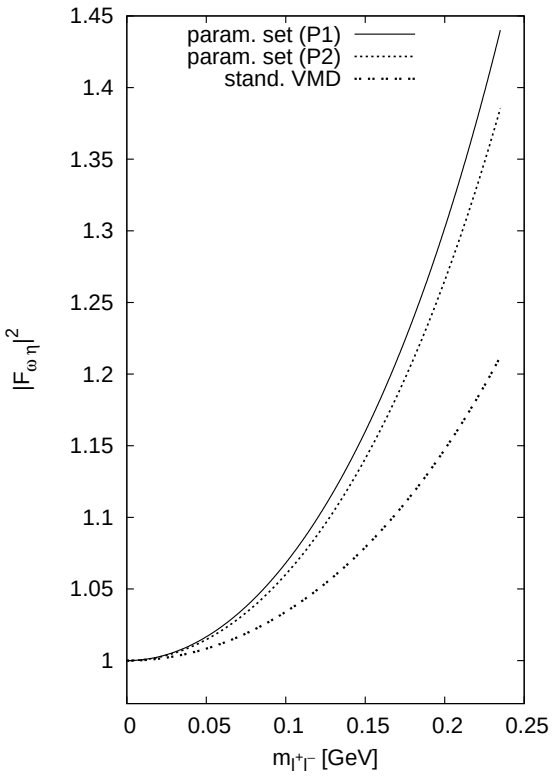

Figure 3.8: Form factor of the decay $\omega \to \eta \, l^+ l^-$ calculated with both parameter sets (P1) and (P2) (solid and dashed line) and with the VMD model (dot-dashed line).

3.3.2 Single-Differential and Full Partial Decay Widths for the Decays into Dimuon and Dielectron

The single-differential decay widths of the decays of the ω-meson into an η-meson and either a dimuon or a dielectron are plotted in Fig. 3.9 and Fig. 3.10, respectively. For both cases, the calculations with the two parameter sets agree very well and are practically indistinguishable in both figures. The calculation with the VMD model is in disagreement with those calculations for the decay into a dimoun and nearly on top of them in the figure describing the decay into a dielectron. To be able to compare the results for the decay into a dimuon and a dielectron, the single-differential decay width of the decay into a dielectron for $m_{e^+e^-}$ above $2m_\mu$ is given in Fig. 3.11.

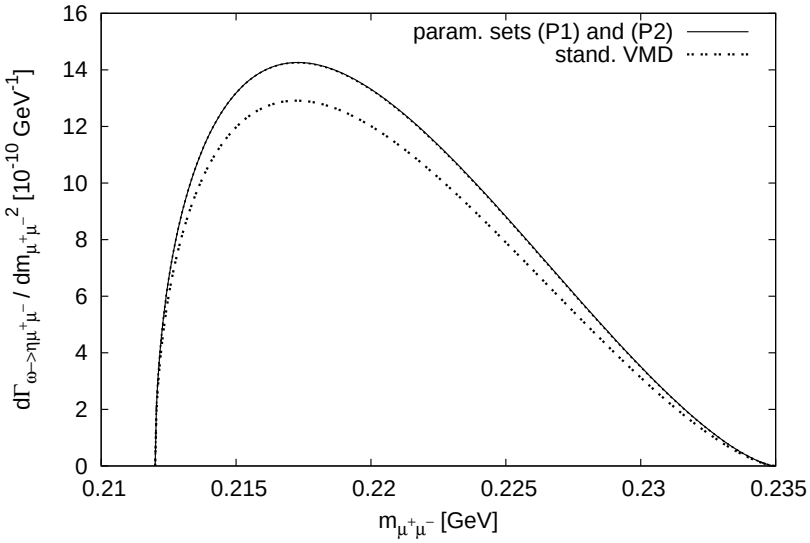

Figure 3.9: Single-differential decay width of the decay $\omega \to \eta\mu^+\mu^-$. As they are practically indistinguishable, the solid line describes the calculations with both parameter sets (P1) and (P2). The dot-dashed line is calculated with the standard VMD model.

The partial decay widths

$$\Gamma_{\omega\to\eta\mu^+\mu^-} = (8.51 \pm 0.01) \cdot 10^{-12}\,\text{GeV}, \tag{3.57}$$
$$\Gamma_{\omega\to\eta e^+e^-} = (2.72 \pm 0.09) \cdot 10^{-8}\,\text{GeV} \tag{3.58}$$

one gets with the Lagrangian $\mathcal{L}_{\omega\eta}$ can only be seen as predictions because there are no experimental data available. Furthermore, the branching ratios of these processes are very small

$$\text{BR}_{\omega\to\eta\mu^+\mu^-} = (1.00 \pm 0.00) \cdot 10^{-9}, \tag{3.59}$$
$$\text{BR}_{\omega\to\eta e^+e^-} = (3.20 \pm 0.10) \cdot 10^{-6}. \tag{3.60}$$

Therefore, it seems quite difficult to measure these processes and thus to judge whether

the approach used in this thesis or the standard VMD model describes the $\omega \to \eta$ transition better. It will be shown in section 4.4 that the normalised form factor for the $\eta' \to \omega$ transition is equal to the one for the $\omega \to \eta$ transition. Since it is possible for the KLOE-2 collaboration to measure the decay $\eta' \to \omega l^+ l^-$ [Kup10], there will be another opportunity to check the results of this section.

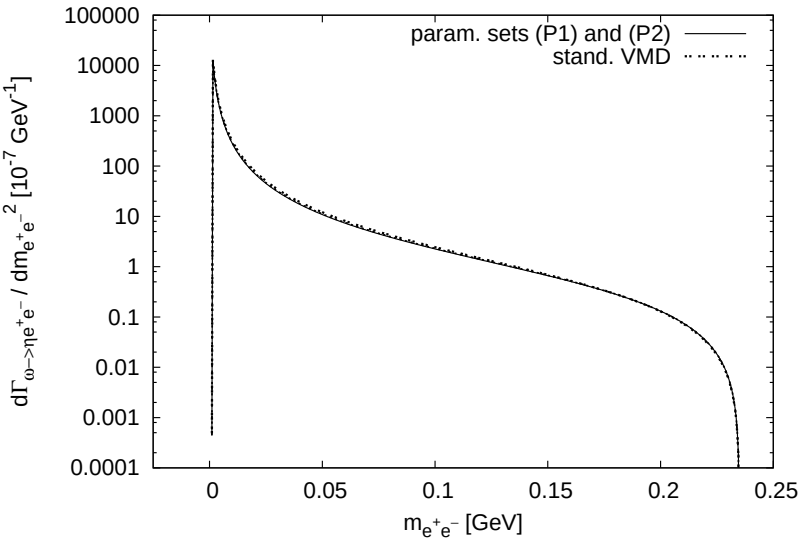

Figure 3.10: Same as Fig. 3.9 but for electrons instead of muons. In this case, the dot-dashed line calculated with the VMD model is on top of the solid line which was calculated with the parameter sets (P1) and (P2).

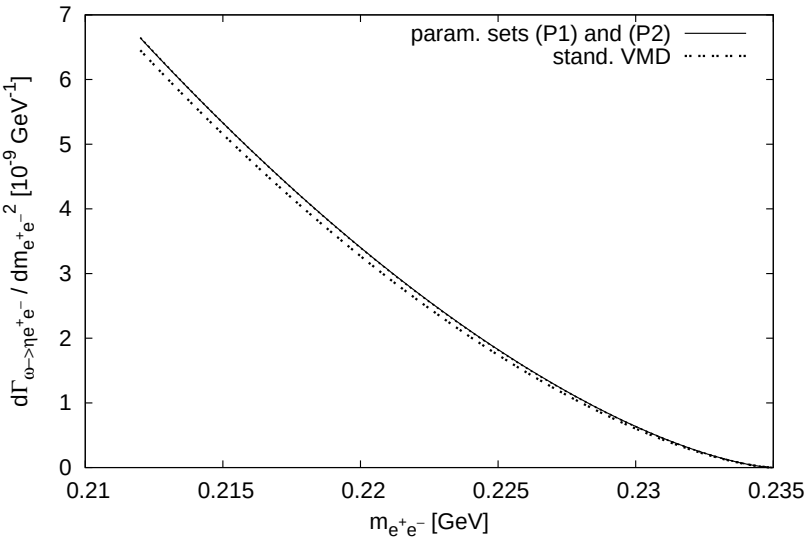

Figure 3.11: Same as Fig. 3.10 but for $m_{e^+e^-} \geq 2m_\mu$ only. Here, the difference between the calculation with both parameter sets (P1) and (P2) (solid line) and the one with the standard VMD calculation (dot-dashed line) are small, but can be observed.

3.4 Decay $\phi \to \eta l^+ l^-$

3.4.1 Form Factor for the $\phi \to \eta$ Transition

For the decay of a ϕ-meson into an η-meson and a, real or virtual, photon the Lagrangian (3.8) becomes $\mathcal{L}_{\phi\eta} = \mathcal{L}_{\phi\eta}^{\text{dir}} + \mathcal{L}_{\phi\eta}^{\text{indir}}$ with

$$\mathcal{L}_{\phi\eta}^{\text{dir}} = -\frac{\sqrt{2}\, e_A}{3\sqrt{3}\, f\, m_V}\, \varepsilon^{\mu\nu\alpha\beta}\, \partial^\tau \phi_{\tau\alpha}\, \partial_\beta \eta\, \partial_\mu A_\nu \tag{3.61}$$

describing the direct decay and

$$\begin{aligned}\mathcal{L}_{\phi\eta}^{\text{indir}} = &\frac{h_A}{2\sqrt{3}\, f}\, \varepsilon^{\mu\nu\alpha\beta}\, \phi_{\mu\nu}\, \left(\partial^\tau \phi_{\tau\alpha}\right)\, \partial_\beta \eta \\ &+ \frac{b_A\, \left(2\bar{m}_K^2 - \bar{m}_\pi^2\right)}{\sqrt{3}\, f}\, \varepsilon^{\mu\nu\alpha\beta}\, \phi_{\mu\nu}\, \phi_{\alpha\beta}\, \eta \\ &+ \frac{\sqrt{2}\, e_V\, m_V}{12}\, \phi^{\mu\nu}\, \partial_\mu A_\nu\end{aligned} \tag{3.62}$$

describing the indirect decay via a virtual vector meson. In agreement with isospin conservation which allows for a decay via a virtual ω- or ϕ-meson and the suppression of the decay via an ω-meson due to the OZI rule (compare sections 3.2.1, 3.3.1), this Lagrangian allows only for a decay via an intermediate ϕ-meson.

The form factor for the $\phi \to \eta$ transition can be determined as

$$\begin{aligned}f_{\phi\eta}(q) = \frac{2m_\phi}{3\sqrt{6} f m_V e}\Bigg[&-e_A + \frac{1}{4} e_V h_A m_V^2 \left(1 + \frac{q^2}{m_\phi^2}\right) S_\phi\left(q^2\right) \\ &-2 b_A e_V m_V^2\, \frac{2\bar{m}_K^2 - \bar{m}_\pi^2}{m_\phi^2}\, S_\phi\left(q^2\right)\Bigg].\end{aligned} \tag{3.63}$$

In Fig. 3.12, the normalised form factor $F_{\phi\eta}(q) = f_{\phi\eta}(q)/f_{\phi\eta}(0)$ and the standard VMD form factor (3.44) for $m_{\text{virtual}} = m_\phi$ are plotted. They are compared to the data taken at the SND detector at the VEPP-2M collider for the decay into a dielectron [A+01]. Although the calculations done with the parameter sets (P1) and (P2) (solid and dashed line, respectively) and the calculation with the standard VMD model (dot-dashed line) differ from each other, all three fit the data due to their relatively large error bars. So, it is not possible to judge which ansatz is better for the $\phi \to \eta$ transition. It is our hope that we will get better data form the KLOE-2 collaboration where the decay $\phi \to \eta e^+ e^-$ can also be measured [Gio10].

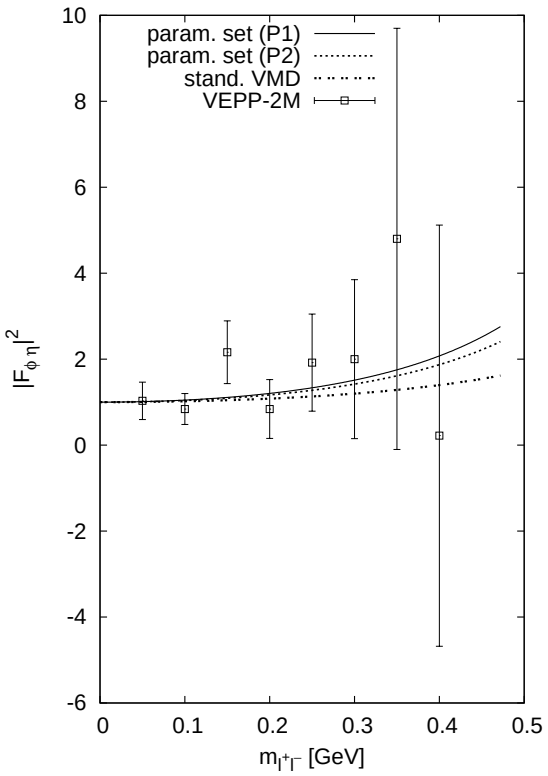

Figure 3.12: Form factor of the decay $\phi \to \eta l^+ l^-$ compared to dielectron data taken at the VEPP-2M collider [A+01]. The solid line describes the form factor calculated with parameter set (P1) and the dotted line the one calculated with parameter set (P2). The dot-dashed line is calculated with the standard VMD model.

3.4.2 Single-Differential and Full Partial Decay Widths for the Decays into Dimuon and Dielectron

The single-differential decay widths of the decays into a dimuon and a dielectron are shown in Fig. 3.13 and Fig. 3.14, respectively. For a better comparability, the single-differential decay width of the decay into a dielectron for an invariant mass $m_{e^+e^-}$ above $2m_\mu$ is plotted in Fig. 3.15. In the case of a decay into a dielectron, all three lines, calculated with parameter set (P1) (solid), parameter set (P2) (dashed) and the VMD model (dot-dashed), agree well, whereas they differ from each other for the decay into a dimuon. The disagreement between the calculations for the decay into a dimuon with both parameter sets (P1) and (P2) is greater than it was for the transition form factor. This is caused by the differences between the partial decay widths of the decay $\phi \to \eta\gamma$ calculated with the different parameter sets (see table 2.2) which has to be inserted in formula (3.30) for the single-differential decay width. Bear in mind that the ϕ-meson is

the heaviest light vector meson and parameter set (P2) was introduced to have a rough estimate for the error of the leading-order calculations performed with parameter set (P1). Consequently, it was expected that the differences between the calculations with the two parameter sets are largest for the decay of the ϕ-meson.

This larger difference is also observable at the full partial decay widths for the decay into a dielectron where the calculated value

$$\Gamma_{\phi\to\eta e^+e^-} = (4.64 \pm 0.26) \cdot 10^{-7}\,\text{GeV} \tag{3.64}$$

has the greatest deviation from the experimental value given in [A+08]

$$\Gamma^{\text{exp}}_{\phi\to\eta e^+e^-} = (4.90 \pm 0.47) \cdot 10^{-7}\,\text{GeV} \tag{3.65}$$

among all partial decay widths for the decays of vector mesons considered in this thesis. Nevertheless, it is still in agreement with the experimental value within the error bars.

For the decay into a dimuon no experimental data are available, so the calculated width

$$\Gamma_{\phi\to\eta\mu^+\mu^-} = (2.75 \pm 0.29) \cdot 10^{-8}\,\text{GeV} \tag{3.66}$$

has to be seen as a prediction.

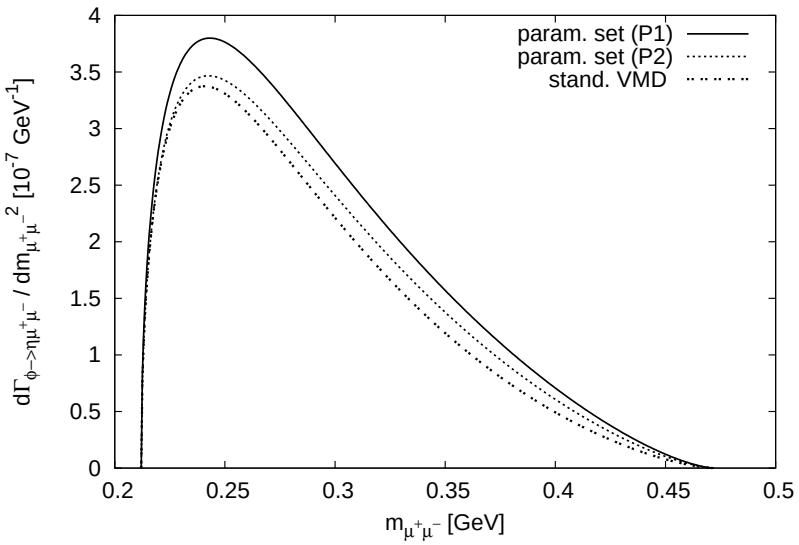

Figure 3.13: Single-differential decay width for the decay $\phi \to \eta\mu^+\mu^-$. The solid and dashed lines are calculated with the parameter set (P1) and (P2), respectively, the dot-dashed one with the VMD model.

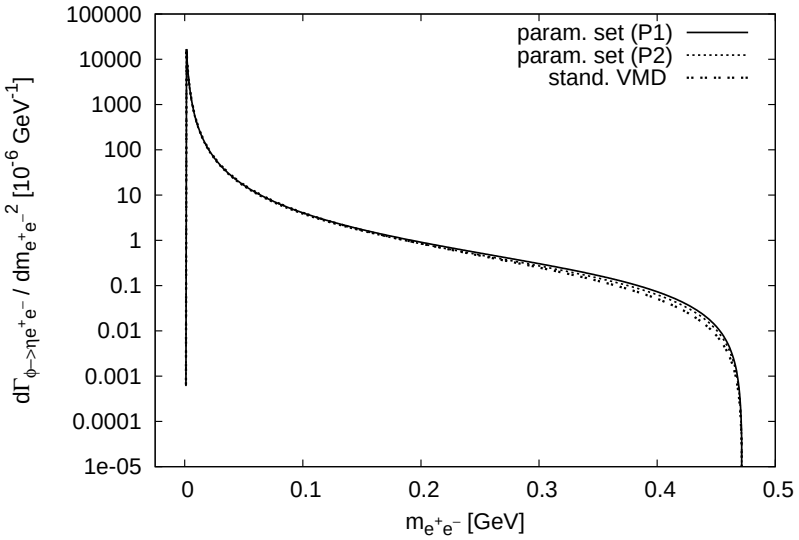

Figure 3.14: Same as in Fig. 3.13 but for electrons instead of muons.

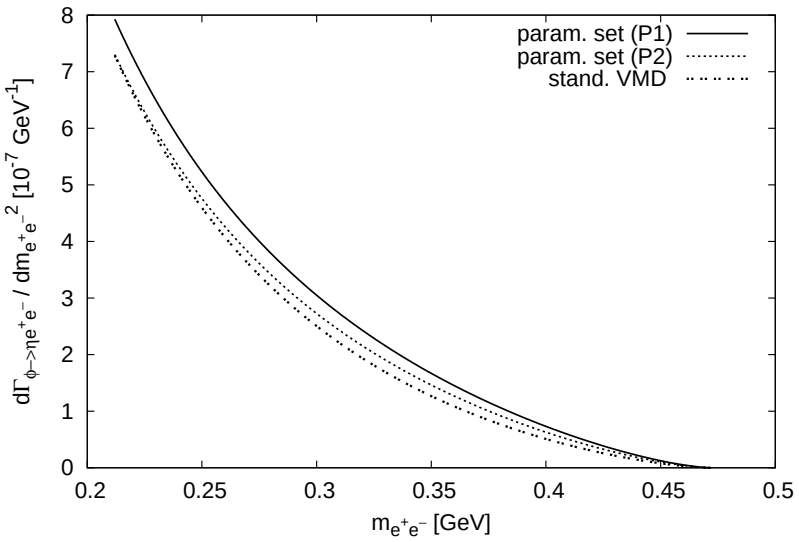

Figure 3.15: Same as in Fig. 3.14 for $m_{e^+e^-} \geq 2m_\mu$.

4 Radiative Two- and Three-Body Decays of Pseudoscalar Mesons

In this chapter, electromagnetic transitions of pseudoscalar mesons A into real photons or vector mesons B are considered, i.e. the processes $A \to \gamma\gamma^{(\star)}$ and $A \to B\gamma^{(\star)}$ with real or virtual photons $\gamma^{(\star)}$.
In section 4.1, the relevant leading-order Lagrangian and the formulas for the partial decay width are derived. Thereby, the leading-order WZW Lagrangian (cf. subsection 2.3.2) describing the direct decay of a pseudoscalar meson into two, real or virtual, photons is also considered. The $\pi^0 \to \gamma$ transition is discussed in the subsequent section 4.2. For the decays of η- and η'-mesons, the mixing of these states has to be considered first (section 4.3). Therewith, the transitions $\eta' \to \omega$, $\eta \to \gamma$ and $\eta' \to \gamma$ are calculated in the later sections 4.4, 4.5 and 4.6.

4.1 Leading-order Lagrangian, Transition Form Factor and Partial Decay Width

4.1.1 The Leading-Order Lagrangian Concerning Vector Mesons

In section 2.5, it was explained that the leading-order Lagrangian which is used in this thesis and is based on the counting scheme (C1), (C2) does not contain all terms describing the decays of pseudoscalar mesons into one or two (real or virtual) vector mesons. Therefore, this kind of decays can only be used as a test for the approach without insisting on being a full leading- or next-to-leading-order calculation.

In this chapter, decays of a pseudoscalar meson P into two real photons, into a photon and vector meson or into a photon and a dilepton will be considered. The relevant parts of the Lagrangian given in section 2.5 are the following:

- Decay $P \to V\gamma$ with a vector meson V:

$$\begin{aligned}\mathcal{L}_1 &= i\,\frac{e_A}{4m_V}\,\varepsilon^{\mu\nu\alpha\beta}\,\mathrm{tr}\left\{\left(f_{\mu\nu}^{+}\left(D^\tau V_{\tau\alpha}\right)+\left(D^\tau V_{\tau\alpha}\right)f_{\mu\nu}^{+}\right)U_\beta\right\}\\ &\approx -\frac{e_A}{4fm_V}\,\varepsilon^{\mu\nu\alpha\beta}\,\mathrm{tr}\left\{\left(Q\left(\partial^\tau V_{\tau\alpha}\right)+\left(\partial^\tau V_{\tau\alpha}\right)Q\right)\partial_\beta\Phi\right\}\,\partial_\mu A_\nu\,. \end{aligned} \tag{4.1}$$

- Decay $P \to VV'$ with two vector mesons V and V':

$$\begin{aligned}\mathcal{L}_{21} &= i\,\frac{h_A}{8}\,\varepsilon^{\mu\nu\alpha\beta}\,\mathrm{tr}\left\{\left(V_{\mu\nu}\left(D^\tau V_{\tau\alpha}\right)+\left(D^\tau V_{\tau\alpha}\right)V_{\mu\nu}\right)U_\beta\right\}\\ &\approx -\frac{h_A}{16f}\,\varepsilon^{\mu\nu\alpha\beta}\,\mathrm{tr}\left\{\left(V_{\mu\nu}\left(\partial^\tau V_{\tau\alpha}\right)+\left(\partial^\tau V_{\tau\alpha}\right)V_{\mu\nu}\right)\partial_\beta\Phi\right\}, \end{aligned} \tag{4.2}$$

$$\begin{aligned}\mathcal{L}_{22} &= i\,\frac{b_A}{8}\,\varepsilon^{\mu\nu\alpha\beta}\,\mathrm{tr}\left\{\left[V_{\mu\nu},V_{\alpha,\beta}\right]_+\chi_-\right\}\\ &\approx -\frac{b_A}{8f}\,\varepsilon^{\mu\nu\alpha\beta}\,\mathrm{tr}\left\{V_{\mu\nu}V_{\alpha\beta}\left[\Phi,\chi_0\right]_+\right\}. \end{aligned} \tag{4.3}$$

- Transition $V \to \gamma$:

$$\begin{aligned}\mathcal{L}_3 &= -\frac{e_V m_V}{8}\,\mathrm{tr}\left\{V^{\mu\nu}f_{\mu\nu}^{+}\right\}\\ &\approx -\frac{e_V m_V}{12}\left[3\left(\rho^0\right)^{\mu\nu}-\sqrt{2}\phi^{\mu\nu}+\omega^{\mu\nu}\right]\partial_\mu A_\nu\,. \end{aligned} \tag{4.4}$$

Hence, the relevant Lagrangian describing both the decay of a pseudoscalar meson into two photons and into a vector meson and a photon equals

$$\begin{aligned}\mathcal{L}^{\text{vec}}_{P\to V\gamma/\gamma\gamma} &= \mathcal{L}_1 + \mathcal{L}_{21} + \mathcal{L}_{22} + \mathcal{L}_3 \\ &= -\frac{e_A}{4fm_V}\,\varepsilon^{\mu\nu\alpha\beta}\,\mathrm{tr}\left\{\left(Q\left(\partial^\tau V_{\tau\alpha}\right) + \left(\partial^\tau V_{\tau\alpha}\right)Q\right)\partial_\beta\Phi\right\}\,\partial_\mu A_\nu \\ &\quad -\frac{h_A}{16f}\,\varepsilon^{\mu\nu\alpha\beta}\,\mathrm{tr}\left\{\left(V_{\mu\nu}\left(\partial^\tau V_{\tau\alpha}\right) + \left(\partial^\tau V_{\tau\alpha}\right)V_{\mu\nu}\right)\partial_\beta\Phi\right\} \\ &\quad -\frac{b_A}{8f}\,\varepsilon^{\mu\nu\alpha\beta}\,\mathrm{tr}\left\{V_{\mu\nu}V_{\alpha\beta}\left[\Phi,\chi_0\right]_+\right\} \\ &\quad -\frac{e_V m_V}{4}\,\mathrm{tr}\left\{V^{\mu\nu}Q\right\}\,\partial_\mu A_\nu. \end{aligned} \tag{4.5}$$

As in the case of a decay of a vector meson (see section 3.1), the e_A term describing the direct decay of a pseudoscalar meson into a (real or virtual) vector meson and a photon will be used for a rough estimate of the intrinsic error of the calculations. Of course, the parameters e_A, h_A and b_A are still fixed by the sets (P1) and (P2).

4.1.2 The Effective Wess-Zumino-Witten Action

As discussed in subsection 2.3.2, the Lagrangian for Goldstone bosons as it was given in subsection 2.3.1 exhibits a larger symmetry than the real world does. Therefore, the Wess-Zumino-Witten (WZW) Lagrangian (2.84) has to be added. For decays of pseudoscalar mesons into two photons the first term $-enA_\mu J^\mu$ in (2.84) does not contribute to tree-level calculations because $J^\mu \in \mathcal{O}\left(\Phi^3\right)$. The trace of the second term becomes

$$-\frac{6i}{f}\,\mathrm{tr}\left\{Q^2\partial_\mu\Phi\right\}$$

and, hence, the relevant part of the WZW Lagrangian equals

$$\mathcal{L}^{\text{WZW}} \approx \frac{3e^2}{8\pi^2 f}\,\varepsilon^{\mu\nu\alpha\beta}\,\partial_\nu A_\alpha\, A_\beta\,\mathrm{tr}\left\{Q^2\partial_\mu\Phi\right\}. \tag{4.6}$$

This Lagrangian describes the direct decay of a pseudoscalar meson into two photons without any vector meson being involved while the Lagrangian (4.5) describes only decays via at least one virtual vector meson.

For the decays of pseudoscalar mesons, the Lagrangian

$$\mathcal{L}_{P\to V\gamma/\gamma\gamma} = \mathcal{L}^{\text{vec}}_{P\to V\gamma/\gamma\gamma} \pm \mathcal{L}^{\text{WZW}}_{P\to V\gamma/\gamma\gamma} \tag{4.7}$$

with $\mathcal{L}^{\text{vec}}_{P\to V\gamma/\gamma\gamma}$ given in Eq. (4.5) and $\mathcal{L}^{\text{WZW}}_{P\to V\gamma/\gamma\gamma}$ given in Eq. (4.6) has to be used. As discussed in subsection 2.3.2, the relative sign between the two parts of the Lagrangian

is not fixed yet. Within the approach of this thesis it is not possible to decide purely theoretically whether it should be a positive or a negative relative sign. The only possibility to fix the sign is a check against experiment: The squared normalised form factor $|F_{P\gamma}(q)|^2$ for the transition of a pseudoscalar meson into a real photon is plotted for both relative signs and both calculations are compared to available experimental data. The sign which describes the data better is taken as the physically realistic sign. In this thesis, the sign is determined as negative by comparing the $\eta \to \gamma$ transition form factor with data taken by the NA60 collaboration for the decay $\eta \to \gamma\mu^+\mu^-$ [A+09] so that

$$\mathcal{L}_{P\to V\gamma/\gamma\gamma} = \mathcal{L}^{\text{vec}}_{P\to V\gamma/\gamma\gamma} - \mathcal{L}^{\text{WZW}}_{P\to V\gamma/\gamma\gamma}\,. \tag{4.8}$$

Keep in mind that a negative relative sign between the two parts of the Lagrangian is, of course, connected to fixing the parameters n of the WZW Lagrangian (4.6) and the parameter h_A of the Lagrangian (4.5) as positive in advance.

4.1.3 Transition Form Factor and Partial Decay Width

Analogical to the definition of the transition matrix element and the transition form factor for the decay of vector mesons (see subsection 3.1.2), the transition matrix element for the decay of a pseudoscalar meson P into a real photon and either another (real) photon or a dilepton l is given by

$$\mathcal{M}_{P\to\gamma\gamma/\gamma l^+l^-} = e f_{P\gamma}(q)\,\varepsilon^{\mu\nu\alpha\beta}\,p_\mu q_\nu\,\varepsilon^*_\alpha(k,\lambda_\gamma)\,l_\beta(q) \tag{4.9}$$

with $l_\beta(q)$ defined by Eq. (3.11), (3.12) and the four-momenta p, q and k of the incoming pseudoscalar meson, the outgoing or intermediate photon and the outgoing photon, respectively.
The transition matrix element for the decay into a vector meson V and either a photon or a dilepton is given by

$$\mathcal{M}_{P\to V\gamma/Vl^+l^-} = e f_{PV}(q)\,\varepsilon^{\mu\nu\alpha\beta}\,p_\mu q_\nu\,\varepsilon_\alpha(k,\lambda_V)\,l_\beta(q) \tag{4.10}$$

with k being the four-momentum of the outgoing vector meson.

The formula for the decay width for the decay of a pseudoscalar meson into a vector meson and a photon or into two (real) photons is in principle given by Eq. (3.24). As pseudoscalar particles have spin 0, the prefactor $\frac{1}{3}$ arising from the average over all incoming vector meson states has to be replaced by the prefactor 1. Additionally, for the decay into two photons a prefactor $\frac{1}{2!}$ has to be included as there are two identical particles in the outgoing channel which cannot be distinguished in a detector. Therefore,

the partial decay widths equal

$$\Gamma_{P\to V\gamma} = \frac{e^2\left(m_P^2 - m_V^2\right)^3}{32\pi\, m_P^3}\,\left|f_{PV}(0)\right|^2, \tag{4.11}$$

$$\Gamma_{P\to 2\gamma} = \frac{e^2\, m_P^3}{64\pi}\,\left|f_{P\gamma}(0)\right|^2. \tag{4.12}$$

Therewith, the single-differential decay width for the decay of a pseudoscalar meson into a vector meson and a dilepton can be calculated by applying formula (3.30) (taking P as the incoming particle instead of A and V instead of B). The single-differential decay width for the decay into a real photon and a dilepton gets an additional factor 2 in comparison to formula (3.30) yielding

$$\frac{\mathrm{d}\Gamma_{P\to\gamma l^+l^-}}{\mathrm{d}q^2\,\Gamma_{P\to 2\gamma}} = \frac{e^2}{6\pi^2}\,\frac{1}{q^2}\,\sqrt{1-\frac{4m_l^2}{q^2}}\,\left(1+\frac{2m_l^2}{q^2}\right)\left(1-\frac{q^2}{m_P^2}\right)^3\left|F_{P\gamma}(q)\right|^2 \tag{4.13}$$

including that $m_\gamma^2 = 0$.

4.2 Decay $\pi^0 \to \gamma l^+ l^-$

4.2.1 Form Factor for the $\pi^0 \to \gamma$ Transition

The relevant leading-order Lagrangian (4.8) for the decays of pseudoscalar mesons yields that the neutral pion can only decay via one virtual ρ^0-meson, one virtual ω-meson or a ρ^0- and an ω-meson into two (real or virtual) photons. As the pion field is proportional to $\bar{u}\gamma_5 u - \bar{d}\gamma_5 d$, an intermediate ϕ-meson is not allowed in leading-order processes according to the OZI rule. As a photon has isospin zero or one, both the decay of a neutral pion into a photon and a ρ^0-meson and the decay into a photon and an ω-meson are in agreement with isospin conservation. But the decay of the pion into two ω-mesons would violate isospin conservation and is therefore forbidden. Additionally, an allowed process should conserve G-parity, i.e. the process should be invariant under the composition of charge conjugation and isospin. As

$$G\pi^0 = -1,\ G\rho^0 = +1,\ G\omega = -1, \tag{4.14}$$

a decay into two ρ^0-mesons is also forbidden and the decay into a ρ^0- and an ω-meson is the only possibility for a decay of a neutral pion into two virtual vector mesons.

Thus, the leading-order Lagrangian $\mathcal{L}_{\pi\gamma}^{\text{vec}}$ equals $\mathcal{L}_{\pi\gamma}^{\text{one virt}} + \mathcal{L}_{\pi\gamma}^{\text{two virt}}$ with

$$\mathcal{L}_{\pi\gamma}^{\text{one virt}} = -\frac{e_A}{6 f m_V}\, \varepsilon^{\mu\nu\alpha\beta} \left[\partial^\tau \rho^0_{\tau\alpha} + 3\partial^\tau \omega_{\tau\alpha}\right] \partial_\beta \pi^0\, \partial_\mu A_\nu \tag{4.15}$$

describing the decay via one virtual vector meson and

$$\begin{aligned}\mathcal{L}_{\pi\gamma}^{\text{two virt}} = &-\frac{h_A}{4f}\, \varepsilon^{\mu\nu\alpha\beta} \left[\omega_{\mu\nu}\left(\partial^\tau \rho^0_{\tau\alpha}\right) + \rho^0_{\tau\alpha}\left(\partial^\tau \omega_{\tau\alpha}\right)\right] \partial_\beta \phi^0 \\ &-\frac{b_A \bar{m}_\pi^2}{f}\, \varepsilon^{\mu\nu\alpha\beta}\, \rho^0_{\mu\nu}\, \omega_{\alpha\beta}\, \pi^0\end{aligned} \tag{4.16}$$

describing the decay via two virtual vector mesons.

The matrix element defined by the Lagrangian $\mathcal{L}_{\pi\gamma}^{\text{vec}}$ can be calculated with the Feynman rules given in the subsection 2.6.1 analogically to the calculations in subsection 3.2.1 (see the two diagrams on the left-hand side in Fig. 4.1). Thereby, all possible virtual vector mesons have to be considered and the results to be added. The calculated matrix element equals

$$\mathcal{M}_{\pi\gamma}^{\text{vec}} = e\, f_{\pi\gamma}^{\text{vec}}(q)\, \varepsilon^{\mu\nu\alpha\beta}\, p_\mu q_\nu\, \varepsilon_\alpha^*(k, \lambda_\gamma)\, l_\beta(q) \tag{4.17}$$

with the vector part of the form factor for the $\pi^0 \to \gamma$ transition

$$f_{\pi\gamma}^{\text{vec}}(q) = \frac{e_V}{12fe}\left[e_V m_V^2\left(\frac{h_A}{8}q^2 - b_A\bar{m}_\pi^2\right)\left(\frac{1}{m_\omega^2}S_\rho\left(q^2\right) + \frac{1}{m_\rho^2}S_\omega\left(q^2\right)\right) + \frac{e_A}{2}\left(S_\rho\left(q^2\right) + S_\omega\left(q^2\right)\right)q^2\right] \tag{4.18}$$

and using $l_\beta(q)$ as defined in subsection 3.1.2. Recall that for the decay into two real photons the form factor has to be evaluated at $q^2 = 0$.

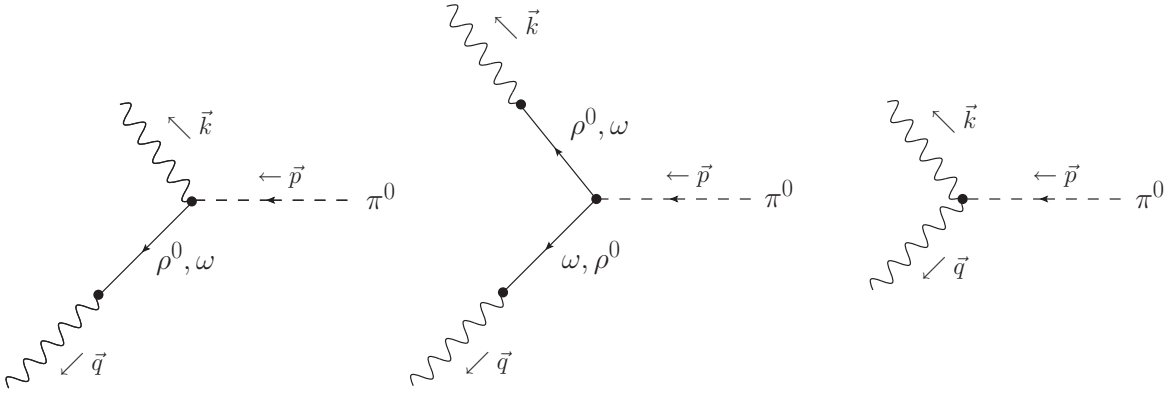

Figure 4.1: Decay of the neutral pion into two (real or virtual) photons via $\mathcal{L}_{\pi\gamma}^{\text{vec}}$ with one or two virtual vector mesons (left and middle) and via $\mathcal{L}_{\pi\gamma}^{\text{WZW}}$ (right).

Additionally, the Lagrangian based on the effective Wess-Zumino-Witten action describing the direct decay of the neutral pion into two photons

$$\mathcal{L}_{\pi\gamma}^{\text{WZW}} = \frac{e^2}{8\pi^2 f}\,\varepsilon^{\mu\nu\alpha\beta}\,\partial_\mu\pi^0\,\partial_\nu A_\alpha\,A_\beta \tag{4.19}$$

has to be considered (see diagram on the right-hand side in Fig. 4.1). It yields the matrix element

$$\begin{aligned} i\mathcal{M}_{\pi\gamma}^{\text{WZW}} &= 2\,(-ip_\mu)\left(+i\frac{e^2}{8\pi^2 f}\,\varepsilon^{\mu\nu\alpha\beta}\right)(ik_\nu)\,\varepsilon_\alpha^*(k,\lambda_\gamma)\,(-l_\beta(q)) \\ &= -\,i\,\frac{e^2}{4\pi^2 f}\,\varepsilon^{\mu\nu\alpha\beta}\,p_\mu k_\nu\,\varepsilon_\alpha^*(k,\lambda_\gamma)\,l_\beta(q) \\ &= +\,i\,\frac{e^2}{4\pi^2 f}\,\varepsilon^{\mu\nu\alpha\beta}\,p_\mu q_\nu\,\varepsilon_\alpha^*(k,\lambda_\gamma)\,l_\beta(q) \end{aligned} \tag{4.20}$$

and, thus, the transition form factor

$$f_{\pi\gamma}^{\text{WZW}} = \frac{e}{4\pi^2 f}\,. \tag{4.21}$$

As already mentioned in subsection 4.1.2, the form factor $f_{\pi\gamma}$ for the $\pi^0 \to \gamma$ transition is the sum of $f_{\pi\gamma}^{\text{vec}}$ and $-f_{\pi\gamma}^{\text{WZW}}$,

$$\begin{aligned} f_{\pi\gamma}(q) &= f_{\pi\gamma}^{\text{vec}}(q) - f_{\pi\gamma}^{\text{WZW}}(q) \\ &= \frac{e_V}{12fe}\left[e_V m_V^2\left(\frac{h_A}{8}q^2 - b_A\bar{m}_\pi^2\right)\left(\frac{1}{m_\omega^2}S_\rho\left(q^2\right) + \frac{1}{m_\rho^2}S_\omega\left(q^2\right)\right)\right. \\ &\quad \left. + \frac{e_A}{2}\left(S_\rho\left(q^2\right) + S_\omega\left(q^2\right)\right)q^2\right] - \frac{e}{4\pi^2 f}\,. \end{aligned} \tag{4.22}$$

On the left-hand side of Fig. 4.2, the normalised form factor $F_{\pi\gamma}(q)$ is plotted. Once again, the calculations with the parameter sets (P1) and (P2) do not differ much. Additionally, the standard VMD form factor which is approximated by

$$F_{\pi\gamma}^{\text{VMD}}(q) = \frac{m_{\text{virtual}}^2}{m_{\text{virtual}}^2 - q^2}\,. \tag{4.23}$$

for $m_\rho \approx m_\omega \approx m_{\text{virtual}} = 774.5\,\text{MeV}$ is plotted in that figure. The calculations with parameter set (P1) and with the standard VMD model lie on top of each other so that the form factor of the $\pi^0 \to \gamma$ transition cannot be used to evaluate our approach in comparison to the standard VMD model. In the figure on the right-hand side, the calculations are compared to the data taken at the Brookhaven National Laboratory [Sam61]. The error bars of the data are relatively large so that an agreement or a disagreement with the calculations with parameters sets (P1), (P2) and the standard VMD form factor cannot be observed.
To be able to find out which part of the $\pi^0 \to \gamma$ transition form factor, the indirect vector term or the direct WZW term, are dominant in which energy regions, the quotient $f_{\pi\gamma}^{\text{vec}}(q)/f_{\pi\gamma}^{\text{WZW}}(q)$ is plotted in Fig. 4.3. The quotient is less than 0.025 for all allowed energies. Thus, the WZW term in the form factor is the dominant one, a decay via one or two virtual vector mesons yields a form factor whose value is at most 2.5% of the WZW term.

4.2.2 Single-Differential and Full Partial Decay Widths for the Decays $\pi^0 \to \gamma\gamma/\gamma e^+ e^-$

For the decay of a neutral pion into two photons and the decay into a photon and a dielectron the partial decay widths are equal to

$$\Gamma_{\pi^0\to\gamma\gamma} = (7.83 \pm 0.14)\cdot 10^{-9}\,\text{GeV}, \tag{4.24}$$

$$\Gamma_{\pi^0\to\gamma e^+e^-} = (9.28 \pm 0.16)\cdot 10^{-11}\,\text{GeV}. \tag{4.25}$$

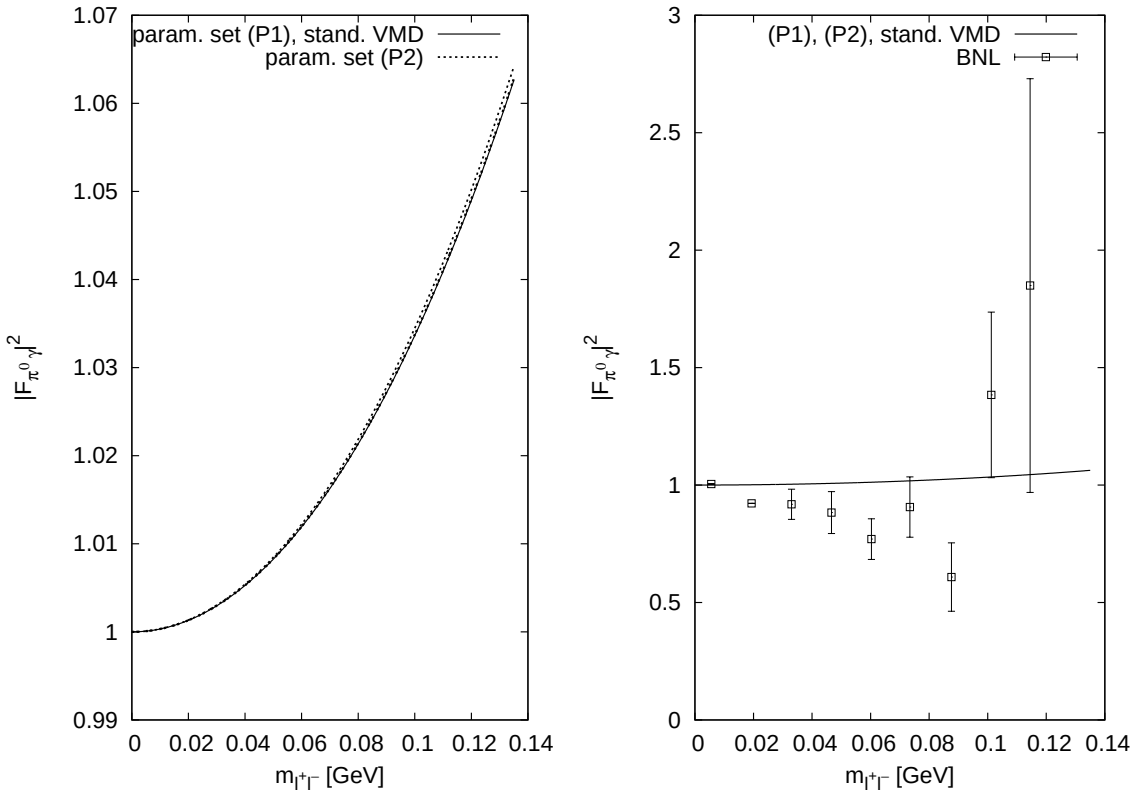

Figure 4.2: On the left-hand side, the (full) form factor of the $\pi^0 \to \gamma$ transition is plotted. The calculations with the parameter sets (P1) and (P2) are described by the solid and the dotted line, respectively; the calculations with the VMD model are practically indistinguishable from the calculations with parameter set (P1). The figure on the right-hand side compares all three calculated form factors with the data taken at the Brookhaven National Laboratory [Sam61]. In that scale, the three curves are indistinguishable and presented by one solid line.

Both agree well with the experimental values taken from [A+08]

$$\Gamma^{\text{exp}}_{\pi^0\to\gamma\gamma} = (7.74 \pm 0.56) \cdot 10^{-9}\,\text{GeV}, \tag{4.26}$$

$$\Gamma^{\text{exp}}_{\pi^0\to\gamma e^+e^-} = (9.20 \pm 0.93) \cdot 10^{-11}\,\text{GeV}. \tag{4.27}$$

The corresponding single-differential decay width for the decay $\pi^0 \to \gamma e^+ e^-$ is plotted in Fig. 4.4 with the calculations done with parameter set (P1) and parameter set (P2) (solid line) in agreement. The calculation done with the standard model (dot-dashed line) differs from those.
Note that a decay into a photon and a dimuon is not possible because the lower kinematic boundary $m_\gamma + 2m_\mu = 2m_\mu = 212\,\text{MeV}$ for such a decay is larger than the mass of the neutral pion $m_{\pi^0} = 135\,\text{MeV}$.

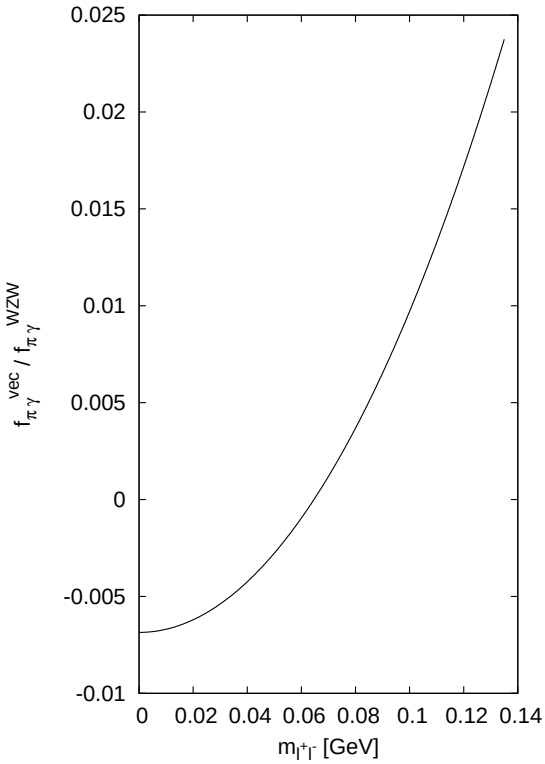

Figure 4.3: The quotient $f_{\pi\gamma}^{\mathrm{vec}}(q)/f_{\pi\gamma}^{\mathrm{WZW}}(q)$ using Eq. (4.18) and Eq. (4.21).

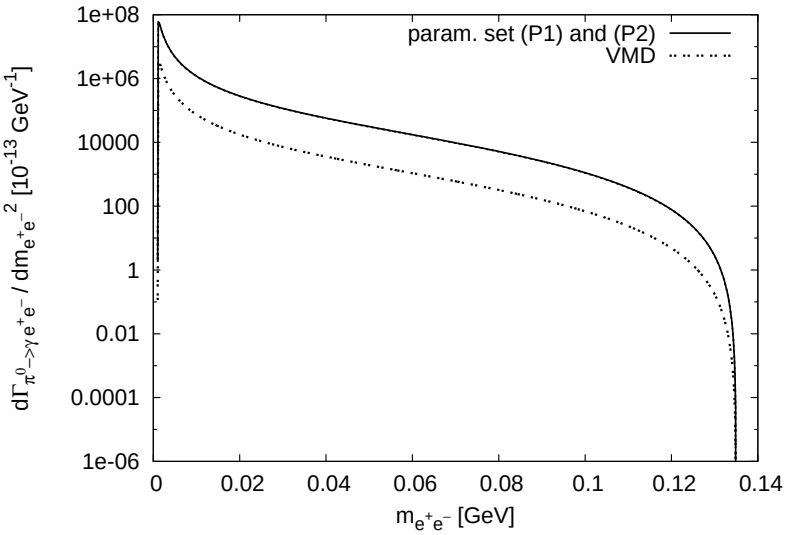

Figure 4.4: Single-differential decay width for the decay $\pi^0 \to \gamma e^+ e^-$. The solid line describes the calculations done with parameter set (P1) and (P2) which are indistinguishable and the dot-dashed line the calculations done with the standard VMD model.

4.3 η-η'-Mixing

In the chapter 3 where the radiative decays of vector mesons were considered, the Goldstone-boson octet described by the matrix Φ defined in Eq. (2.52) was used for decays into η-mesons. Yet, the η-meson included in Φ is not equal to the physical η-meson. This meson is a combination of the octet η-state, from now on called η_8, and the singlet η-state η_1. For decays of vector mesons into an η-meson and a dilepton it is adequate to consider the η_8-state instead of the physical η-meson but for the description of decays of η-mesons it is necessary to use the physical η-meson as the results calculated with an unmixed $\eta = \eta_8$ state and with the physical η-meson differ much (see section 4.5). Correspondingly, the physical η'-meson cannot be described adequately as an η_1 state but consists of an η_8- and an η_1-part. Again, there are significant differences between the calculations done with the unmixed $\eta' = \eta_1$ state and the physical η'-meson (see section 4.6). To take this mixture of octet and singlet into account, the Goldstone-boson matrix $\Phi =: \Phi_{\text{old}}$ defined in (2.52), which only includes the η_8-state, is modified by adding a matrix describing the singlet:

$$\Phi \mapsto \Phi_{\text{old}} + \sqrt{\frac{2}{3}} \begin{pmatrix} \eta_1 & 0 & 0 \\ 0 & \eta_1 & 0 \\ 0 & 0 & \eta_1 \end{pmatrix}. \tag{4.28}$$

The aim is to describe the η- and the η'-meson with one at this point still arbitrary mixing angle θ as

$$\eta = \cos\theta\eta_8 - \sin\theta\eta_1, \tag{4.29}$$
$$\eta' = \sin\theta\eta_8 + \cos\theta\eta_1. \tag{4.30}$$

To determine this mixing angle, the mass terms in the Lagrangian have to be considered. For the Goldstone octet, the mass terms are the terms of second order in the fields in the symmetry breaking term $\mathcal{L}_{\text{s.b.}}$ of the Lagrangian for the Goldstone bosons (2.73). With $\chi = \chi_0 = 2B_0M$ and the quark-mass matrix $M = \text{diag}\,(m_u, m_d, m_s)$ this symmetry breaking term equals

$$\begin{aligned} \mathcal{L}_{\text{s.b.}} &= \frac{1}{4} f^2 \,\text{tr}\{\chi_0 U^\dagger + U\chi_0^\dagger\} = \frac{B_0}{2} f^2 \,\text{tr}\{MU^\dagger + UM\} \\ &\approx -\frac{B_0}{2} \,\text{tr}\{\Phi_{\text{old}}^2 M\} + \text{const.} \end{aligned} \tag{4.31}$$

As constants are irrelevant in Lagrangians, $\mathcal{L}_{\text{s.b.}}$ is simplified as

$$\begin{aligned}\mathcal{L}_{\text{s.b.}} &\approx -\frac{B_0}{2}\,\text{tr}\{\Phi_{\text{old}}^2 M\} \\ &= -\frac{B_0}{2}\Big[2(m_u+m_d)\pi^+\pi^- + 2(m_u+m_s)K^+K^- + 2(m_d+m_s)K^0\bar{K}^0 \\ &\quad +(m_u+m_d)\pi^0\pi^0 + \frac{2}{\sqrt{3}}(m_u-m_d)\pi^0\eta_8 + \frac{m_u+m_d+4m_s}{3}\,\eta_8^2\Big]. \end{aligned} \tag{4.32}$$

In the isospin-symmetric limit $m_u = m_d = m$, the term proportional to $\pi^0\eta_8$ turns to zero and there is no π^0-η_8-mixing. The values for $B_0 m$ and $B_0 m_s$ can therewith be determined via

$$\overline{m}_\pi^2 = 2B_0 m,\ \overline{m}_K^2 = B_0(m+m_s) \tag{4.33}$$

by the masses of the Goldstone bosons pion, $\overline{m}_\pi \approx 138\,\text{MeV}$, and kaon, $\overline{m}_K = 496\,\text{MeV}$, as

$$B_0 m = \frac{1}{2}\overline{m}_\pi^2,\ B_0 m_s = \overline{m}_K^2 - \frac{1}{2}\overline{m}_\pi^2. \tag{4.34}$$

To involve also the pseudoscalar singlet, an additional mass term

$$-\frac{1}{2}\,m_1^2\,\eta_1^2 \tag{4.35}$$

is needed [EGPdR89]. Thus, by modifying the Goldstone-boson matrix Φ according to (4.28), the Lagrangian to determine the masses and the mixing angle of η- and η'-mesons equals

$$\mathcal{L}_{\text{mass}} = -\frac{1}{2}B_0\,\text{tr}\{\Phi^2 M\} - \frac{1}{2}m_1^2\eta_1^2. \tag{4.36}$$

If only terms proportional to η_8 or η_1 are considered, this term will reduce to

$$\begin{aligned}\mathcal{L}_{\text{mass}}(\eta_8,\eta_1) &= -\frac{1}{2}\left[\frac{2}{3}B_0\left((m+2m_s)\eta_8^2 + 2\sqrt{2}(m-m_s)\eta_8\eta_1 + (2m+m_s)\eta_1^2\right) + m_1^2\eta_1^2\right] \\ &= -\frac{1}{2}\begin{pmatrix}\eta_8 & \eta_1\end{pmatrix}\underbrace{\begin{pmatrix}\frac{2}{3}B_0(m+2m_s) & \frac{2\sqrt{2}}{3}(m-m_s) \\ \frac{2\sqrt{2}}{3}B_0(m-m_s) & \frac{2}{3}B_0(2m+m_s)+m_1^2\end{pmatrix}}_{=:\,M(\eta_8,\eta_1)}\begin{pmatrix}\eta_8 \\ \eta_1\end{pmatrix}. \end{aligned} \tag{4.37}$$

The physical states η- and η'-meson are defined as a multiplication of $(\eta_8,\eta_1)^T$ with a unitary matrix U as defined by (4.29), (4.30). As there is no mixing of the physical

η- and η'-meson, all terms proportional to $\eta\,\eta'$ should vanish. Therefore, the matrix $M(\eta,\eta') := U^T M(\eta_8,\eta_1)U$ has to be diagonal[1]. Hence, the mass term equals

$$\begin{aligned}\mathcal{L}_{\text{mass}}(\eta_8,\eta_1) &= -\frac{1}{2}\begin{pmatrix}\eta_8 & \eta_1\end{pmatrix} U^T\, U M(\eta_8,\eta_1) U^T\, U \begin{pmatrix}\eta_8\\ \eta_1\end{pmatrix} = -\frac{1}{2}\begin{pmatrix}\eta & \eta'\end{pmatrix} M(\eta,\eta') \begin{pmatrix}\eta\\ \eta'\end{pmatrix} \\ &= -\frac{1}{2}\left[d_1\eta^2 + d_2\eta'^2\right] \end{aligned} \tag{4.38}$$

with the diagonal elements d_1 and d_2 of the mass matrix $M(\eta,\eta')$. The first diagonal element d_1 has to be equal to the squared mass m_η^2 of the η-meson and the second one d_2 to the squared mass $m_{\eta'}^2$ of the η'-meson. Both diagonal elements d_1 and d_2 are defined by $M(\eta,\eta') := U^T M(\eta_8,\eta_1)U$ and depend on $B_0 m$, $B_0 m_s$ and m_1. As $B_0 m$ and $B_0 m_s$ are fixed by the averaged pion and kaon mass via Eq. (4.34), the mass m_1 can be calculated by solving the Eq. $d_2 = m_{\eta'}^2 = (958\,\text{MeV})^2$ and is determined as

$$m_1 \approx 819\,\text{MeV}. \tag{4.39}$$

If this result is inserted into the Eq. $d_1 = m_\eta^2$, the mass of the η-meson will equal

$$m_\eta \approx 495\,\text{MeV} \tag{4.40}$$

which is in acceptable agreement with the experimental value $m_\eta = 548\,\text{MeV}$ taken from [A+08]. Inserting the values for $B_0 m$, $B_0 m_s$ and m_1 in $U(\eta_8,\eta_1)^T = (\eta,\eta')^T$ with the physical states η and η' as defined in (4.29) and (4.30), respectively, fixes the mixing angle as

$$\theta \approx -19.7^\circ. \tag{4.41}$$

This result also agrees well with the generally appointed value $\theta = -19.5^\circ$ [ABBC92] for the mixing angle which is used within this thesis.

[1] The unitary matrix U which diagonalizes $M(\eta_8,\eta_1)$ can be determined via the eigenvectors of $M(\eta_8,\eta_1)$.

4.4 Form Factor for the $\eta' \to \omega$ Transition

As explained in the previous section 4.3, the η'-meson is a linear combination of the octet state η_8 and the singlet state η_1. Thus, for all calculations concerning the decays of an η'-meson both the Lagrangian describing the decay of the η_8 state and the one describing the decay of the η_1 state are needed. The relevant Lagrangians for the decays into an ω-meson and a, real or virtual, photon are

$$\begin{aligned}\mathcal{L}_{\eta_8\omega} = &- \frac{e_A}{6\sqrt{3}fm_V}\,\varepsilon^{\mu\nu\alpha\beta}\,\partial^\tau\omega_{\tau\alpha}\,\partial_\beta\eta_8\,\partial_\mu A_\nu \\ &- \frac{h_A}{4\sqrt{3}f}\,\varepsilon^{\mu\nu\alpha\beta}\,\partial^\tau\omega_{\tau\alpha}\,\omega_{\mu\nu}\,\partial_\beta\eta_8 \\ &- \frac{b_A\bar{m}_\pi^2}{2\sqrt{3}f}\,\varepsilon^{\mu\nu\alpha\beta}\,\omega_{\mu\nu}\,\omega_{\alpha\beta}\,\eta_8 \\ &- \frac{e_V m_V}{12}\,\omega^{\mu\nu}\,\partial_\mu A_\nu \end{aligned} \tag{4.42}$$

describing the decay of the η_8 state and

$$\begin{aligned}\mathcal{L}_{\eta_1\omega} = &- \frac{\sqrt{2}e_A}{6\sqrt{3}fm_V}\,\varepsilon^{\mu\nu\alpha\beta}\,\partial^\tau\omega_{\tau\alpha}\,\partial_\beta\eta_1\,\partial_\mu A_\nu \\ &- \frac{\sqrt{2}h_A}{4\sqrt{3}f}\,\varepsilon^{\mu\nu\alpha\beta}\,\partial^\tau\omega_{\tau\alpha}\,\omega_{\mu\nu}\,\partial_\beta\eta_1 \\ &- \frac{\sqrt{2}b_A\bar{m}_\pi^2}{2\sqrt{3}f}\,\varepsilon^{\mu\nu\alpha\beta}\,\omega_{\mu\nu}\,\omega_{\alpha\beta}\,\eta_1 \\ &- \frac{e_V m_V}{12}\,\omega^{\mu\nu}\,\partial_\mu A_\nu \end{aligned} \tag{4.43}$$

describing the decay of the η_1 state. Obviously, the first three terms in $\mathcal{L}_{\eta_1\omega}$ are equal to the first three terms in $\mathcal{L}_{\eta_8\omega}$ multiplied with $\sqrt{2}$. The last term for the decay of the virtual ω-meson into a photon is, of course, the same for both Lagrangians. Therefore, the matrix element $\mathcal{M}_{\eta_1\omega}$ equals $\sqrt{2}\,\mathcal{M}_{\eta_8\omega\gamma}$. Hence, the definition $\eta' = \sin\theta\eta_8 + \cos\theta\eta_1$ yields

$$\begin{aligned}\mathcal{M}_{\eta'\omega} &= \sin\theta\mathcal{M}_{\eta_8\omega} + \cos\theta\mathcal{M}_{\eta_1\omega} = \left[\sin\theta + \sqrt{2}\cos\theta\right]\mathcal{M}_{\eta_8\omega} \\ &= e\left[\sin\theta + \sqrt{2}\cos\theta\right] f_{\eta_8\omega}(q)\,\varepsilon^{\mu\nu\alpha\beta}\,p_\mu q_\nu\,\varepsilon_\alpha(k,\lambda_\omega)\,l_\beta(q)\end{aligned} \tag{4.44}$$

with the four-momenta p, q and k of the incoming η'-meson, the outgoing (real or virtual) photon and the outgoing ω-meson, respectively.
Hence, to calculate $\mathcal{M}_{\eta'\omega}$ only $f_{\eta_8\omega}(q)$ has to be determined. Calculated analogically to the $\pi^0 \to \gamma$ transition form factor in subsection 4.2.1, the form factor for the $\eta_8 \to \omega$

transition is determined as

$$f_{\eta_8\omega}(q) = -\frac{m_\omega}{6\sqrt{3}fm_V e}\left[-e_A + \frac{1}{4}e_V\, h_A\, m_V^2\left(1+\frac{q^2}{m_\omega^2}\right)S_\omega\left(q^2\right) - 2b_A\, e_V\, m_V^2\,\frac{\bar{m}_\pi^2}{m_\omega^2}\,S_\omega\left(q^2\right)\right]. \tag{4.45}$$

This form factor is equal to (-1) times the form factor (3.56) for the $\omega \to \eta$ transition given in subsection 3.3.1. Hence, the normalised form factor for the $\eta' \to \omega$ transition equals

$$\begin{aligned} F_{\eta'\omega}(q) &= \frac{\sin\theta f_{\eta_8\omega}(q) + \cos\theta f_{\eta_1\omega}(q)}{\sin\theta f_{\eta_8\omega}(0) + \cos\theta f_{\eta_1\omega}(0)} = \frac{\left[\sin\theta + \sqrt{2}\cos\theta\right] f_{\eta_8\omega}(q)}{\left[\sin\theta + \sqrt{2}\cos\theta\right] f_{\eta_8\omega}(0)} \\ &= \frac{f_{\eta_8\omega}(q)}{f_{\eta_8\omega}(0)} = \frac{-f_{\omega\eta}(q)}{-f_{\omega\eta}(0)} \\ &= F_{\omega\eta} \end{aligned} \tag{4.46}$$

as already anticipated in subsection 3.3.1.

The partial decay width for the decay of the η'-meson into an ω-meson and a photon can be calculated with formula (4.11) and equals

$$\Gamma_{\eta'\to\omega\gamma} = (5.54 \pm 0.16)\cdot 10^{-6}\,\text{GeV} \tag{4.47}$$

in good agreement with the experimental value [A+08]

$$\Gamma^{\text{exp}}_{\eta'\to\omega\gamma} = (6.16 \pm 1.09)\cdot 10^{-6}\,\text{GeV}. \tag{4.48}$$

On this basis, the partial decay width and the branching ratio for the decay into a dielectron[2] are calculated as

$$\Gamma_{\eta'\to\omega e^+e^-} = (3.78 \pm 0.10)\cdot 10^{-8}\,\text{GeV}, \tag{4.49}$$

$$\text{BR}_{\eta'\to\omega e^+e^-} = (1.85 \pm 0.19)\cdot 10^{-4}. \tag{4.50}$$

As there is no experimental data available, these values have to be seen as predictions. Note that the order of magnitude of the branching ratio is much larger than the branching ratio for the decay of the ω-meson into an η-meson and a dielectron which is of the order of 10^{-6}. Therefore, it should be easier to verify the form factor $F_{\eta'\omega} = F_{\omega\eta}$ shown in Fig. 3.8 by measuring decays of η'-mesons.

[2] A decay into a dimuon is not possible since the minimal mass of the dimuon equals $2m_\mu = 212\,\text{MeV}$ and is therewith greater than the maximal available energy $m_{\eta'} - m_\omega = 175\,\text{MeV}$.

4.5 Decay $\eta \to \gamma l^+ l^-$

4.5.1 Form Factor for the $\eta \to \gamma$ Transition

For the decay of the η-meson one has to consider again the decays of the η_8 and the η_1 state as described in section 4.4 with one or two intermediate vector mesons. An η_8- or η_1-state can decay via one virtual ρ^0-, ω- or ϕ-meson into two photons (without violating isospin conservation). As the state is proportional to $\bar{u}\gamma_5 u + \bar{d}\gamma_5 d - \bar{s}\gamma_5 s$, none of these possibilities is suppressed by the OZI rule in leading order. Additionally, isospin conservation allows only the vector meson combinations $\rho^0\rho^0$, $\omega\omega$, $\omega\phi$ and $\phi\phi$ for the decay of an η-state into two (virtual) vector mesons. In leading order, the decay into an ω- and a ϕ-meson is suppressed by the OZI rule (see Fig. 4.5).

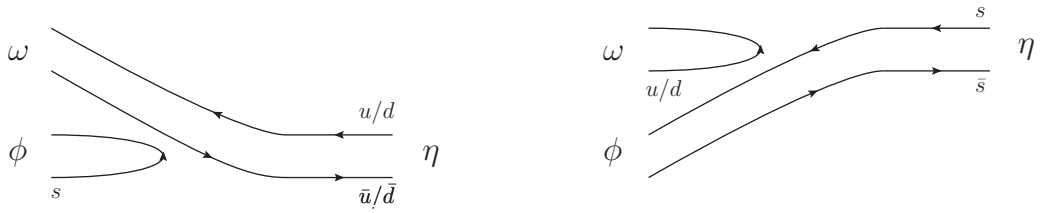

Figure 4.5: The possibilities of an η-meson to decay into an ω- and a ϕ-meson.

Therewith, the leading-order Lagrangian for the decay of the η_8 state equals

$$\begin{aligned}
\mathcal{L}^{\text{vec}}_{\eta_8\gamma} = &- \frac{e_A}{6\sqrt{3}m_V f}\,\varepsilon^{\mu\nu\alpha\beta}\left[3\partial^\tau\rho^0_{\tau\alpha} + \partial^\tau\omega_{\tau\alpha} + 2\sqrt{2}\partial^\tau\phi_{\tau\alpha}\right]\partial_\beta\eta_8\,\partial_\mu A_\nu \\
&- \frac{h_A}{4\sqrt{3}f}\,\varepsilon^{\mu\nu\alpha\beta}\left[\rho^0_{\mu\nu}\partial^\tau\rho^0_{\tau\alpha} + \omega_{\mu\nu}\partial^\tau\omega_{\tau\alpha} - 2\phi_{\mu\nu}\partial^\tau\phi_{\tau\alpha}\right]\partial_\beta\eta_8 \\
&- \frac{b_A}{2\sqrt{3}f}\,\varepsilon^{\mu\nu\alpha\beta}\left[\bar{m}_\pi^2\rho^0_{\mu\nu}\rho^0_{\alpha\beta} + \bar{m}_\pi^2\omega_{\mu\nu}\omega_{\alpha\beta} - 2\left(2\bar{m}_K^2 - \bar{m}_\pi^2\right)\phi_{\mu\nu}\phi_{\alpha\beta}\right]\eta_8 \\
&- \frac{e_V m_V}{12}\left[3\left(\rho^0\right)^{\mu\nu} + \omega^{\mu\nu} - \sqrt{2}\phi^{\mu\nu}\right]\partial_\mu A_\nu
\end{aligned} \tag{4.51}$$

and the one for the decay of the η_1 state

$$\begin{aligned}
\mathcal{L}^{\text{vec}}_{\eta_1\gamma} = &- \frac{e_A}{6\sqrt{3}m_V f}\,\varepsilon^{\mu\nu\alpha\beta}\left[3\sqrt{2}\partial^\tau\rho^0_{\tau\alpha} + \sqrt{2}\partial^\tau\omega_{\tau\alpha} - 2\sqrt{2}\partial^\tau\phi_{\tau\alpha}\right]\partial_\beta\eta_1\,\partial_\mu A_\nu \\
&- \frac{\sqrt{2}h_A}{4\sqrt{3}f}\,\varepsilon^{\mu\nu\alpha\beta}\left[\rho^0_{\mu\nu}\partial^\tau\rho^0_{\tau\alpha} + \omega_{\mu\nu}\partial^\tau\omega_{\tau\alpha} + \phi_{\mu\nu}\partial^\tau\phi_{\tau\alpha}\right]\partial_\beta\eta_1 \\
&- \frac{\sqrt{2}b_A}{2\sqrt{3}f}\,\varepsilon^{\mu\nu\alpha\beta}\left[\bar{m}_\pi^2\rho^0_{\mu\nu}\rho^0_{\alpha\beta} + \bar{m}_\pi^2\omega_{\mu\nu}\omega_{\alpha\beta} + \left(2\bar{m}_K^2 - \bar{m}_\pi^2\right)\phi_{\mu\nu}\phi_{\alpha\beta}\right]\eta_1 \\
&- \frac{e_V m_V}{12}\left[3\left(\rho^0\right)^{\mu\nu} + \omega^{\mu\nu} - \sqrt{2}\phi^{\mu\nu}\right]\partial_\mu A_\nu\,.
\end{aligned} \tag{4.52}$$

The transition form factor for the η_8 state is calculated as

$$f^{\text{vec}}_{\eta_8\gamma}(q) = \frac{e_V}{36\sqrt{3}fe} \sum_{V=\rho^0,\omega,\phi} \left[\left(\frac{e_A}{2} x_{81}(V) y(V) + \frac{h_A e_V m_V^2}{8} \frac{1}{m^2(V)} x_{82}(V) y^2(V) \right) q^2 \right.$$
$$\left. - b_A e_V m_V^2 \frac{1}{m^2(V)} x_{83}(V) y^2(V) \right] S_V\left(q^2\right) \tag{4.53}$$

with the following parameters depending on the type of the virtual vector meson:

$$x_{81}(V) = \begin{cases} 3, & \text{if } V = \rho^0 \\ 1, & \text{if } V = \omega \\ 2\sqrt{2}, & \text{if } V = \phi \end{cases}, \quad x_{82}(V) = \begin{cases} 1, & \text{if } V = \rho^0 \\ 1, & \text{if } V = \omega \\ -2, & \text{if } V = \phi \end{cases}$$

$$x_{83}(V) = \begin{cases} \bar{m}_\pi^2, & \text{if } V = \rho^0 \\ \bar{m}_\pi^2, & \text{if } V = \omega \\ -2\left(2\bar{m}_K^2 - \bar{m}_\pi^2\right), & \text{if } V = \phi \end{cases}, \quad y(V) = \begin{cases} 3, & \text{if } V = \rho^0 \\ 1, & \text{if } V = \omega \\ -\sqrt{2}, & \text{if } V = \phi \end{cases}.$$

For the η_1 state the transition form factor equals

$$f_{\eta_1\gamma}(q)^{\text{vec}} = \frac{e_V}{36\sqrt{3}fe} \sum_{V=\rho^0,\omega,\phi} \left[\left(\frac{e_A}{2} x_{11}(V) y(V) + \frac{\sqrt{2} h_A e_V m_V^2}{8} \frac{1}{m^2(V)} y^2(V) \right) q^2 \right.$$
$$\left. - \sqrt{2} b_A e_V m_V^2 \frac{1}{m^2(V)} x_{13}(V) y^2(V) \right] S_V\left(q^2\right) \tag{4.54}$$

with the parameters

$$x_{11}(V) = \begin{cases} 3\sqrt{2}, & \text{if } V = \rho^0 \\ \sqrt{2}, & \text{if } V = \omega \\ -2, & \text{if } V = \phi \end{cases}, \quad x_{13}(V) = \begin{cases} \bar{m}_\pi^2, & \text{if } V = \rho^0 \\ \bar{m}_\pi^2, & \text{if } V = \omega \\ 2\bar{m}_K^2 - \bar{m}_\pi^2, & \text{if } V = \phi \end{cases}.$$

Additionally, the leading-order WZW Lagrangians for the η_8 state

$$\mathcal{L}^{\text{WZW}}_{\eta_8\gamma} = \frac{e^2}{8\sqrt{3}\pi^2 f} \varepsilon^{\mu\nu\alpha\beta} \partial_\mu \eta_8 \partial_\nu A_\alpha A_\beta \tag{4.55}$$

and for the η_1 state

$$\mathcal{L}^{\text{WZW}}_{\eta_1\gamma} = \frac{e^2}{2\sqrt{6}\pi^2 f} \varepsilon^{\mu\nu\alpha\beta} \partial_\mu \eta_1 \partial_\nu A_\alpha A_\beta \tag{4.56}$$

are needed. The corresponding form factors are

$$f^{\text{WZW}}_{\eta_8\gamma}(q) = \frac{e}{4\sqrt{3}\,\pi^2\, f}\,, \tag{4.57}$$

$$f^{\text{WZW}}_{\eta_1\gamma}(q) = \frac{e}{\sqrt{6}\,\pi^2\, f}\,. \tag{4.58}$$

As already mentioned in subsection 4.1.2, the relative sign between the terms in the Lagrangian describing decays via virtual vector mesons and the WZW term describing the direct decay into two photons cannot be determined within the framework of the theory. Instead, it is fixed by comparing the normalised form factors for both possible relative signs with experimental data. The form factor for the $\eta \to \gamma$ transition is thereby calculated as

$$\begin{aligned} f_{\eta\gamma}(q) &= \cos\theta f_{\eta_8\gamma}(q) - \sin\theta f_{\eta_1\gamma}(q) \\ &= \cos\theta \left[f^{\text{vec}}_{\eta_8\gamma}(q) \pm f^{\text{WZW}}_{\eta_8\gamma}(q) \right] - \sin\theta \left[f^{\text{vec}}_{\eta_1\gamma}(q) \pm f^{\text{WZW}}_{\eta_1\gamma}(q) \right]. \end{aligned} \tag{4.59}$$

In Fig. 4.6, the normalised form factor is plotted for both signs in comparison with by data taken at the NA60 collaboration for the decay $\eta \to \gamma\mu^+\mu^-$ [A+09]. As the calculations for the two different parameter sets (P1) and (P2) are indistinguishable, they are plotted in one line. Obviously, the form factor calculated with a negative relative sign fits the data very well whereas the one calculated with a positive relative sign does not. Therefore, the sign will be fixed as negative yielding

$$f_{\eta_8\gamma}(q) = f^{\text{vec}}_{\eta_8\gamma}(q) - f^{\text{WZW}}_{\eta_8\gamma}(q), \tag{4.60}$$

$$f_{\eta_1\gamma}(q) = f^{\text{vec}}_{\eta_1\gamma}(q) - f^{\text{WZW}}_{\eta_1\gamma}(q). \tag{4.61}$$

In the panel on the left-hand side of Fig. 4.7, the form factor for an η-meson being a mixture of η_8 and η_1 state (solid line) and the form factor for the unmixed case $\eta = \eta_8$ (dotted line) are plotted. Both are compared to the experimental data for the decay $\eta \to \gamma\mu^+\mu^-$ taken by the NA60 collaboration. As mentioned above, the calculations for the different parameter sets (P1) and (P2) are not distinguishable. Additionally, the standard VMD form factor defined in Eq. (2.88) is plotted (dot-dashed line). It can be calculated by identifying $\frac{g_{PV\gamma}}{2f_V}$ with the prefactors from the terms proportional to e_A in the Lagrangians (4.51), (4.52) and normalising such that the form factor holds $F^{\text{VMD}}_{\eta\gamma}(0) = 1$. Therewith, the standard VMD form factor equals

$$\begin{aligned} F^{\text{VMD}}_{\eta\gamma}(q) = \frac{1}{6\left(\cos\theta - 2\sqrt{2}\sin\theta\right)} \Bigg[& 9\left(\cos\theta - \sqrt{2}\sin\theta\right) \frac{m_\rho^2}{m_\rho^2 - q^2} \\ & + \left(\cos\theta - \sqrt{2}\sin\theta\right) \frac{m_\omega^2}{m_\omega^2 - q^2} - 2\left(2\cos\theta + \sqrt{2}\sin\theta\right) \frac{m_\phi^2}{m_\phi^2 - q^2} \Bigg]. \end{aligned} \tag{4.62}$$

The plot shows that the calculations for the mixed case and the standard VMD form factor are very close together and all three calculations fit the data quite well.

On the right-hand side of Fig. 4.7, the quotient $f^{\text{vec}}_{\eta\gamma}(q)/f^{\text{WZW}}_{\eta\gamma}(q)$ for the mixed, physical η-meson is plotted. The quotient is smaller than one, i.e. the WZW term in the form factor is dominant, until the invariant mass is near the upper kinematic boundary $m_\eta - m_\gamma = 548\,\text{MeV}$. Only in the last part of the allowed energetic region, the term describing decays via virtual vector mesons is dominant.

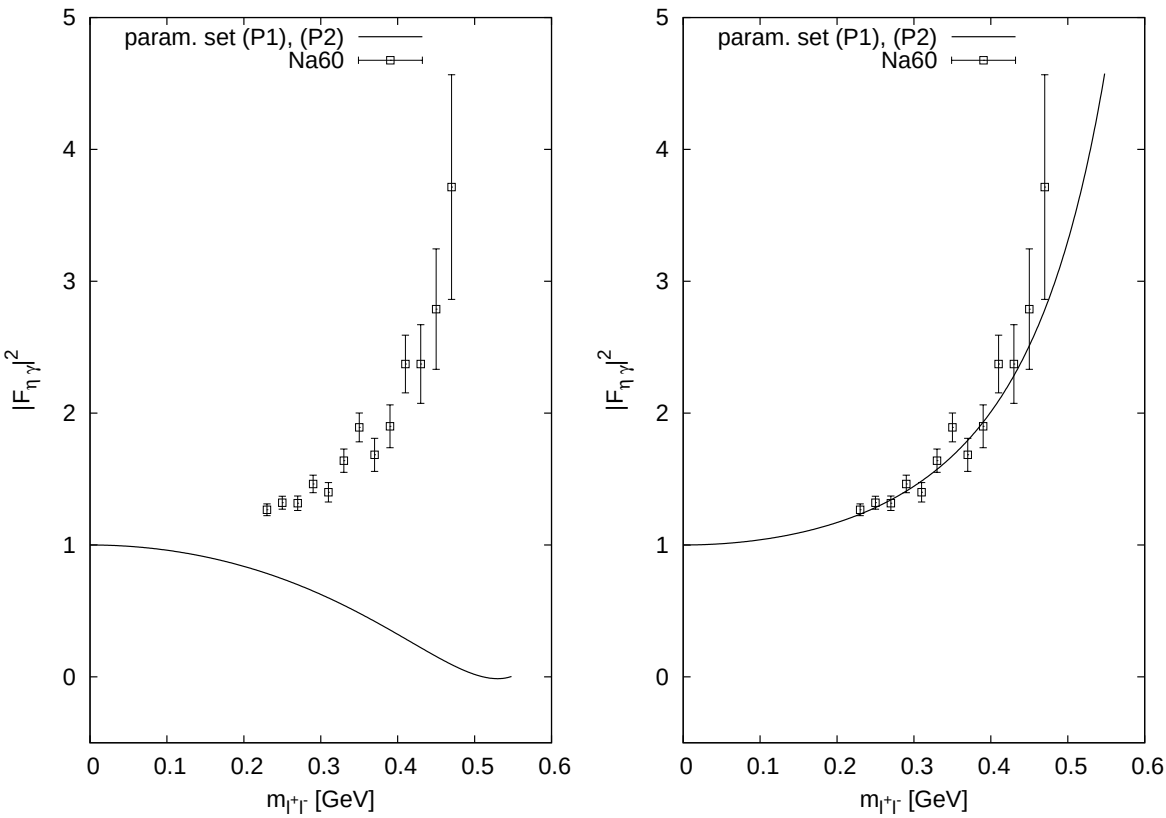

Figure 4.6: Normalised form factor for the $\eta \to \gamma$ transition plotted for a positive relative sign between the vector and the WZW part of the form factor on the left-hand side and for a negative relative sign on the right-hand side. Both calculations are compared to data taken by the NA60 collaboration for the decay $\eta \to \gamma\mu^+\mu^-$ [A+09].

4.5.2 Single-Differential and Full Partial Decay Widths

For the decay $\eta \to \gamma\gamma$ one gets the partial decay widths

$$\Gamma_{\eta\to\gamma\gamma}^{\text{unmixed}} = (2.13 \pm 0.14) \cdot 10^{-7}\,\text{GeV}, \tag{4.63}$$

$$\Gamma_{\eta\to\gamma\gamma}^{\text{mixed}} = (6.71 \pm 0.10) \cdot 10^{-7}\,\text{GeV} \tag{4.64}$$

for the unmixed $\eta = \eta_8$ state and the mixed η-meson, respectively. While the value for the unmixed η state does not fit the experimental value given in [A+08]

$$\Gamma_{\eta\to\gamma\gamma}^{\text{exp}} = (5.11 \pm 0.30) \cdot 10^{-7}\,\text{GeV}, \tag{4.65}$$

the value for the mixed η-meson does agrees much better.

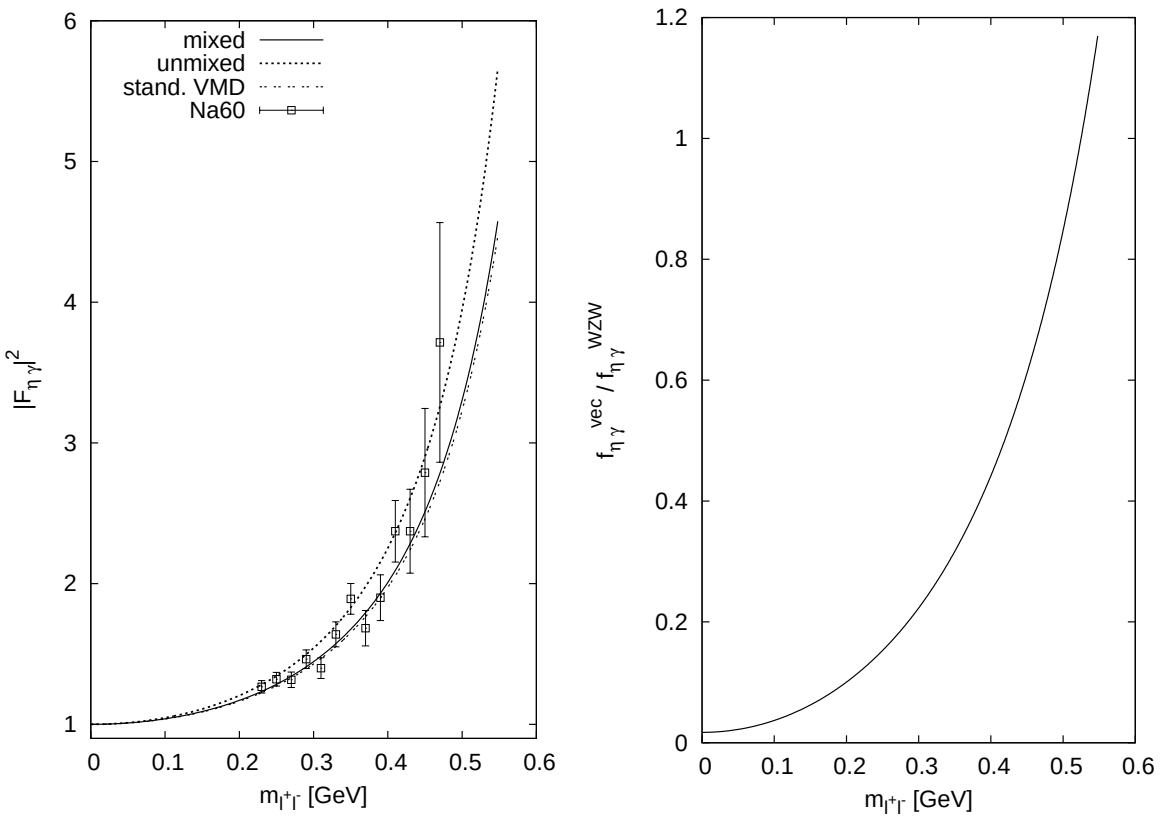

Figure 4.7: In the panel on the left-hand side, the normalised form factor for the decay $\eta \to \gamma l^+ l^-$ is plotted and compared to the experimental data for the decay $\eta \to \gamma \mu^+ \mu^-$ taken by the NA60 collaboration [A+09]. The calculation for the mixed form factor (solid line), the unmixed form factor (dotted line) and the standard VMD form factor (dot-dashed line) are all in agreement with the data. The quotient $f_{\eta\gamma}^{\mathrm{vec}}(q)/f_{\eta\gamma}^{\mathrm{WZW}}(q)$ for the mixed case is plotted in the figure on the right-hand side.

In Fig. 4.8, the single-differential decay width for the decay of an η-meson into a photon and a dimuon is plotted for both the unmixed $\eta = \eta_8$ state (dotted line) and the physical, mixed η-meson (solid line). The difference between the two curves is much larger than the small difference between the normalised form factors for the unmixed case $F_{\eta_8\gamma}$ and the mixed case $F_{\eta\gamma}$ plotted in Fig. 4.7. This is caused by the large difference between the full widths for the decay into two real photons, $\Gamma_{\eta\to\gamma\gamma}^{\mathrm{unmixed}}$ and $\Gamma_{\eta\to\gamma\gamma}^{\mathrm{mixed}}$, which are contained in the formula for the single-differential decay width (4.12). Additionally, the single-differential decay width calculated with the VMD model is plotted (dot-dashed line) which is, as expected, close to the result for the mixed case. The same is done for the single-differential decay width of the decay into a dielectron in Fig. 4.9 and, for a better comparability with the one for the decay into a dimuon, it is plotted for $m_{e^+e^-}$ above

$2m_\mu$ only in Fig. 4.10. One always observes the same pattern: The mixed case and the VMD result are close together.
The experimental values for the full partial decay widths taken from [A+08]

$$\Gamma^{\text{exp}}_{\eta\to\gamma\mu^+\mu^-} = (4.03 \pm 0.74) \cdot 10^{-10}\,\text{GeV}, \tag{4.66}$$
$$\Gamma^{\text{exp}}_{\eta\to\gamma e^+e^-} = (9.10 \pm 1.40) \cdot 10^{-9}\,\text{GeV} \tag{4.67}$$

are again much better described by the values for the decay of a physical mixed η state

$$\Gamma^{\text{mixed}}_{\eta\to\gamma\mu^+\mu^-} = (5.39 \pm 0.09) \cdot 10^{-10}\,\text{GeV}, \tag{4.68}$$
$$\Gamma^{\text{mixed}}_{\eta\to\gamma e^+e^-} = (11.24 \pm 0.16) \cdot 10^{-9}\,\text{GeV} \tag{4.69}$$

than by those for the decay of an unmixed $\eta = \eta_8$ state

$$\Gamma^{\text{unmixed}}_{\eta\to\gamma\mu^+\mu^-} = (1.83 \pm 0.11) \cdot 10^{-10}\,\text{GeV}, \tag{4.70}$$
$$\Gamma^{\text{unmixed}}_{\eta\to\gamma e^+e^-} = (3.59 \pm 0.01) \cdot 10^{-9}\,\text{GeV}. \tag{4.71}$$

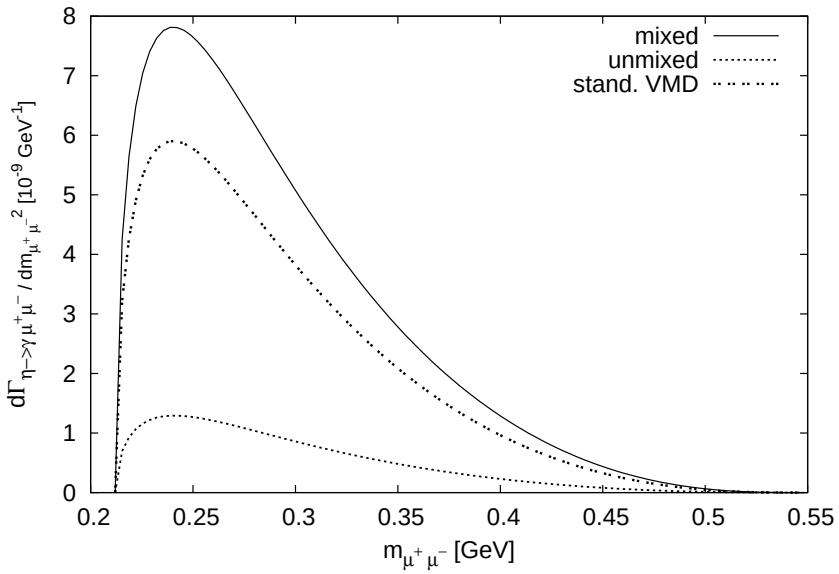

Figure 4.8: Single-differential decay width of the decay $\eta \to \gamma\mu^+\mu^-$. The solid line is calculated for the decay of a mixed η state, the dotted one for the decay of an unmixed one. The dot-dashed line describes the calculation with the standard VMD model.

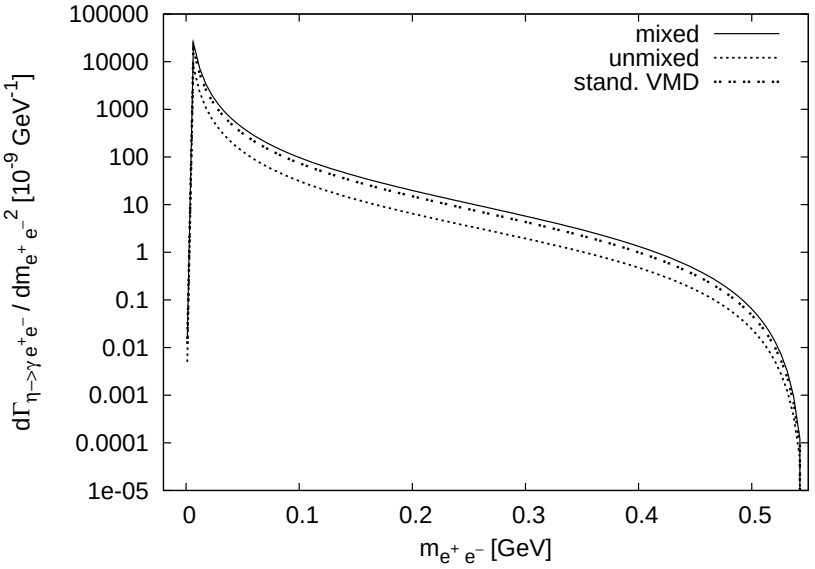

Figure 4.9: Single-differential decay width of the decay $\eta \to \gamma e^+ e^-$ calculated for the decay of a mixed η state (solid line), the decay of an unmixed one (dotted line) and the calculation with the standard VMD model (dot-dashed line).

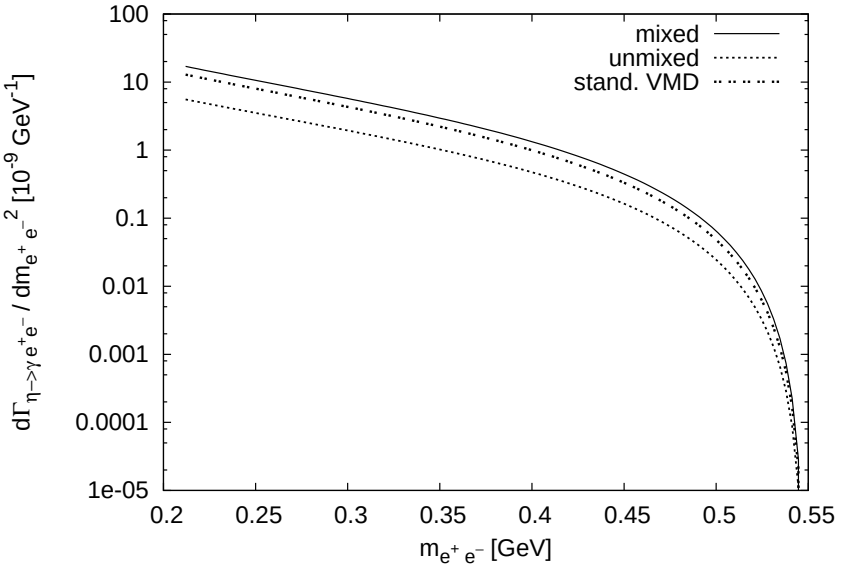

Figure 4.10: Same as Fig. 4.9 for $m_{e^+e^-} \geq 2m_\mu$ only.

4.6 Decay $\eta' \to \gamma l^+ l^-$

4.6.1 Form Factor for the $\eta' \to \gamma$ Transition

For the physical η'-meson $\eta' = \sin\theta\eta_8 + \cos\theta\eta_1$, the form factor for the transition into a real photon equals

$$f_{\eta'\gamma}(q) = \sin\theta f_{\eta_8\gamma}(q) + \cos\theta f_{\eta_1\gamma}(q) \tag{4.72}$$

with the form factors $f_{\eta_8\gamma}$ and $f_{\eta_1\gamma}$ given in subsection 4.5.1 for the $\eta_8 \to \gamma$ and $\eta_1 \to \gamma$ transition, respectively. For the $\eta' \to \gamma$ transition, the upper kinematic boundary is equal to $m_{\eta'} - m_\gamma = m_{\eta'} = 958\,\text{MeV}$ and therewith greater than the mass $m_\omega = 783\,\text{MeV}$ of the ω-meson and the mass $m_\rho = 776\,\text{MeV}$ of the ρ^0-meson. Hence, the propagator for these virtual vector mesons cannot be simplified as

$$S_V\left(q^2\right) \approx \frac{1}{q^2 - m(V)^2} \tag{4.73}$$

as it was done for the decays discussed so far. Instead, the propagator

$$S_V\left(q^2\right) = \frac{1}{q^2 - m(V)^2 + i\sqrt{q^2}\,\Gamma_V\left(q^2\right)} \tag{4.74}$$

with the energy-dependent width $\Gamma_V\left(q^2\right)$ given in subsection 2.6.1 has to be used.

On the left-hand side of Fig. 4.11, the normalised form factor (solid line) is plotted in comparison with the form factor for the unmixed $\eta' = \eta_1$ state (dotted line) and the standard VMD form factor (dot-dashed line). Analogical to the $\eta \to \gamma$ transition (see subsection 4.5.1), the standard VMD form factor can be calculated as

$$\begin{aligned} F_{\eta'\gamma}^{\text{VMD}}(q) = &-\frac{1}{6\left(\sin\theta + 2\sqrt{2}\cos\theta\right)}\Big[9\left(\sin\theta + \sqrt{2}\cos\theta\right)m_\rho^2 S_\rho(q^2) \\ &+ \left(\sin\theta + \sqrt{2}\cos\theta\right)m_\omega S_\omega(q^2) - 2\left(2\sin\theta - \sqrt{2}\cos\theta\right)m_\phi S_\phi(q^2)\Big]. \end{aligned} \tag{4.75}$$

Additionally, the absolute value of the quotient $f_{\eta'\gamma}^{\text{vec}}(q)/f_{\eta'\gamma}^{\text{WZW}}(q)$ is plotted in the figure on the right-hand side of Fig. 4.11. The absolute value has to be considered since the propagators for virtual ρ^0- and ω-mesons have to include the energy-dependent width $\Gamma_V\left(q^2\right)$ and, therefore, are not real anymore. As for the decays discussed before, the WZW part is important in the low-energy region. For higher energies, the vector part becomes more important. The absolute value $|f_{\eta'\gamma}^{\text{vec}}(q)|$ is equal to up to approximately 10 times the absolute value of the WZW term for $m_{l^+l^-} \approx 0.8\,\text{GeV}$. This greater importance decreases again near the kinematic boundary $m_{\eta'}$. Obviously, none of the two terms can be neglected for the form factor calculations.

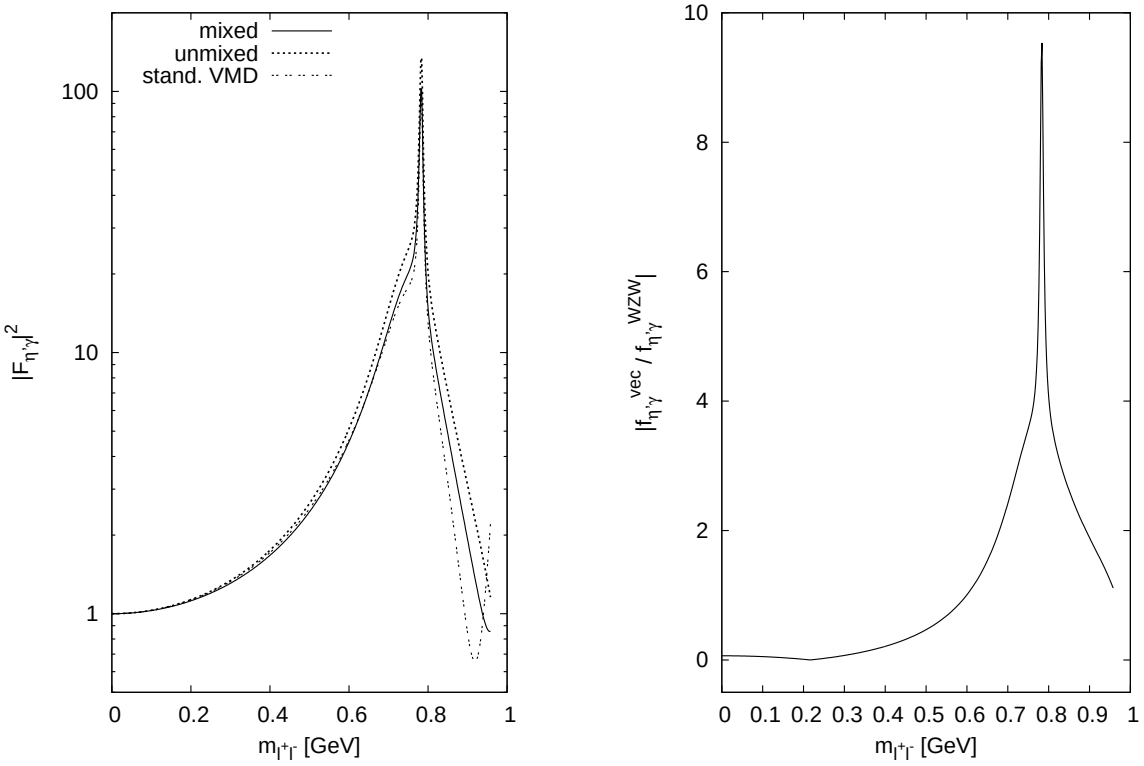

Figure 4.11: On the left-hand side, the normalised form factor for the $\eta' \to \gamma$ transition is plotted. The solid line describes the form factor for a mixed η'-meson, the dotted line the one for an unmixed $\eta' = \eta_1$ state and the dot-dashed line the standard VMD form factor. The plot on the right-hand side shows the quotient $|f^{\mathrm{vec}}_{\eta'\gamma}(q)/f^{\mathrm{WZW}}_{\eta'\gamma}(q)|$ for a mixed η'-meson.

4.6.2 Single-Differential and Full Partial Decay Widths

With formula (4.12) the full partial decay widths for the decays of an unmixed $\eta' = \eta_1$ state and the mixed physical η'-meson into two photons can be calculated:

$$\Gamma^{\mathrm{unmixed}}_{\eta'\to\gamma\gamma} = (7.08 \pm 0.29) \cdot 10^{-6}\,\mathrm{GeV}, \tag{4.76}$$

$$\Gamma^{\mathrm{mixed}}_{\eta'\to\gamma\gamma} = (4.63 \pm 0.27) \cdot 10^{-6}\,\mathrm{GeV}. \tag{4.77}$$

The width for the decay of the mixed η' state agrees with the experimental value [A+08]

$$\Gamma^{\mathrm{exp}}_{\eta'\to\gamma\gamma} = (4.28 \pm 0.56) \cdot 10^{-6}\,\mathrm{GeV} \tag{4.78}$$

quite well while the width for the decay of the unmixed state fails to do so. A similar observation has been done for the decay of an η-meson in subsection 4.5.2.

In Figs. 4.12, 4.13 and 4.14, the single-differential decay widths for the decays of an η'-meson into a real photon and a dimuon and into a photon and a dielectron in comparison

to the calculations done with the VMD model are plotted. As for the decay of an η-meson, great differences between the decays of an unmixed $\eta' = \eta_1$ state and a physical mixed η'-meson can be observed. Furthermore, the plots show a good agreement between the standard VMD calculation and the calculations done with the mixed physical η'-meson.

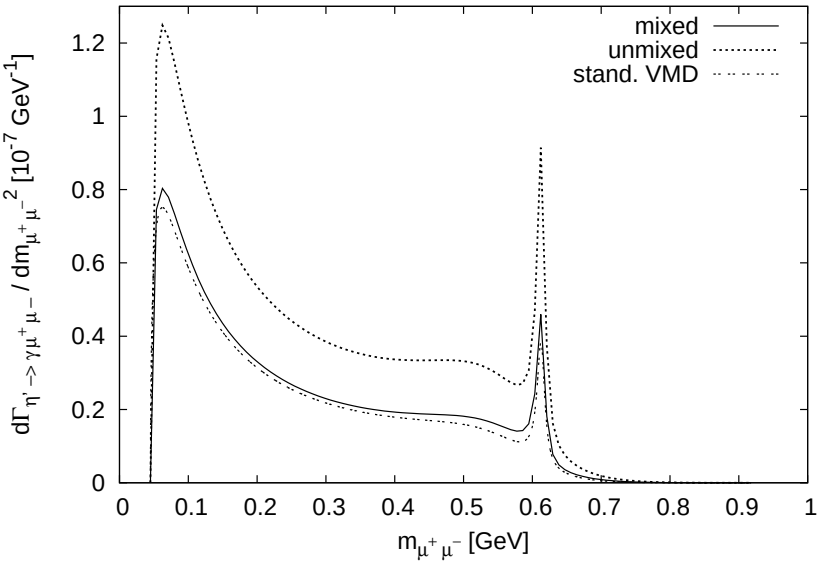

Figure 4.12: Single-differential decay width of the decay $\eta' \to \gamma\mu^+\mu^-$. The solid line is calculated for the decay of a mixed η state, the dotted one for the decay of an unmixed one. The dot-dashed line describes the calculation done with the standard VMD model.

For the decay into a dimuon, the value for the full partial decay width for the decay of the mixed η' state

$$\Gamma^{\text{mixed}}_{\eta' \to \gamma\mu^+\mu^-} = (1.77 \pm 0.21) \cdot 10^{-8}\,\text{GeV} \tag{4.79}$$

agrees with the experimental value taken from [A+08]

$$\Gamma^{\text{exp}}_{\eta' \to \gamma\mu^+\mu^-} = (2.10 \pm 0.68) \cdot 10^{-8}\,\text{GeV}. \tag{4.80}$$

Again, the value for the decay of the unmixed state

$$\Gamma^{\text{unmixed}}_{\eta' \to \gamma\mu^+\mu^-} = (2.96 \pm 0.09) \cdot 10^{-8}\,\text{GeV} \tag{4.81}$$

fails to do so.

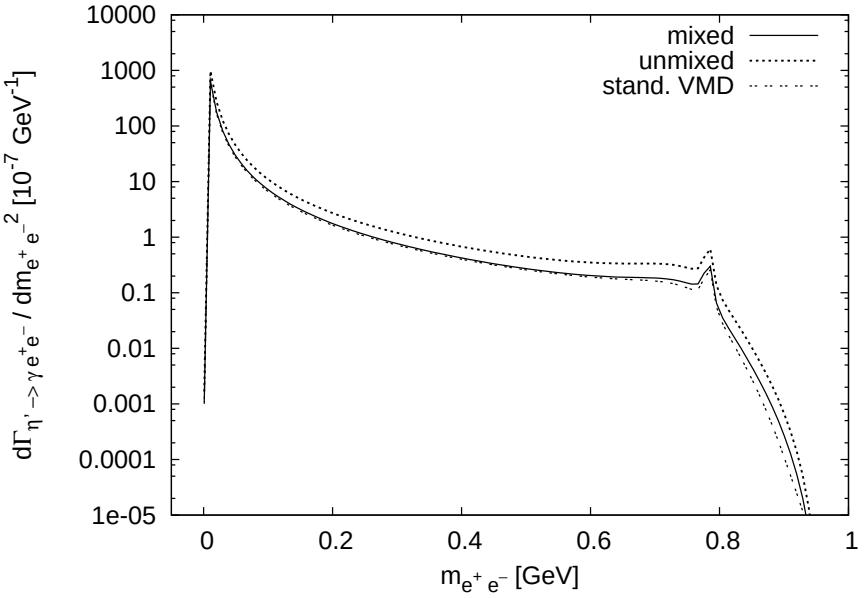

Figure 4.13: Single-differential decay width of the decay $\eta' \to \gamma e^+ e^-$ calculated for the decay of a mixed η state (solid), the decay of an unmixed one (dotted line) and with the standard VMD model (dot-dashed line).

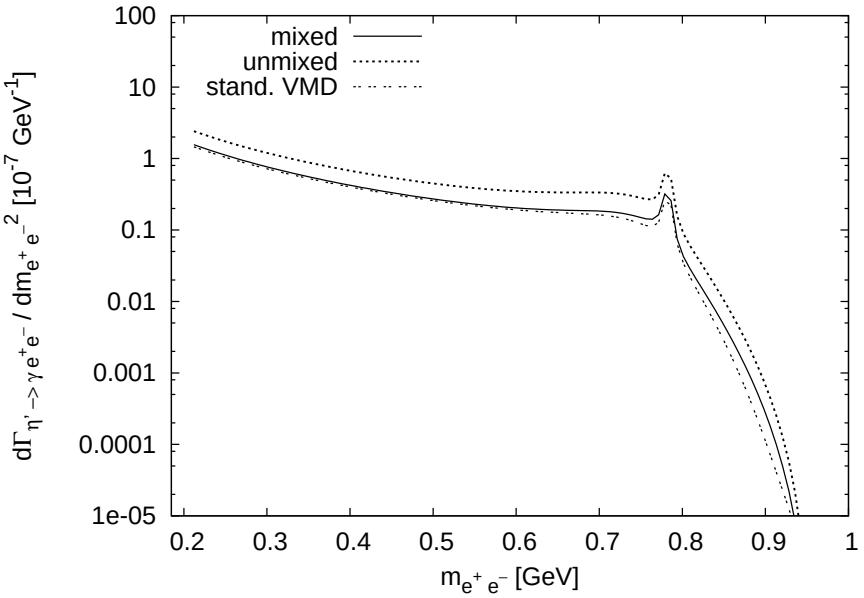

Figure 4.14: Same as Fig. 4.13 but for $m_{e^+e^-} \geq 2m_\mu$ only.

For the decay into a dielectron only an upper boundary

$$\Gamma^{\text{exp}}_{\eta' \to e^+e^-} < 1.836 \cdot 10^{-7}\,\text{GeV} \tag{4.82}$$

for the experimental partial decay width is available [A+08]. Thus, the widths for the decay of both the mixed and the unmixed η' state

$$\Gamma^{\text{mixed}}_{\eta' \to e^+e^-} = (9.41 \pm 0.46) \cdot 10^{-8}\,\text{GeV}, \tag{4.83}$$

$$\Gamma^{\text{unmixed}}_{\eta' \to e^+e^-} = (1.47 \pm 0.00) \cdot 10^{-7}\,\text{GeV} \tag{4.84}$$

agree with the experimental value.

From basically all results achieved here and in the previous section 4.5 it is obvious that the η-η' mixing is a necessary ingredient to obtain a satisfying agreement with the experimental data.

5 Decays of Pseudoscalar Mesons into Two Dileptons

In this chapter, decays of pseudoscalar mesons into two dileptons are considered. Thereby, one has to distinguish between decays into two different kinds of dileptons and decays into two identical dileptons. The decay width for decays into two different kinds of dileptons is developed in section 5.1 and the one for decays into two identical dileptons in section 5.2. In the subsequent sections 5.3, 5.4 and 5.5, the results for the decays of neutral pions, η- and η'-mesons into two dileptons are presented.

5.1 Decay Width For the Decay into Two Different Kinds of Dileptons

If a pseudoscalar meson decays into two different kinds of dileptons, the production of the measured four-momenta q_1 and q_2 of the first dilepton l_1 and the momenta q_3 and q_4 of the second dilepton $l_2 \neq l_1$ can be illustrated by two Feynman diagrams (Fig. 5.1). Either the "upper" virtual photon decays into the dilepton l_1 and the "lower" one into the dilepton l_2 (left-hand side of Fig. 5.1) or vice versa (right-hand side of Fig. 5.1). Then, the transition matrix element for the decay of a pseudoscalar meson P into two different kinds of dileptons l_1 and $l_2 \neq l_1$ with masses m_1 and m_2 equals

$$\begin{aligned}
&\mathcal{M}_{P\to l_1^+ l_1^- l_2^+ l_2^-} \\
&\quad = e^2 f_P(k^2,q^2)\,\varepsilon^{\mu\nu\alpha\beta}\,q_\mu k_\nu\,\frac{1}{k^2 q^2}\,\bar{u}_s(q_1)\gamma_\alpha v_{s'}(q_2)\,\bar{u}_\sigma(q_3)\gamma_\beta v_{\sigma'}(q_4) \\
&\qquad + e^2 f_P(q^2,k^2)\,\varepsilon^{\mu\nu\alpha\beta}\,k_\mu q_\nu\,\bar{u}_\sigma(q_3)\gamma_\alpha v_{\sigma'}(q_4)\,\frac{1}{q^2 k^2}\,\bar{u}_s(q_1)\gamma_\beta v_{s'}(q_2) \\
&\quad = e^2\left[f_P(k^2,q^2)+f_P(q^2,k^2)\right]\varepsilon^{\mu\nu\alpha\beta}\,q_\mu k_\nu\,\frac{1}{k^2 q^2}\bar{u}_s(q_1)\gamma_\alpha v_{s'}(q_2)\,\bar{u}_\sigma(q_3)\gamma_\beta v_{\sigma'}(q_4)
\end{aligned} \tag{5.1}$$

with the momenta of the virtual photons $k = q_1 + q_2$ and $q = q_3 + q_4$ analogical to the previous chapter 4.

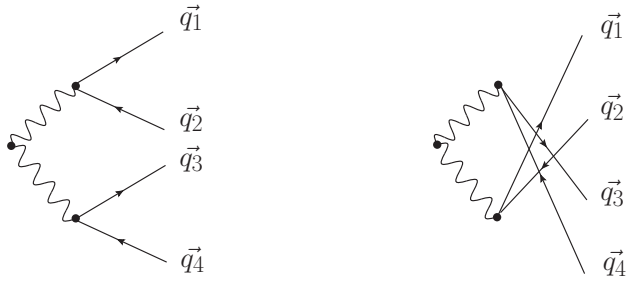

Figure 5.1: Feynman diagrams for the possibilities of a pseudoscalar meson to decay into two different kind of dileptons l_1 and $l_2 \neq l_1$ with four-momenta q_1, q_2 and q_3, q_4, respectively.

For the averaged squared matrix element the sum over the possible spins of the outgoing particles

$$\begin{aligned}
&\sum_{s,s',\sigma,\sigma'} \bar{u}_s(q_1)\gamma_\alpha v_{s'}(q_2)\;\bar{u}_\sigma(q_3)\gamma_\beta v_{\sigma'}(q_4)\cdot\bar{v}_{\sigma'}(q_4)\gamma_{\bar{\beta}} u_\sigma(q_3)\;\bar{v}_{s'}(q_2)\gamma_{\bar{\alpha}} u_s(q_1) \\
&\quad = \sum_{s,s',\sigma,\sigma'} (\bar{u}_s(q_1))_a(\gamma_\alpha)_{ab}(v_{s'}(q_2))_b\;(\bar{u}_\sigma(q_3))_c(\gamma_\beta)_{cd}(v_{\sigma'}(q_4))_d \\
&\qquad\qquad \cdot(\bar{v}_{\sigma'}(q_4))_e(\gamma_{\bar{\beta}})_{ef}(u_\sigma(q_3))_f\;(\bar{v}_{s'}(q_2))_g(\gamma_{\bar{\alpha}})_{gh}(u_s(q_1))_h
\end{aligned} \tag{5.2}$$

has to be calculated. Using $\sum_s u_s(p)\bar{u}_s(p) = \not{p} + m$ and $\sum_s v_s(p)\bar{v}_s(p) = \not{p} - m$, this can be simplified as

$$\begin{aligned}&(\not{q}_1 + m)_{ha}(\gamma_\alpha)_{ab}(\not{q}_2 - m)_{bg}(\gamma_{\bar{\alpha}})_{gh} \cdot (\not{q}_3 + m)_{fc}(\gamma_\beta)_{cd}(\not{q}_4 - m)_{de}(\gamma_{\bar{\beta}})_{ef} \\ &\quad = \operatorname{tr}\{(\not{q}_1 + m)\gamma_\alpha(\not{q}_2 - m)\gamma_{\bar{\alpha}}\}\ \operatorname{tr}\{(\not{q}_3 + m)\gamma_\beta(\not{q}_4 - m)\gamma_{\bar{\beta}}\}. \end{aligned} \tag{5.3}$$

Therewith, the averaged squared matrix element equals

$$\begin{aligned}\overline{\left|\mathcal{M}_{P\to l_1^+ l_1^- l_2^+ l_2^-}\right|^2} = W^{\alpha\beta\bar{\alpha}\bar{\beta}}(k^2, q^2)\ &\operatorname{tr}\{(\not{q}_1 + m_1)\gamma_\alpha(\not{q}_2 - m_1)\gamma_{\bar{\alpha}}\} \\ &\cdot \operatorname{tr}\{(\not{q}_3 + m_2)\gamma_\beta(\not{q}_4 - m_2)\gamma_{\bar{\beta}}\}\end{aligned} \tag{5.4}$$

with the abbreviation

$$W^{\alpha\beta\bar{\alpha}\bar{\beta}}(k^2, q^2) := e^4 \left| f_P(k^2, q^2) + f_P(q^2, k^2)\right|^2 \varepsilon^{\mu\nu\alpha\beta}\, \varepsilon^{\bar{\mu}\bar{\nu}\bar{\alpha}\bar{\beta}}\, q_\mu k_\nu\, q_{\bar{\mu}} k_{\bar{\nu}}\, \frac{1}{k^4 q^4}\,. \tag{5.5}$$

The general formula for the partial decay width of a decay of a particle P into four decay particles equals

$$\Gamma_{P\to 4 \text{ particles}} = \int \mathrm{d}\Phi_4\,(p; q_1, q_2, q_3, q_4)\ \frac{(2\pi)^4}{2m_P}\ \overline{\left|\mathcal{M}_{P\to 4 \text{ particles}}\right|^2} \tag{5.6}$$

with the four-body phase-space element

$$\mathrm{d}\Phi_4\,(p; q_1, q_2, q_3, q_4) = \delta^{(4)}\left(p - \sum_{i=1}^{4} q_i\right) \prod_{i=1}^{4} \frac{\mathrm{d}^3 q_i}{(2\pi)^3\, 2E_i} \tag{5.7}$$

including the four-momentum p of the decaying particle and the energies $E_1, \ldots, E_4$ of the four decay particles. Using notation (5.4) and inserting

$$1 = \int \delta^{(4)}\,(k - (q_1 + q_2))\ \delta^{(4)}\,(q - (q_3 + q_4))\ \mathrm{d}^4 k\, \mathrm{d}^4 q, \tag{5.8}$$

the partial decay width for the decay of a pseudoscalar particle into two different kinds of dileptons can be written as

$$\begin{aligned}&\Gamma_{P\to l_1^+ l_1^- l_2^+ l_2^-} \\ &\quad = \int \delta^{(4)}\left(p - \sum_{i=1}^{4} q_i\right) \prod_{i=1}^{4} \frac{\mathrm{d}^3 q_i}{(2\pi)^3\, 2E_i}\, \delta^{(4)}\,(k - (q_1 + q_2))\ \delta^{(4)}\,(q - (q_3 + q_4))\ \mathrm{d}^4 k\, \mathrm{d}^4 q \\ &\qquad \frac{(2\pi)^4}{2m_P}\, W^{\alpha\beta\bar{\alpha}\bar{\beta}}(k^2, q^2)\ \operatorname{tr}\{(\not{q}_1 + m_1)\gamma_\alpha(\not{q}_2 - m_1)\gamma_{\bar{\alpha}}\}\ \operatorname{tr}\{(\not{q}_3 + m_2)\gamma_\beta(\not{q}_4 - m_2)\gamma_{\bar{\beta}}\}.\end{aligned} \tag{5.9}$$

This integral can be splitted into an outer integration over $\mathrm{d}^4k\,\mathrm{d}^4q$ and an inner integration over $\mathrm{d}^3q_1 \ldots \mathrm{d}^3q_4$:

$$\begin{aligned}
&\int \delta^{(4)}\left(p - \sum_{i=1}^{4} q_i\right)\, \mathrm{d}^4k\,\mathrm{d}^4q\, \frac{1}{(2\pi)^8\, 2m_P} W^{\alpha\beta\bar{\alpha}\bar{\beta}}(k^2, q^2) \\
&\cdot \int \delta^{(4)}\left(k - q_1 - q_2\right)\, \delta^{(4)}\left(q - q_3 - q_4\right)\, \frac{\mathrm{d}q_1^3}{2E_1} \ldots \frac{\mathrm{d}^3q_4}{2E_4}\, \mathrm{tr}\{(\not{q}_1 + m_1)\gamma_\alpha(\not{q}_2 - m_1)\gamma_{\bar{\alpha}}\} \\
&\quad \mathrm{tr}\{(\not{q}_3 + m_2)\gamma_\beta(\not{q}_4 - m_2)\gamma_{\bar{\beta}}\} \\
&=: \int \delta^{(4)}\left(p - \sum_{i=1}^{4} q_i\right)\, \mathrm{d}^4k\,\mathrm{d}^4q\, \frac{1}{(2\pi)^8\, 2m_P} W^{\alpha\beta\bar{\alpha}\bar{\beta}}(k^2, q^2) \cdot J_{\alpha\beta\bar{\alpha}\bar{\beta}}(k, q). \qquad (5.10)
\end{aligned}$$

The outer integral only depends on the momenta k and q of the virtual photons and does not explicitly depend on the single momenta $q_1, \ldots, q_4$ of leptons and antileptons anymore. Therefore, the inner integral $J_{\alpha\beta\bar{\alpha}\bar{\beta}}(k, q)$ over $\mathrm{d}^3q_1 \ldots \mathrm{d}^3q_4$ can be calculated independently of the outer integral. As it will be shown in the next subsection, this integrations can be performed analytically. For that, the integral $J_{\alpha\beta\bar{\alpha}\bar{\beta}}(k, q)$ is split into two integrals concerning the integration over d^3q_1 and d^3q_2 on the one hand and the integration over d^3q_3 and d^3q_4 on the other hand and equals

$$\begin{aligned}
J_{\alpha\beta\bar{\alpha}\bar{\beta}}(k, q) = &\int \frac{\mathrm{d}^3q_1}{2E_1} \frac{\mathrm{d}^3q_2}{2E_2}\, \mathrm{tr}\{(\not{q}_1 + m_1)\gamma_\alpha(\not{q}_2 - m_1)\gamma_{\bar{\alpha}}\}\, \delta^{(4)}(k - q_1 - q_2) \\
&\cdot \int \frac{\mathrm{d}^3q_3}{2E_3} \frac{\mathrm{d}^3q_4}{2E_4}\, \mathrm{tr}\{(\not{q}_3 + m_2)\gamma_\beta(\not{q}_4 - m_2)\gamma_{\bar{\beta}}\}\, \delta^{(4)}(q - q_3 - q_4) \\
= 16 &\int \frac{\mathrm{d}^3q_1}{2E_1} \frac{\mathrm{d}^3q_2}{2E_2}\, \left[(q_1)_\alpha(q_2)_{\bar{\alpha}} + (q_1)_{\bar{\alpha}}(q_2)_\alpha - g_{\alpha\bar{\alpha}}(q_1 \cdot q_2 + m_1^2)\right] \delta^{(4)}(k - q_1 - q_2) \\
&\cdot \int \frac{\mathrm{d}^3q_3}{2E_3} \frac{\mathrm{d}^3q_4}{2E_4}\, \left[(q_3)_\beta(q_4)_{\bar{\beta}} + (q_3)_{\bar{\beta}}(q_4)_\beta - g_{\beta\bar{\beta}}(q_3 \cdot q_4 + m_2^2)\right] \delta^{(4)}(q - q_3 - q_4). \qquad (5.11)
\end{aligned}$$

5.1.1 Solving the Integral $J_{\alpha\beta\bar{\alpha}\bar{\beta}}(k, q)$

To solve the integral $J_{\alpha\beta\bar{\alpha}\bar{\beta}}(k, q)$, integrals of the type

$$\int \frac{\mathrm{d}^3x}{2E_x} \frac{\mathrm{d}^3y}{2E_y}\, \delta^{(4)}(z - x - y)\, h(x, y) = \int \frac{\mathrm{d}^3x}{2E_x} \frac{\mathrm{d}^3y}{2E_y}\, \delta^{(4)}(z - x - y)\, h(x, z - x) \qquad (5.12)$$

have to be solved including a function $h(x, z - x)$ only depending on z^2 and on linearly appearing factors $x_{\rho_1}, x_{\rho_2}, \ldots, y_{\sigma_1}, y_{\sigma_2}, \ldots$. Using $y_\sigma = z_\sigma - x_\sigma$, the following integrals

including the energies $E_x = \sqrt{m^2 + \vec{x}^2}$ and $E_y = \sqrt{m^2 + \vec{y}^2}$ are those types needed to evaluate $J_{\alpha\beta\bar{\alpha}\bar{\beta}}(k, q)$:

$$I(z^2) := \int \frac{\mathrm{d}^3x}{2E_x} \frac{\mathrm{d}^3y}{2E_y} \delta^{(4)}(z - x - y), \tag{5.13}$$

$$I_\rho(z) := \int \frac{\mathrm{d}^3x}{2E_x} \frac{\mathrm{d}^3y}{2E_y} \delta^{(4)}(z - x - y)\, x_\rho, \tag{5.14}$$

$$I_{\rho\sigma}(z) := \int \frac{\mathrm{d}^3x}{2E_x} \frac{\mathrm{d}^3y}{2E_y} \delta^{(4)}(z - x - y)\, x_\rho x_\sigma. \tag{5.15}$$

As a first step, the integral $I(z^2)$ has to be evaluated. This integral is Lorentz invariant and thus can be calculated in the frame where $\vec{z} = 0$ because only z with $z^2 > 0$ are of interest. Then, $I(z^2)$ equals

$$\begin{aligned} I(z^2) &= \int \frac{\mathrm{d}^3x}{2E_x} \frac{\mathrm{d}^3y}{2E_y} \delta(\sqrt{z^2} - E_x - E_y)\, \delta^{(3)}(\vec{x} + \vec{y}) \\ &= \int \frac{\mathrm{d}^3x}{2E_x} \frac{1}{2\sqrt{m^2 + \vec{x}^2}} \delta(\sqrt{z^2} - E_x - \sqrt{m^2 + \vec{x}^2}) \\ &= \int |\vec{x}|^2 \,\mathrm{d}\,|\vec{x}|\; \mathrm{d}\cos\theta_x \,\mathrm{d}\phi_x \frac{1}{4E_x^2} \delta(\sqrt{z^2} - 2E_x) \\ &= \pi \int_0^\infty \mathrm{d}\,|\vec{x}|\; |\vec{x}|^2 \; \frac{1}{E_x^2} \delta(\sqrt{z^2} - 2E_x). \end{aligned}$$

After the substitution $|\vec{x}| = \sqrt{E_x^2 - m^2}$,$|\vec{x}|\,\mathrm{d}\,|\vec{x}| = E_x \mathrm{d}E_x$. Hence, the integral equals

$$\begin{aligned} I(z^2) &= \pi \int_m^\infty \mathrm{d}E_x\, E_x \sqrt{E_x^2 - m^2}\, \frac{1}{E_x^2} \delta(\sqrt{z^2} - 2E_x) \\ &= \frac{1}{2}\pi \sqrt{\frac{1}{4}z^2 - m^2}\, \frac{1}{\frac{1}{2}\sqrt{z^2}}\, \Theta\left(\sqrt{z^2} - 2m\right) \\ &= \frac{1}{2}\pi \frac{\sqrt{z^2 - 4m^2}}{\sqrt{z^2}}\, \Theta\left(\sqrt{z^2} - 2m\right). \end{aligned} \tag{5.16}$$

The integral $I_\rho(z)$ only depends on the four-vector z and, thus, it has the general form

$$I_\rho(z) = A(z^2) z_\rho. \tag{5.17}$$

If both sides are multiplied with z^ρ and the sum over ρ is performed, $A(z^2)$ will be determined as

$$A(z^2) = \frac{1}{z^2}\, z^\rho I_\rho(z) \tag{5.18}$$

with $z^\rho I_\rho$ being equal to

$$z^\rho I_\rho(z) = \int \frac{\mathrm{d}^3x}{2E_x}\frac{\mathrm{d}^3y}{2E_y}\,\delta^{(4)}(z-x-y)\,z\cdot x.$$

Since the scalar product $z\cdot x$ can be written as

$$(x+y)\cdot x = x^2 + y\cdot x = x^2 + \frac{1}{2}(z^2-x^2-y^2) = m^2 + \frac{1}{2}(z^2-m^2-m^2) = \frac{1}{2}z^2,$$

the integral above equals

$$\int \frac{\mathrm{d}^3x}{2E_x}\frac{\mathrm{d}^3y}{2E_y}\,\delta^{(4)}(z-x-y)\,\frac{1}{2}z^2 = \frac{1}{2}z^2 I(z^2).$$

Hence, $A(z^2)$ and therewith $I_\rho(z)$ can be determined as

$$I_\rho(z) = \frac{1}{2}I(z^2)z_\rho. \tag{5.19}$$

The general form for the last of the needed integrals equals

$$I_{\rho\sigma}(z) = B(z^2)g_{\rho\sigma} + C(z^2)z_\rho z_\sigma. \tag{5.20}$$

To determine $B(z^2)$ and $C(z^2)$ the integrals

$$\begin{aligned} I_\rho{}^\rho(z) &= I_{\rho\sigma}(z)g^{\rho\sigma} = 4B(z^2) + z^2C(z^2),\\ z^\rho z^\sigma I_{\rho\sigma}(z) &= z^2B(z^2) + z^4C(z^2) \end{aligned}$$

are used yielding the following representation for $B(z^2)$ and $C(z^2)$:

$$\begin{aligned} B(z^2) &= \frac{1}{3}I_\rho{}^\rho(z) - \frac{1}{3z^2}z^\rho z^\sigma I_{\rho\sigma}(z),\\ C(z^2) &= -\frac{1}{3z^2}I_\rho{}^\rho(z) + \frac{4}{3z^4}z^\rho z^\sigma I_{\rho\sigma}(z). \end{aligned}$$

As those integrals can be calculated as

$$\begin{aligned} I_\rho{}^\rho(z) &= \int \frac{\mathrm{d}^3x}{2E_x}\frac{\mathrm{d}^3y}{2E_y}\,\delta^{(4)}(z-x-y)\,x^2 = m^2 I(z^2),\\ z^\rho z^\sigma I_{\rho\sigma}(z) &= \int \frac{\mathrm{d}^3x}{2E_x}\frac{\mathrm{d}^3y}{2E_y}\,\delta^{(4)}(z-x-y)\,(z\cdot x)^2 = \frac{1}{4}z^4 I(z^2), \end{aligned}$$

the considered integral equals

$$I_{\rho\sigma}(z) = \frac{1}{3}I(z^2)\left[-\frac{1}{4}(z^2-4m^2)g_{\rho\sigma} + (z^2-m^2)\frac{z_\rho z_\sigma}{z^2}\right]. \tag{5.21}$$

To evaluate $J_{\alpha\beta\bar{\alpha}\bar{\beta}}(k,q)$ the following integral has to be calculated (cf. (5.11)):

$$\begin{aligned}
&\int \frac{\mathrm{d}^3x}{2E_x}\,\frac{\mathrm{d}^3y}{2E_y}\,\delta^{(4)}(z-x-y)\,\Big[x_\rho y_\sigma + x_\sigma y_\rho - g_{\rho\sigma}(x\cdot y + m^2)\Big] \\
&\quad= \int \frac{\mathrm{d}^3x}{2E_x}\,\frac{\mathrm{d}^3y}{2E_y}\,\delta^{(4)}(z-x-y)\,\Big[x_\rho z_\sigma - x_\rho x_\sigma + x_\sigma z_\rho - x_\sigma x_\rho - g_{\rho\sigma}(\frac{1}{2}z^2 - m^2 + m^2)\Big] \\
&\quad= I_\rho(z) z_\sigma - I_{\rho\sigma}(z) + I_\sigma(z) z_\rho - I_{\sigma\rho}(z) - \frac{1}{2}z^2 I(z^2) g_{\rho\sigma} \\
&\quad= 2I_\rho(z) z_\sigma - 2I_{\rho\sigma}(z) - \frac{1}{2}z^2 I(z^2) g_{\rho\sigma} \\
&\quad= \frac{1}{3}(z^2+2m^2)\, I(z^2)\,\left[\frac{z_\rho z_\sigma}{z^2} - g_{\rho\sigma}\right].
\end{aligned} \tag{5.22}$$

Thus, the wanted result is

$$\begin{aligned}
J_{\alpha\beta\bar{\alpha}\bar{\beta}} = &\frac{4}{9}\pi^2\,\frac{\sqrt{k^2-4m_1^2}}{\sqrt{k^2}}\,(k^2+2m_1^2)\,\frac{\sqrt{q^2-4m_2^2}}{\sqrt{q^2}}\,(q^2+2m_2^2)\,\left[\frac{k_\alpha k_{\bar{\alpha}}}{k^2} - g_{\alpha\bar{\alpha}}\right]\left[\frac{q_\beta q_{\bar{\beta}}}{q^2} - g_{\beta\bar{\beta}}\right] \\
&\cdot \Theta\left(\sqrt{k^2}-2m_1\right)\,\Theta\left(\sqrt{q^2}-2m_2\right).
\end{aligned} \tag{5.23}$$

5.1.2 Calculation of the Full Decay Width

To evaluate the decay width, the factors $W^{\alpha\beta\bar{\alpha}\bar{\beta}}(k^2,q^2)$ and $J_{\alpha\beta\bar{\alpha}\bar{\beta}}(k,q)$ have to be multiplied and contracted. As $\varepsilon^{\mu\nu\alpha\beta}q_\mu k_\nu k_\alpha = \varepsilon^{\mu\nu\alpha\beta}q_\mu k_\nu q_\beta = 0$, only terms of $J_{\alpha\beta\bar{\alpha}\bar{\beta}}(k,q)$ not including k_α or q_β have to be considered. By inserting

$$g_{\alpha\bar{\alpha}}g_{\beta\bar{\beta}}\,\varepsilon^{\mu\nu\alpha\beta}\,\varepsilon^{\bar{\mu}\bar{\nu}\bar{\alpha}\bar{\beta}}\,q_\mu k_\nu\,q_{\bar{\mu}}k_{\bar{\nu}} = 2\left[(k\cdot q)^2 - k^2q^2\right] \tag{5.24}$$

the full partial decay width becomes

$$\begin{aligned}
\Gamma_{P\to l_1^+ l_1^- l_2^+ l_2^-} = &\int \delta^{(4)}(p-(q+k))\,\mathrm{d}^4k\,\mathrm{d}^4q\,\frac{1}{(2\pi)^8\,2m_P}\,g_{\alpha\bar{\alpha}}g_{\beta\bar{\beta}}\,W^{\alpha\beta\bar{\alpha}\bar{\beta}}(k^2,q^2) \\
&\cdot\frac{4}{9}\pi^2\,\frac{\sqrt{k^2-4m_1^2}}{\sqrt{k^2}}\,(k^2+2m_1^2)\,\frac{\sqrt{q^2-4m_2^2}}{\sqrt{q^2}}\,(q^2+2m_2^2) \\
&\cdot\Theta\left(\sqrt{k^2}-2m_1\right)\,\Theta\left(\sqrt{q^2}-2m_2\right) \\
= &\frac{e^4}{(2\pi)^6\,9m_P}\int \delta^{(4)}(p-(q+k))\,\mathrm{d}^4k\,\mathrm{d}^4q\,\left|f_P(k^2,q^2)+f_P(q^2,k^2)\right|^2\,\frac{1}{k^4q^4} \\
&\cdot\left[(k\cdot q)^2-k^2q^2\right]\,\frac{\sqrt{k^2-4m_1^2}}{\sqrt{k^2}}\,(k^2+2m_1^2)\,\frac{\sqrt{q^2-4m_2^2}}{\sqrt{q^2}}\,(q^2+2m_2^2) \\
&\cdot\,\Theta\left(\sqrt{k^2}-2m_1\right)\,\Theta\left(\sqrt{q^2}-2m_2\right).
\end{aligned} \tag{5.25}$$

This integral includes only the four-vector momenta k and q of the virtual photons. Therefore, the problem is reduced to a decay into two particles. These particles would have the masses $m_k = \sqrt{k^2}$ and $m_q = \sqrt{q^2}$. Then, the following relations hold in the rest frame of the decaying pseudoscalar meson P [A+08]:

$$\begin{aligned} \left|\vec{k}\right| = \left|\vec{q}\right| &= \frac{1}{2m_P}\left[\left(m_P^2 - \left(\sqrt{k^2}+\sqrt{q^2}\right)^2\right)\left(m_P^2 - \left(\sqrt{k^2}-\sqrt{q^2}\right)^2\right)\right]^{1/2}, \\ k\cdot q &= \frac{1}{2}\left[m_P^2 - (k^2+q^2)\right]. \end{aligned} \tag{5.26}$$

Furthermore, the four-dimensional integral $\int \mathrm{d}^4 z$ can be written as $\int \mathrm{d}z^2 \, \frac{\mathrm{d}^3 z}{2E_z}$ if the integration over z_0 is restricted to positive values. Therewith, the following transformations can be performed:

$$\begin{aligned} \int \mathrm{d}^4k \, \mathrm{d}^4q \, \delta^{(4)}\left(p-(k+q)\right) &= (2\pi)^6 \int \mathrm{d}k^2 \, \mathrm{d}q^2 \int \frac{\mathrm{d}^3k}{(2\pi)^3\, 2E_k} \frac{\mathrm{d}^3q}{(2\pi)^3\, 2E_q} \, \delta^{(4)}\left(p-(k+q)\right) \\ &= (2\pi)^6 \int \mathrm{d}k^2 \, \mathrm{d}q^2 \int \mathrm{d}\Phi_2(p;k,q). \end{aligned} \tag{5.27}$$

As $\int \mathrm{d}\Phi_2(p;k,q) = \left[(2\pi)^5\, 2m_P\right]^{-1} \left|\vec{k}\right|$ [PS95], this equals

$$\frac{\pi}{m_P} \int \mathrm{d}k^2 \, \mathrm{d}q^2 \, \left|\vec{k}\right|. \tag{5.28}$$

Including all previous calculations, the full partial decay width equals

$$\begin{aligned} \Gamma_{P\to l_1^+ l_1^- l_2^+ l_2^-} = &\frac{e^4}{(2\pi)^5\, 36 m_P^3} \int \mathrm{d}k^2 \, \mathrm{d}q^2 \, \left|f_P(k^2,q^2) + f_P(q^2,k^2)\right|^2 \, \frac{(k^2+2m_1^2)(q^2+2m_2^2)}{k^4 q^4} \\ &\frac{\sqrt{k^2-4m_1^2}}{\sqrt{k^2}} \, \frac{\sqrt{q^2-4m_2^2}}{\sqrt{q^2}} \, \sqrt{\left(m_P^2 - (\sqrt{k^2}+\sqrt{q^2})^2\right)\left(m_P^2 - (\sqrt{k^2}-\sqrt{q^2})^2\right)} \\ &\left[\frac{1}{4}\left(m_P^2 - (k^2+q^2)\right)^2 - k^2q^2\right] \\ = &\frac{e^4}{(2\pi)^5\, 18 m_P^3} \int \mathrm{d}k^2 \, \mathrm{d}q^2 \, \left|f_P(k^2,q^2) + f_P(q^2,k^2)\right|^2 \, \frac{(k^2+2m_1^2)(q^2+2m_2^2)}{k^4 q^4} \\ &\frac{\sqrt{k^2-4m_1^2}}{\sqrt{k^2}} \, \frac{\sqrt{q^2-4m_2^2}}{\sqrt{q^2}} \, \left[\frac{1}{4}\left(m_P^2 - (k^2+q^2)\right)^2 - k^2q^2\right]^{3/2} \end{aligned} \tag{5.29}$$

with k^2 running from $4m_1^2$ to $(m_P - 2m_2)^2$ and q^2 from $4m_2^2$ to $(m_P - \sqrt{k^2})^2$.

5.2 Decay Width For the Decay into Two Identical Dileptons

5.2.1 The General Squared Matrix Element

In the case of a decay of a pseudoscalar particle into two identical dileptons, the measured momenta q_1 and q_3 of the leptons and q_2 and q_4 of the antileptons can be produced from all of the possibilities shown in Fig. 5.2[1]. As leptons are fermions, each exchange of two leptons or antileptons according to the first possibility produces an extra minus sign.

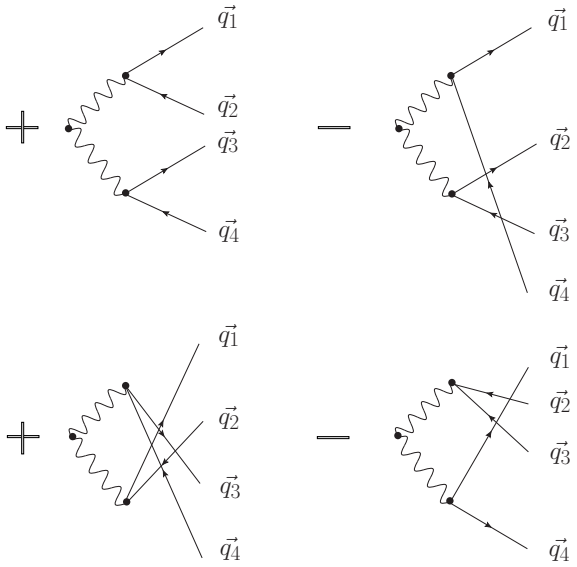

Figure 5.2: The four different possibilities to produce the measured momenta q_1 and q_3 of the leptons and q_2 and q_4 of the antileptons in the case of a decay into two identical dileptons.

These possibilities yield a transition matrix element consisting of four terms, each one including one of the factors

$$
\begin{aligned}
a_1 &:= +\,\bar{u}_s(q_1)\gamma_\alpha v_{s'}(q_2)\;\bar{u}_\sigma(q_3)\gamma_\beta v_{\sigma'}(q_4),\\
a_2 &:= -\,\bar{u}_s(q_1)\gamma_\alpha v_{s'}(q_4)\;\bar{u}_\sigma(q_3)\gamma_\beta v_{\sigma'}(q_2),\\
a_3 &:= +\,\bar{u}_s(q_3)\gamma_\alpha v_{s'}(q_4)\;\bar{u}_\sigma(q_1)\gamma_\beta v_{\sigma'}(q_2),\\
a_4 &:= -\,\bar{u}_s(q_3)\gamma_\alpha v_{s'}(q_2)\;\bar{u}_\sigma(q_1)\gamma_\beta v_{\sigma'}(q_4)
\end{aligned}
$$

[1] In section 5.1, the first and the third possibility have been chosen to describe the decay into two different kinds of dileptons. Taking the second and the third possibility would only produce an overall negative sign which would not be relevant for any observables.

with signs defined relative to a_1. As only the squared matrix element is contained in observables, the absolute sign of a_1 is irrelevant.

For the calculation of a single-differential or full partial decay width the averaged squared matrix element is needed. The full transition matrix element has the form

$$\begin{aligned}\mathcal{M} = {} & g(q_1+q_2, q_3+q_4)a_1 + g(q_1+q_4, q_3+q_2)a_2 \\ & + g(q_3+q_4, q_1+q_2)a_3 + g(q_3+q_2, q_1+q_4)a_4 \end{aligned} \tag{5.30}$$

with not yet fixed functions $g(q_{I_1}+q_{I_2}, q_{I_3}+q_{I_4})$ which amongst others include the transition form factor. To evaluate a partial decay width, an integration over $\mathrm{d}^3 q_i$ has to be performed for all $i = 1, \ldots, 4$. Hence, the variables $q_1, \ldots, q_4$ can be renamed yielding $a_i \bar{a}_j = a_j \bar{a}_i$ for all $i, j = 1, \ldots, 4$. Thus, the squared matrix element equals

$$\begin{aligned}|\mathcal{M}|^2 = {} & \Big[|g(q_1+q_2, q_3+q_4)|^2 |a_1|^2 + |g(q_1+q_4, q_3+q_2)|^2 |a_2|^2 \\ & + |g(q_3+q_4, q_1+q_2)|^2 |a_3|^2 + |g(q_3+q_2, q_1+q_4)|^2 |a_4|^2 \\ & + 2g(q_1+q_2, q_3+q_4)\, \overline{g(q_1+q_4, q_3+q_2)} a_1 \bar{a}_2 \\ & + 2g(q_1+q_2, q_3+q_4)\, \overline{g(q_3+q_4, q_1+q_2)} a_1 \bar{a}_3 \\ & + 2g(q_1+q_2, q_3+q_4)\, \overline{g(q_3+q_2, q_1+q_4)} a_1 \bar{a}_4 \\ & + 2g(q_1+q_4, q_3+q_2)\, \overline{g(q_3+q_4, q_1+q_2)} a_2 \bar{a}_3 \\ & + 2g(q_1+q_4, q_3+q_2)\, \overline{g(q_3+q_2, q_1+q_4)} a_2 \bar{a}_4 \\ & + 2g(q_3+q_4, q_1+q_2) \overline{g(q_3+q_2, q_1+q_4)} a_3 \bar{a}_4 \Big] . \end{aligned} \tag{5.31}$$

Some of these terms are equal. E.g., after renaming q_1 as q_3 and q_2 as q_4 in the fifth term, the fifth and the tenth term will be equal. Furthermore, after renaming variables the first four terms, the terms 6 and 9 and the terms 7 and 8 will be equal. So, the squared matrix element reduces to

$$\begin{aligned}|\mathcal{M}|^2 = 4 \Big[& |g(q_1+q_2, q_3+q_4)|^2 \, |a_1|^2 \\ & + g(q_1+q_2, q_3+q_4)\, \overline{g(q_1+q_4, q_3+q_2)} \; a_1 \bar{a}_2 \\ & + g(q_1+q_2, q_3+q_4)\, \overline{g(q_3+q_4, q_1+q_2)} \; a_1 \bar{a}_3 \\ & + g(q_1+q_2, q_3+q_4)\, \overline{g(q_3+q_2, q_1+q_4)} \; a_1 \bar{a}_4 \Big] \end{aligned} \tag{5.32}$$

with $a_1 \bar{a}_2$ and $a_1 \bar{a}_4$ producing a negative sign. Thus, the four combinations involving a_1 are the only ones which have to be considered. Analogically to the determination of Eq.

(5.3) one gets the following relations including the mass m of the leptons:

$$\sum_{s,s',\sigma,\sigma'} |a_1|^2 = \operatorname{tr}\{(\not{q}_1 + m)\gamma_\alpha(\not{q}_2 - m)\gamma_{\bar{\alpha}}\}\ \operatorname{tr}\{(\not{q}_3 + m)\gamma_\beta(\not{q}_4 - m)\gamma_{\bar{\beta}}\}, \tag{5.33}$$

$$\sum_{s,s',\sigma,\sigma'} a_1\bar{a}_2 = -\operatorname{tr}\{(\not{q}_1 + m)\gamma_\alpha(\not{q}_2 - m)\gamma_{\bar{\beta}}(\not{q}_3 + m)\gamma_\beta(\not{q}_4 - m)\gamma_{\bar{\alpha}}\}, \tag{5.34}$$

$$\sum_{s,s',\sigma,\sigma'} a_1\bar{a}_3 = \operatorname{tr}\{(\not{q}_1 + m)\gamma_\alpha(\not{q}_2 - m)\gamma_{\bar{\beta}}\}\operatorname{tr}\{(\not{q}_3 + m)\gamma_\beta(\not{q}_4 - m)\gamma_{\bar{\alpha}}\}, \tag{5.35}$$

$$\sum_{s,s',\sigma,\sigma'} a_1\bar{a}_4 = -\operatorname{tr}\{(\not{q}_1 + m)\gamma_\alpha(\not{q}_2 - m)\gamma_{\bar{\alpha}}(\not{q}_3 + m)\gamma_\beta(\not{q}_4 - m)\gamma_{\bar{\beta}}\}. \tag{5.36}$$

5.2.2 Calculating Integrals over $\mathrm{d}\Phi_4\,(p; q_1, q_2, q_3, q_4)$

The formula for the decay width for a decay of a pseudoscalar meson into two identical dileptons is much more complicated than the one for the decay into two different kinds of dileptons. Some of the terms the averaged squared matrix element consists of cannot be integrated by using the tricks given in section 5.1. In such cases, the integral depends on all the combinations $q_1 + q_2$, $q_3 + q_4$, $q_1 + q_4$ and $q_3 + q_2$. Thus, it is not possible to separate the integration over the three-momenta $\vec{q_1}, \ldots, \vec{q_4}$ from the integration over $(q_1 + q_2)^2, \ldots, (q_3 + q_2)^2$ and one has to integrate numerically over the full four-body phase space $\mathrm{d}\Phi_4\,(p; q_1, q_2, q_3, q_4)$ defined in Eq. (5.7). In this subsection, a possibility to reduce this integral to a less-dimensional integral will be presented.

As a first step, the four-body phase space is expanded by an additional δ-function yielding

$$\begin{aligned}
\mathrm{d}\Phi_4\,(p; q_1, q_2, q_3, q_4) &= \delta^{(4)}\left(p - \sum_{i=1}^{4} q_i\right) \prod_{i=1}^{4} \frac{\mathrm{d}^3 q_i}{(2\pi)^3\, 2E_i} \\
&= \int \delta^{(4)}\left(p - \sum_{i=1}^{4} q_i\right) \delta\left(q_4^2 - m^2\right) \Theta\left(E_4 - m\right) \frac{\mathrm{d}^4 q_4}{(2\pi)^3} \prod_{k=1}^{3} \frac{\mathrm{d}^3 q_k}{(2\pi)^3\, 2E_k} \\
&= \frac{1}{8\,(2\pi)^{12}}\, \delta\left[\left(p - \sum_{k=1}^{3} q_k\right)^2 - m^2\right] \Theta\left(E_4 - m\right) \prod_{k=1}^{3} \frac{\mathrm{d}^3 q_k}{E_k}
\end{aligned} \tag{5.37}$$

and reducing the twelve-dimensional integral to a nine-dimensional integral including $E_4 = p_0 - E_1 - E_2 - E_3$. In spherical coordinates, this integral can be represented as

$$\frac{1}{8\,(2\pi)^{12}}\, \delta\left[\left(p - \sum_{k=1}^{3} q_k\right)^2 - m^2\right] \Theta\left(E_4 - m\right) \prod_{k=1}^{3} \frac{|\vec{q}_k|^2}{E_k}\, \mathrm{d}|\vec{q}_k|\, \mathrm{d}\cos\theta_k\, \mathrm{d}\phi_k. \tag{5.38}$$

The limits of the integral over $\mathrm{d}\Phi_4\,(p; q_1, q_2, q_3, q_4)$ are given by the considered decay and will be specified in the next subsection.

If the integration over $\mathrm{d}q_3$ is performed first, the axes of the coordinate system can be chosen in such a way that the spherical representations of $\vec{q}_1$, $\vec{q}_2$ and $\vec{q}_3$ equal

$$\vec{q}_1 = |\vec{q}_1|\,\vec{e}_z, \tag{5.39}$$
$$\vec{q}_2 = |\vec{q}_2|\,(\sin\theta_2\,\vec{e}_x + \cos\theta_2\,\vec{e}_z)\,, \tag{5.40}$$
$$\vec{q}_3 = |\vec{q}_3|\,(\sin\theta_3\cos\phi_3\,\vec{e}_x + \sin\theta_3\sin\phi_3\,\vec{e}_y + \cos\theta_3\,\vec{e}_z) \tag{5.41}$$

with the unit vectors $\vec{e}_x$, $\vec{e}_y$ and $\vec{e}_z$. In this representation, the integrand of the integral over $\mathrm{d}\Phi_4\,(p; q_1, \ldots, q_4)$ is independent of $\cos\theta_1$, ϕ_1 and ϕ_2 and therefore the integration over these variables only yields a factor $2 \cdot 2\pi \cdot 2\pi = 8\pi^2$.

In the rest frame of the decaying meson P, the argument of the δ-function equals

$$\begin{aligned}
\left(p - \sum_{k=1}^{3} q_k\right)^2 - m^2 &= \left(m_P - \sum_{k=1}^{3} E_k, -\vec{q}_1 - \vec{q}_2 - \vec{q}_3\right)^2 - m^2 \\
&= \left(m_P - \sum_{k=1}^{3} E_k\right)^2 - |\vec{q}_1|^2 - |\vec{q}_2|^2 - |\vec{q}_3|^2 - 2\,[\vec{q}_1\cdot\vec{q}_2 + \vec{q}_1\cdot\vec{q}_3 + \vec{q}_2\cdot\vec{q}_3] - m^2 \\
&= \left(m_P - \sum_{k=1}^{3} E_k\right)^2 - |\vec{q}_1|^2 - |\vec{q}_2|^2 - |\vec{q}_3|^2 - m^2 - 2\,[|\vec{q}_1||\vec{q}_2|\cos\theta_2 + |\vec{q}_1||\vec{q}_3|\cos\theta_3 \\
&\quad + |\vec{q}_2||\vec{q}_3|\,(\sin\theta_2\sin\theta_3\cos\phi_3 + \cos\theta_2\cos\theta_3)]\,.
\end{aligned} \tag{5.42}$$

Using this representation, the integration over $\mathrm{d}\phi_3$ of a function G depending on $\cos\phi_3$ times the δ function $\delta\left[\left(p - \sum_{k=1}^{3} q_k\right)^2 - m^2\right]$ is of the form

$$\int_0^{2\pi} \delta(a - b\cos\phi_3)\,\mathrm{d}\phi_3\,G(\cos\phi_3) \tag{5.43}$$

where the abbreviations a and b stand for

$$\begin{aligned}
a = &\left(m_P - \sum_{k=1}^{3} E_k\right)^2 - |\vec{q}_1|^2 - |\vec{q}_2|^2 - |\vec{q}_3|^2 - 2\,[|\vec{q}_1||\vec{q}_2|\cos\theta_2 + |\vec{q}_1||\vec{q}_3|\cos\theta_3 \\
&+ |\vec{q}_2||\vec{q}_3|\cos\theta_2\cos\theta_3] - m^2,
\end{aligned} \tag{5.44}$$
$$b = 2|\vec{q}_2||\vec{q}_3|\sin\theta_2\sin\theta_3. \tag{5.45}$$

Such an integral is calculated as

$$\begin{aligned}
&\int_0^{2\pi} \delta(a - b\cos\phi_3)\,\mathrm{d}\phi_3\, G(\cos\phi_3) \\
&\quad= \int_0^{\pi} \delta(a - b\cos\phi_3)\,\mathrm{d}\phi_3\, G(\cos\phi_3) + \int_{\pi}^{2\pi} \delta(a - b\cos\phi_3)\,\mathrm{d}\phi_3\, G(\cos\phi_3) \\
&\quad= \int_0^{\pi} \mathrm{d}\phi_3\, \left[\delta(a - b\cos\phi_3)\, G(\cos\phi_3) + \delta(a + b\cos\phi_3)\, G(-\cos\phi_3)\right] \\
&\quad= \int_{-1}^{+1} \mathrm{d}x\, \left[\delta(a - bx)\, G(x) + \delta(a + bx)\, G(-x)\right] \frac{1}{\sqrt{1 - x^2}} \\
&\quad= \frac{2}{|b|} \frac{1}{\sqrt{1 - \left(\frac{a}{b}\right)^2}}\, G\left(\frac{a}{b}\right)\, \Theta\left(1 - \left|\frac{a}{b}\right|\right). \qquad (5.46)
\end{aligned}$$

Hence, the integration of a function G depending on $(|\vec{q}_1|, |\vec{q}_2|, |\vec{q}_3|, \cos\theta_2, \cos\theta_3)$ and $\cos\phi_3$ over $\mathrm{d}\Phi_4(p; q_1, q_2, q_3, q_4)$ equals

$$\begin{aligned}
&\int \mathrm{d}\Phi_4(p; q_1, q_2, q_3, q_4)\, G\left((|\vec{q}_1|, |\vec{q}_2|, |\vec{q}_3|, \cos\theta_2, \cos\theta_3), \cos\phi_3\right) \\
&= \frac{1}{4\,(2\pi)^{10}} \int \mathrm{d}|\vec{q}_1|\,\mathrm{d}|\vec{q}_2|\,\mathrm{d}|\vec{q}_3|\,\mathrm{d}\cos\theta_2\,\mathrm{d}\cos\theta_3\; \Theta\left(E_4 - m\right)\, \Theta\left(1 - \left|\frac{a}{b}\right|\right) \frac{|\vec{q}_1|^2\,|\vec{q}_2|^2\,|\vec{q}_3|^2}{E_1\,E_2\,E_3} \\
&\quad \frac{2}{|b|} \frac{1}{\sqrt{1 - \left(\frac{a}{b}\right)^2}}\, G\left((|\vec{q}_1|, |\vec{q}_2|, |\vec{q}_3|, \cos\theta_2, \cos\theta_3), \frac{a}{b}\right) \\
&= \frac{1}{4\,(2\pi)^{10}} \int \mathrm{d}|\vec{q}_1|\,\mathrm{d}|\vec{q}_2|\,\mathrm{d}|\vec{q}_3|\,\mathrm{d}\cos\theta_2\,\mathrm{d}\cos\theta_3\; \theta\left(E_4 - m\right)\, \Theta\left(1 - \left|\frac{a}{b}\right|\right) \frac{|\vec{q}_1|^2\,|\vec{q}_2|\,|\vec{q}_3|}{E_1\,E_2\,E_3} \\
&\quad \frac{1}{\sqrt{1 - \cos^2\theta_2}\sqrt{1 - \cos^2\theta_3}\sqrt{1 - \left(\frac{a}{b}\right)^2}}\, G\left((|\vec{q}_1|, |\vec{q}_2|, |\vec{q}_3|, \cos\theta_2, \cos\theta_3), \frac{a}{b}\right) \qquad (5.47)
\end{aligned}$$

with a and b given in (5.44) and (5.45). Therewith, the integral over the four-body phase space which was primary twelve-dimensional is reduced to a five-dimensional integral.

5.2.3 The Partial Decay Width

The partial decay width for the decay of a pseudoscalar meson into two identical dileptons is given as

$$\Gamma_{P\to 2l^+2l^-} = \frac{1}{2!\,2!} \int \mathrm{d}\Phi_4\left(p; q_1, q_2, q_3, q_4\right) \frac{(2\pi)^4}{2m_P} \overline{|\mathcal{M}|^2}\,. \qquad (5.48)$$

Thereby, the symmetry factor $\frac{1}{2!\,2!}$ is caused by the decay into two identical particles, two leptons and two antileptons. According to Eq. (5.32) the squared matrix element consists of the terms

$$|g(q_1+q_2,q_3+q_4)|^2\,|a_1|^2, \tag{5.49}$$

$$g(q_1+q_2,q_3+q_4)\,\overline{g(q_1+q_4,q_3+q_2)}\,a_1\bar{a}_2, \tag{5.50}$$

$$g(q_1+q_2,q_3+q_4)\,\overline{g(q_3+q_4,q_1+q_2)}\,a_1\bar{a}_3, \tag{5.51}$$

$$g(q_1+q_2,q_3+q_4)\,\overline{g(q_3+q_2,q_1+q_4)}\,a_1\bar{a}_4 \tag{5.52}$$

yielding the averaged squared matrix element

$$\overline{|\mathcal{M}|^2} = 4 \sum_{\text{lepton spins}} [(5.49)+(5.50)+(5.51)+(5.52)]\,. \tag{5.53}$$

In the following sections it will be shown that $g\left(q_{i_1}+q_{i_2},q_{i_3}+q_{i_4}\right)$ with distinct indices $i_1,\ldots,i_4$ out of $\{1,\ldots,4\}$ is of the type

$$e^2\,f_P\left(\left(q_{i_1}+q_{i_2}\right)^2,\left(q_{i_3}+q_{i_4}\right)^2\right)\,\varepsilon^{\mu\nu\alpha\beta}\,\frac{1}{\left(q_{i_1}+q_{i_2}\right)^2\left(q_{i_3}+q_{i_4}\right)^2}\,. \tag{5.54}$$

The first term (5.49) and the third term (5.51) only depend on the sums $k := q_1+q_2$ and $q := q_3+q_4$ of the lepton momenta q_1, q_2, q_3 and q_4.. Additionally, Eqs. (5.3) and (5.35) yield

$$\begin{aligned}
&\varepsilon^{\mu\nu\alpha\beta}\,\varepsilon^{\bar{\mu}\bar{\nu}\bar{\alpha}\bar{\beta}}\,q_\mu k_\nu\,k_{\bar{\mu}}q_{\bar{\nu}} \sum_{\text{lepton spins}} a_1\bar{a}_4 \\
&\quad= \varepsilon^{\mu\nu\alpha\beta}\,\varepsilon^{\bar{\mu}\bar{\nu}\bar{\alpha}\bar{\beta}}\,q_\mu k_\nu\,k_{\bar{\mu}}q_{\bar{\nu}}\,\operatorname{tr}\{(\not{q}_1+m)\gamma_\alpha(\not{q}_2-m)\gamma_{\bar{\beta}}\}\,\operatorname{tr}\{(\not{q}_3+m)\gamma_\beta(\not{q}_4-m)\gamma_{\bar{\alpha}}\} \\
&\quad= \varepsilon^{\mu\nu\alpha\beta}\,\varepsilon^{\bar{\mu}\bar{\nu}\bar{\alpha}\bar{\beta}}\,q_\mu k_\nu\,q_{\bar{\mu}}k_{\bar{\nu}}\,\operatorname{tr}\{(\not{q}_1+m)\gamma_\alpha(\not{q}_2-m)\gamma_{\bar{\alpha}}\}\,\operatorname{tr}\{(\not{q}_3+m)\gamma_\beta(\not{q}_4-m)\gamma_{\bar{\beta}}\} \\
&\quad= \varepsilon^{\mu\nu\alpha\beta}\,\varepsilon^{\bar{\mu}\bar{\nu}\bar{\alpha}\bar{\beta}}\,q_\mu k_\nu\,q_{\bar{\mu}}k_{\bar{\nu}} \sum_{\text{lepton spins}} |a_1|^2.
\end{aligned} \tag{5.55}$$

So, the integral over the first and third term

$$\Gamma^{(13)}_{P\to 2l^+2l^-} = \int \mathrm{d}\Phi_4\left(p;q_1,q_2,q_3,q_4\right)\frac{(2\pi)^4}{2m_P}\sum_{\text{lepton spins}}[(5.49)+(5.51)] \tag{5.56}$$

can be calculated with formula (5.29) by replacing $\left|f_P(k^2,q^2)+f_P(q^2,k^2)\right|^2$ by $f_P(k^2,q^2)\cdot\left[f_P^\dagger(k^2,q^2)+f_P^\dagger(q^2,k^2)\right]$ with $k=q_1+q_2$ and $q=q_3+q_4$ and the mass of leptons and antileptons $m_1=m_2=m$.

The integrals over the second term (5.50) and the fourth term (5.52) depend on all possible combinations q_1+q_2, q_3+q_4, q_1+q_4 and q_3+q_2. Therefore, the integral

$$\Gamma^{(24)}_{P\to 2l^+2l^-} = \int \mathrm{d}\Phi_4\left(p;q_1,q_2,q_3,q_4\right)\frac{(2\pi)^4}{2m_P}\sum_{\text{lepton spins}}[(5.50)+(5.52)] \tag{5.57}$$

has to be calculated numerically using the simplification of the four-body phase space done in the previous subsection. $\cos\theta_1$ and $\cos\theta_2$ are integrated over $[-1,1]$ and the integration interval for the absolute values of the three-momenta $\vec{q}_1$, $\vec{q}_2$ and $\vec{q}_3$ can be reduced to $[0,\sqrt{m_P^2-m^2}]$ by using the equality $E_k^2 = m^2 + |\vec{q}_k|^2$ for $k = 1,2,3$. Furthermore, the constraints for k, q, $k' = q_1+q_4$ and $q' = q_3+q_2$ are included in form of θ-functions by multiplying the integrand with

$$\begin{aligned}\Theta_{q_1,q_2,q_3,q_4} = \Theta\left(k^2-4m^2\right)\,\Theta\left((m_P-m)^2-k^2\right)\,\Theta\left(q^2-4m^2\right)\Theta\left(\left(m_P-\sqrt{k^2}\right)^2-q^2\right)\\ \cdot\,\Theta\left(k'^2-4m^2\right)\,\Theta\left((m_P-m)^2-k'^2\right)\,\Theta\left(q'^2-4m^2\right)\Theta\left(\left(m_P-\sqrt{k^2}\right)^2-q'^2\right).\end{aligned} \tag{5.58}$$

Then, $\Gamma^{(24)}_{P\to 2l^+2l^-}$ is evaluated with formula (5.47) for

$$G\left(\left(|\vec{q}_1|,|\vec{q}_2|,|\vec{q}_3|,\cos\theta_2,\cos\theta_3\right),\cos\phi_3\right) = \frac{(2\pi)^4}{2m_P}\sum_{\text{lepton spins}}\left[(5.50)+(5.52)\right]\Theta_{q_1,q_2,q_3,q_4}. \tag{5.59}$$

Since Eqs. (5.34) and (5.36) yield

$$\varepsilon^{\mu\nu\alpha\beta}\,\varepsilon^{\bar{\mu}\bar{\nu}\bar{\alpha}\bar{\beta}}\,k_\mu q_\nu\,k'_{\bar{\mu}}q'_{\bar{\nu}}\,a_1\bar{a}_2 = \varepsilon^{\mu\nu\alpha\beta}\,\varepsilon^{\bar{\mu}\bar{\nu}\bar{\alpha}\bar{\beta}}\,k_\mu q_\nu\,q'_{\bar{\mu}}k'_{\bar{\nu}}\,a_1\bar{a}_4, \tag{5.60}$$

the sum (5.50) + (5.52) can be combined as

$$e^4\,f(k^2,q^2)\left[f^\dagger(k'^2,q'^2)+f^\dagger(q'^2,k'^2)\right]\varepsilon^{\mu\nu\alpha\beta}\,\varepsilon^{\bar{\mu}\bar{\nu}\bar{\alpha}\bar{\beta}}\,k_\mu q_\nu\,k'_{\bar{\mu}}q'_{\bar{\nu}}\,a_1\bar{a}_2. \tag{5.61}$$

With the arguments given above the full partial decay width equals

$$\Gamma_{P\to 2l^+2l^-} = \frac{1}{4}\cdot 4\left[\Gamma^{(13)}_{P\to 2l^+2l^-}+\Gamma^{(24)}_{P\to 2l^+2l^-}\right] = \Gamma^{(13)}_{P\to 2l^+2l^-}+\Gamma^{(24)}_{P\to 2l^+2l^-}\,. \tag{5.62}$$

Keep in mind that $\Gamma^{(24)}_{P\to 2l^+2l^-}$ has a negative sign relative to $\Gamma^{(13)}_{P\to 2l^+2l^-}$ (see definition of a_1, a_2, a_3 and a_4 in subsection 5.2.1).

As the five-fold integral for $\Gamma^{(24)}_{P\to 2l^+2l^-}$ has to be integrated numerically and is hence quite difficult to determine, the whole partial decay width is approximated by $\Gamma^{(13)}_{P\to 2l^+2l^-}$ in most applications. This is justified if $\Gamma^{(24)}_{P\to 2l^+2l^-}$ is small compared to $\Gamma^{(13)}_{P\to 2l^+2l^-}$. In this thesis, both $\Gamma^{(13)}_{P\to 2l^+2l^-}$ and $\Gamma^{(24)}_{P\to 2l^+2l^-}$ are calculated so that the influence of $\Gamma^{(24)}_{P\to 2l^+2l^-}$ on the full width can be evaluated.

5.3 Decay of a Neutral Pion into Two Dileptons

5.3.1 Transition Matrix Element and Form Factor

The matrix element for the decay of a neutral pion into two dielectrons equals

$$\mathcal{M}_\pi = \sum_{n=1,\dots,4} e^2\, f_\pi(k^2,q^2)\, \varepsilon^{\mu\nu\alpha\beta}\, q_\mu k_\nu\, \frac{1}{k^2 q^2}\, (-1)^{I_n}\, \bar{u}_s(q_{I_{n,1}})\gamma_\alpha v_{s'}(q_{I_{n,2}})\, \bar{u}_\sigma(q_{I_{n,3}})\gamma_\beta v_{\sigma'}(q_{I_{n,4}})\,. \tag{5.63}$$

Hereby, the vector $I_n \in \{(q_1,q_2,q_3,q_4),\ (q_1,q_4,q_3,q_2),\ (q_3,q_4,q_1,q_2),\ (q_3,q_2,q_1,q_4)\}$ with $I_n = (I_{n,1}, I_{n,2}, I_{n,3}, I_{n,4})$,

$$(-1)^{(q_1,q_2,q_3,q_4)} = (-1)^{(q_3,q_4,q_1,q_2)} = +1,\ (-1)^{(q_1,q_4,q_3,q_2)} = (-1)^{(q_3,q_2,q_1,q_4)} = -1,$$

$k^2 = (q_{I_{n,1}} + q_{I_{n,2}})^2$ and $q^2 = (q_{I_{n,3}} + q_{I_{n,4}})^2$. The form factor

$$\begin{aligned} f_\pi(k^2,q^2) = \frac{e_V}{24 f}\Big[& e_A\left(S_\rho(q^2) + S_\omega(q^2)\right) q^2 + e_V m_V^2 \left(-\frac{1}{4} h_A q^2 + b_A \bar{m}_\pi^2\right) \\ & \cdot \left(S_\rho(k^2) S_\omega(q^2) + S_\omega(k^2) S_\rho(q^2)\right)\Big] - \frac{e^2}{8\pi^2 f} \end{aligned} \tag{5.64}$$

describes decays via at least one virtual vector meson and the direct decay into two photons given by the WZW Lagrangian[2]. In Fig. 5.3, the squared symmetrised and normalised form factor

$$\left|F_\pi^{\text{symm}}(k^2,q^2)\right|^2 = \frac{\left|f_\pi(k^2,q^2) + f_\pi(q^2,k^2)\right|^2}{4\left|f_\pi(0,0)\right|^2} \tag{5.65}$$

is plotted.
As the mass of the neutral pion $m_{\pi^0} = 135\,\text{MeV}$ is smaller than the mass of a dimuon $2m_\mu = 212\,\text{MeV}$, neither the decay of a neutral pion into a dielectron and a dimuon nor the decay into two dimuons is possible.

5.3.2 Decay Width for the Decay into Two Dielectrons

As discussed in section 5.2, the partial decay width for the decay of a pseudoscalar meson into two identical dileptons consists of two terms

$$\Gamma_{P\to 2l^+2l^-} = \Gamma^{(13)}_{P\to 2l^+2l^-} + \Gamma^{(24)}_{P\to 2l^+2l^-} \tag{5.66}$$

with $\Gamma^{(13)}_{P\to 2l^+2l^-}$ and $\Gamma^{(24)}_{P\to 2l^+2l^-}$ defined in Eq. (5.56) and Eq. (5.57), respectively.

[2]The form factor given by the WZW Lagrangian is equal to the last term multiplied with -1 since the relative sign between the WZW form factor and the form factor describing decays via virtual vector mesons was determined as negative in chapter 4.

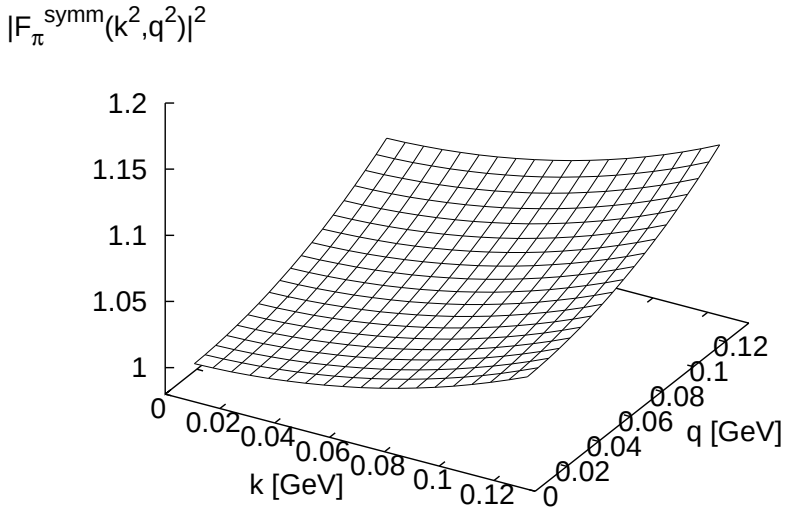

Figure 5.3: Squared symmetrised and normalised form factor $|F_\pi^{\text{symm}}(k^2, q^2)|^2$ for the decay of a neutral pion into two dileptons.

For the decay of a neutral pion into two dielectrons the dominant part equals

$$\Gamma^{(13)}_{\pi^0\to 2e^+2e^-} = (2.30 \pm 0.04) \cdot 10^{-13}\,\text{GeV} \tag{5.67}$$

and the less dominant part

$$\Gamma^{(24)}_{\pi^0\to 2e^+2e^-} = (-0.02 \pm 0.00) \cdot 10^{-13}\,\text{GeV}. \tag{5.68}$$

This yields a full partial decay width of

$$\Gamma_{\pi^0\to 2e^+2e^-} = (2.28 \pm 0.04) \cdot 10^{-13}\,\text{GeV}. \tag{5.69}$$

The derivation of the full partial width from the approximation $\Gamma^{(13)}_{\pi^0\to 2e^+2e^-}$ is approximately 1% and therewith confirms the treatment of $\Gamma^{(24)}_{\pi^0\to 2e^+2e^-}$ as negligible. Thereby, this relation is the overall value. It could be quite different in parts of the energetically allowed region.

Furthermore, the partial decay width agrees with the experimental one [A+08]

$$\Gamma^{\text{exp}}_{\pi^0\to 2e^+2e^-} = (2.62 \pm 0.31) \cdot 10^{-13}\,\text{GeV}. \tag{5.70}$$

5.4 Decay of an η-Meson into Two Dileptons

5.4.1 Transition Matrix Element and Form Factor

As for the decays of η- or η'-mesons into a real photon and a dilepton in chapter 4, the matrix elements for the decays of the η_8 and the η_1 state are needed to describe the decay of an η-meson into two dileptons.

Analogically to Eq. (5.63), the matrix element for the decay of the η-meson is of the type

$$\mathcal{M}_\eta = \sum_{n=1,\dots,4} e^2\, f_\eta(k^2,q^2)\, \varepsilon^{\mu\nu\alpha\beta}\, q_\mu k_\nu\, \frac{1}{k^2 q^2}\, (-1)^{I_n}\, \bar{u}_s(q_{I_{n,1}})\gamma_\alpha v_{s'}(q_{I_{n,2}})\, \bar{u}_\sigma(q_{I_{n,3}})\gamma_\beta v_{\sigma'}(q_{I_{n,4}}) \tag{5.71}$$

including the form factor $f_\eta = \cos\theta f_{\eta_8} - \sin\theta f_{\eta_1}$. The form factor for the decay of the η_8 state equals

$$\begin{aligned} f_{\eta_8}(k^2,q^2) = \frac{e_V}{72\sqrt{3}\,f} \sum_{V=\rho^0,\omega,\phi} S_V(q^2) \Big[\Big(e_A\, x_{81}(V)\, y(V) - \frac{1}{4} h_A e_V m_V^2\, x_{82}\, y^2(V)\, S_V(k^2) \Big) q^2 \\ + b_A e_V m_V^2\, x_{83}(V)\, y^2(V)\, S_V(k^2) \Big] - \frac{e^2}{8\sqrt{3}\,\pi^2\, f} \end{aligned} \tag{5.72}$$

and the one for the decay of the η_1 state

$$\begin{aligned} f_{\eta_1}(k^2,q^2) = \frac{\sqrt{2}}{72\sqrt{3}\,f} \sum_{V=\rho^0,\omega,\phi} S_V(q^2) \Big[\Big(\frac{1}{\sqrt{2}}\, e_A\, x_{11}(V)\, y(V) - \frac{1}{4} h_A e_V m_V^2\, y^2(V)\, S_V(k^2) \Big) q^2 \\ + b_A e_V m_V^2\, x_{13}(V)\, y^2(V)\, S_V(k^2) \Big] - \frac{\sqrt{2}\, e^2}{4\sqrt{3}\,\pi^2\, f} \end{aligned} \tag{5.73}$$

with the coefficients $x_{81}(V)$, $x_{82}(V)$, $x_{83}(V)$, $x_{11}(V)$, $x_{13}(V)$ and $y(V)$ given in subsection 4.5.1. The squared symmetrised and normalised form factor $\left|F_\eta^{\text{symm}}(k^2,q^2)\right|^2$ is plotted in Fig. 5.4.

For the decay into two different dileptons only two of the four combinations $I_1,\dots,I_4$ for the momenta of leptons and antileptons are allowed (compare section 5.2.1, in particular Fig. 5.2). Without loss of generality, I_1 and I_3 are chosen as these allowed combinations[3]. For this case, the matrix element simplifies to the form given in Eq. (5.1) in section 5.1.

[3] As argued before, the negative sign associated with the combinations I_2 and I_4 does not change any observables since only the squared matrix element is included in the formulas for them.

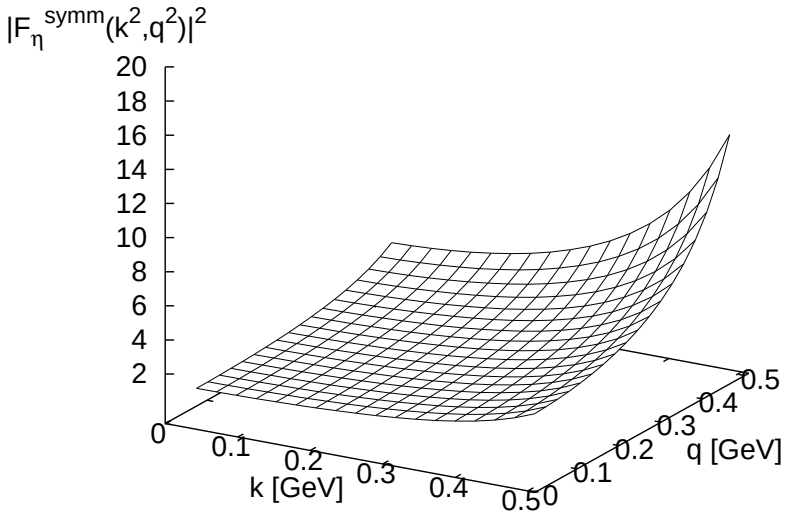

Figure 5.4: Squared symmetrised and normalised form factor $|F_\eta^{\text{symm}}(k^2, q^2)|^2$ for the decay of an η-meson into two dileptons.

5.4.2 Partial Decay Widths

The partial decay width for the decay of an η-meson into a dimuon and a dielectron is calculated as

$$\Gamma_{\eta\to\mu^+\mu^-\,e^+e^-} = (3.92 \pm 0.07) \cdot 10^{-12}\,\text{GeV} \tag{5.74}$$

in agreement with the experimental constraint [A+08]

$$\Gamma^{\text{exp}}_{\eta\to\mu^+\mu^-\,e^+e^-} < 2.08 \cdot 10^{-10}\,\text{GeV}. \tag{5.75}$$

As explained in subsection 5.2.3, the partial decay width for the decay into two identical dileptons is a sum of the dominant part $\Gamma^{(13)}_{\eta\to 2l^+2l^-}$ and the subdominant part $\Gamma^{(24)}_{\eta\to 2l^+2l^-}$. For the decay into two dielectrons, those equal

$$\Gamma^{(13)}_{\eta\to 2e^+2e^-} = (3.07 \pm 0.05) \cdot 10^{-11}\,\text{GeV}, \tag{5.76}$$

$$\Gamma^{(24)}_{\eta\to 2e^+2e^-} = (-0.03 \pm 0.00) \cdot 10^{-11}\,\text{GeV}. \tag{5.77}$$

As the value for $\Gamma^{(24)}_{\eta\to 2e^+2e^-}$ is about 1% of $\Gamma^{(13)}_{\eta\to 2e^+2e^-}$, it is justified to approximate the full partial decay width by $\Gamma^{(13)}_{\eta\to 2e^+2e^-}$. The full partial decay width including the dominant and the subdominant part equals

$$\Gamma_{\eta\to 2e^+2e^-} = (3.04 \pm 0.05) \cdot 10^{-11}\,\text{GeV} \tag{5.78}$$

which again agrees with the experimental constraint [A+08]

$$\Gamma^{\text{exp}}_{\eta\to 2e^+2e^-} < 8.97 \cdot 10^{-11}\,\text{GeV} \tag{5.79}$$

For the decay into two dimuons the dominant part equals

$$\Gamma^{(13)}_{\eta\to 2\mu^+2\mu^-} = (6.94 \pm 0.09) \cdot 10^{-15}\,\text{GeV}. \tag{5.80}$$

The integration for $\Gamma^{(24)}_{\eta\to 2\mu^+2\mu^-}$ was not numerically fully stable for the calculations performed for this thesis. Thus, only an interval instead of a fixed number can be given. The value of the subdominant part of the full partial decay width is then given as

$$\Gamma^{(24)}_{\eta\to 2\mu^+2\mu^-} \in ([0.40, 0.42] \pm 0.03) \cdot 10^{-15}\,\text{GeV}. \tag{5.81}$$

This yields a full partial decay width of

$$\Gamma_{\eta\to 2\mu^+2\mu^-} \in ([7.34, 7.36] \pm 0.12) \cdot 10^{-15}\,\text{GeV}. \tag{5.82}$$

As the difference between the borders of the interval is smaller than the error of the partial decay width, the interval can be approximated by its mean value yielding the partial decay width

$$\Gamma_{\eta\to 2\mu^+2\mu^-} = (7.35 \pm 0.13) \cdot 10^{-15}\,\text{GeV}. \tag{5.83}$$

For this decay, $\Gamma^{(24)}_{\eta\to 2\mu^+2\mu^-}$ adds up to 6% of $\Gamma^{(13)}_{\eta\to 2\mu^+2\mu^-}$ and, hence, the full partial decay width cannot be approximated as $\Gamma^{(13)}_{\eta\to 2\mu^+2\mu^-}$ easily. Nevertheless, both the approximation and the full partial decay width agree with the experimental constraint [A+08]

$$\Gamma^{\text{exp}}_{\eta\to 2\mu^+2\mu^-} < 4.68 \cdot 10^{-10}\,\text{GeV}. \tag{5.84}$$

5.5 Decay of an η'-Meson into Two Dileptons

5.5.1 Transition Matrix Element and Form Factor

Analogically to the decay of an η-meson, the matrix element for the decay of an η'-meson into two identical dileptons is given by Eq. (5.63) and the one for the decay into two different dileptons by Eq. (5.1). Thereby, the form factor $f_{\eta'}(k^2, q^2)$ equals $\sin\theta f_{\eta_1}(k^2, q^2) + \cos\theta f_{\eta_8}(k^2, q^2)$ including the form factors (5.72) and (5.73) for the decays of an η_8 and an η_1 state, respectively. The squared symmetrised and normalised form factor $\left|F_{\eta'}^{\text{symm}}(k^2, q^2)\right|^2$ is plotted in Fig. 5.5. As for the decay of an η'-meson into a real photon and a dilepton (section 4.6), the propagators have to include the widths of the ρ^0- and the ω-resonance since the mass of the η'-meson $m_{\eta'} = 958\,\text{MeV}$ is larger than the mass of the ρ^0- and the ω-meson.

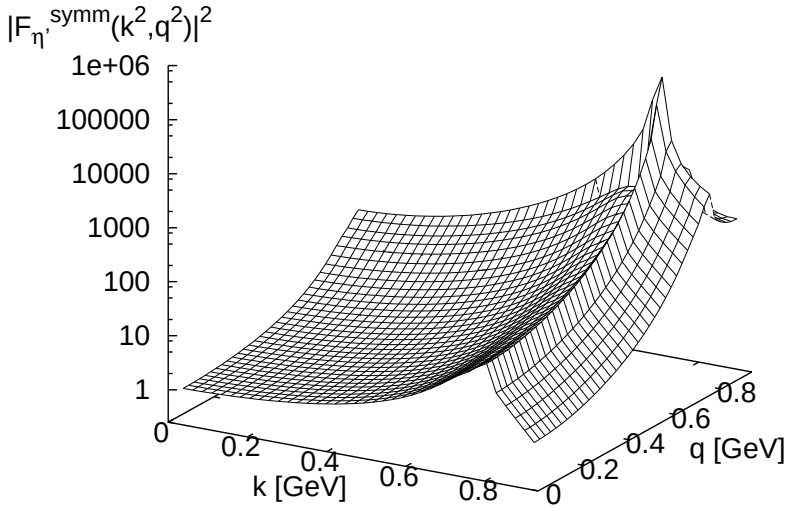

Figure 5.5: Squared symmetrised and normalised form factor $|F_{\eta'}^{\text{symm}}(k^2, q^2)|^2$ for the decay of an η'-meson into two dileptons.

5.5.2 Partial Decay Widths

For decays of an η'-meson into two dileptons no experimental data are available and, therefore, all values given in this subsection have to be seen as predictions.

The partial decay width for the decay into a dimuon and a dielectron is calculated as

$$\Gamma_{\eta' \to \mu^+\mu^- e^+e^-} = (1.50 \pm 0.04) \cdot 10^{-10}\,\text{GeV} \tag{5.85}$$

yielding a relative small branching ratio in the order of 10^{-6}.

For the decay into two dielectrons one gets

$$\Gamma^{(13)}_{\eta'\to 2e^+2e^-} = (3.76 \pm 0.18) \cdot 10^{-10}\,\mathrm{GeV}, \tag{5.86}$$

$$\Gamma^{(24)}_{\eta'\to 2e^+2e^-} = (-0.04 \pm 0.00) \cdot 10^{-10}\,\mathrm{GeV}. \tag{5.87}$$

The part $\Gamma^{(24)}_{\eta'\to 2e^+2e^-}$ equals about 1% of the dominant part and, therewith, the whole partial decay width

$$\Gamma_{\eta'\to 2e^+2e^-} = (3.72 \pm 0.18) \cdot 10^{-10}\,\mathrm{GeV} \tag{5.88}$$

can be approximated by $\Gamma^{(13)}_{\eta'\to 2e^+2e^-}$ within the accuracy of the approach this thesis is based on.

The value for the less dominant term for the decay into two dimuons is again numerically not fully stable,

$$\Gamma^{(24)}_{\eta'\to 2\mu^+2\mu^-} \in (-\,[0.56, 0.59] \pm 0.04) \cdot 10^{-12}\,\mathrm{GeV}. \tag{5.89}$$

As it is between 11 and 12% of the dominant part,

$$\Gamma^{(13)}_{\eta'\to 2\mu^+2\mu^-} = (4.98 \pm 0.22) \cdot 10^{-12}\,\mathrm{GeV}, \tag{5.90}$$

an approximation of the full partial decay width by the dominant part $\Gamma^{(13)}_{\eta'\to 2\mu^+2\mu^-}$ is not justified. The full width $\Gamma^{(13)}_{\eta'\to 2\mu^+2\mu^-} + \Gamma^{(24)}_{\eta'\to 2\mu^+2\mu^-}$ is given as

$$\Gamma_{\eta'\to 2\mu^+2\mu^-} = (4.40 \pm 0.28) \cdot 10^{-12}\,\mathrm{GeV}. \tag{5.91}$$

6 Summary and Outlook

In this thesis, the decays of

- vector mesons into a pseudoscalar meson and a dilepton (chapter 3),
- pseudoscalar mesons into a dilepton and either a real photon or a vector meson (chapter 4) and
- pseudoscalar mesons into two dileptons (chapter 5)

were calculated in leading order. Therefor, the leading-order chiral Lagrangian including both the pseudoscalar Goldstone bosons and the light vector mesons (see sections 2.3, 2.5) was used whereat the leading-order terms where identified according to the counting rules (C1), (C2) proposed in [LL08]. Additionally, a particular next-to-leading-order term (2.107) was added to get a rough estimate about the intrinsic error of the leading-order calculations. The calculations done with the Lagrangian including this next-to-leading-order term did not differ much from the real leading-order calculations for all decays considered in this thesis.

For the decays of vector mesons, all calculated values agreed well with the available data. In Tab. 6.1, the values for the partial decay widths are listed. Compared to the calculation performed with the standard vector meson dominance model (see subsection 2.4.1), the $\omega \to \pi^0$ form factor data taken by the NA60 collaboration for the decay $\omega \to \pi^0\mu^+\mu^-$ could be described much better with the calculation based on the counting rules (C1), (C2).

Table 6.1: Partial decay widths for the decays of vector mesons into a pseudoscalar meson and a dilepton compared to the experimental values given in [A$^+$08].

decay	calculated value [GeV]	experimental value [GeV]
$\omega \to \pi^0\gamma$	$(7.14 \pm 0.20) \cdot 10^{-4}$	$(7.03 \pm 0.30) \cdot 10^{-4}$
$\omega \to \pi^0\mu^+\mu^-$	$(9.85 \pm 0.58) \cdot 10^{-7}$	$(8.15 \pm 2.13) \cdot 10^{-7}$
$\omega \to \pi^0 e^+e^-$	$(6.93 \pm 0.09) \cdot 10^{-6}$	$(6.54 \pm 0.54) \cdot 10^{-6}$
$\omega \to \eta\gamma$	$(3.71 \pm 0.12) \cdot 10^{-6}$	$(3.91 \pm 0.38) \cdot 10^{-6}$
$\omega \to \eta\mu^+\mu^-$	$(8.51 \pm 0.01) \cdot 10^{-12}$	not available
$\omega \to \eta e^+e^-$	$(2.72 \pm 0.09) \cdot 10^{-8}$	not available
$\phi \to \eta\gamma$	$(5.38 \pm 0.26) \cdot 10^{-5}$	$(5.58 \pm 0.15) \cdot 10^{-5}$
$\phi \to \eta\mu^+\mu^-$	$(2.75 \pm 0.29) \cdot 10^{-8}$	not available
$\phi \to \eta e^+e^-$	$(4.64 \pm 0.26) \cdot 10^{-7}$	$(4.90 \pm 0.47) \cdot 10^{-7}$

The leading-order Lagrangian describing the decays of vector mesons and the leading-order Wess-Zumino-Witten Lagrangian (2.84) were used as a test approach to describe

the decays of pseudoscalar mesons. For the radiative two- and three-body decays, the calculated values were again in fair agreement with the available experimental data but not as good as those for the decays of vector mesons. The partial decay widths are listed in Tab. 6.2. In all cases, the partial widths calculated for an η- or an η'-meson described as a mixing of the octet η_8 state and the singlet η_1 state agreed much better with the experimental values than the ones calculated for unmixed $\eta = \eta_8$ and $\eta' = \eta_1$ states (see sections 4.5, 4.6).

Table 6.2: Partial decay widths for the radiative two- and three-body decays of pseudoscalar mesons compared to the experimental values given in [A+08].

decay	calculated value [GeV]	experimental value [GeV]
$\pi^0 \to \gamma\gamma$	$(7.83 \pm 0.14) \cdot 10^{-9}$	$(7.74 \pm 0.56) \cdot 10^{-9}$
$\pi^0 \to \gamma e^+ e^-$	$(9.28 \pm 0.16) \cdot 10^{-11}$	$(9.20 \pm 0.93) \cdot 10^{-11}$
$\eta \to \gamma\gamma$	$(6.71 \pm 0.10) \cdot 10^{-7}$	$(5.11 \pm 0.30) \cdot 10^{-7}$
$\eta \to \gamma\mu^+\mu^-$	$(5.39 \pm 0.09) \cdot 10^{-10}$	$(4.03 \pm 0.74) \cdot 10^{-10}$
$\eta \to \gamma e^+ e^-$	$(11.24 \pm 0.16) \cdot 10^{-9}$	$(9.10 \pm 1.40) \cdot 10^{-9}$
$\eta' \to \gamma\gamma$	$(4.63 \pm 0.27) \cdot 10^{-6}$	$(4.28 \pm 0.56) \cdot 10^{-6}$
$\eta' \to \gamma\mu^+\mu^-$	$(1.77 \pm 0.21) \cdot 10^{-8}$	$(2.10 \pm 0.68) \cdot 10^{-8}$
$\eta' \to \gamma e^+ e^-$	$(9.41 \pm 0.46) \cdot 10^{-8}$	$< 1.836 \cdot 10^{-7}$
$\eta' \to \omega\gamma$	$(5.54 \pm 0.16) \cdot 10^{-6}$	$(6.16 \pm 0.19) \cdot 10^{-6}$
$\eta' \to \omega e^+ e^-$	$(3.78 \pm 0.10) \cdot 10^{-8}$	not available

Furthermore, the available form factor data were described as well with the calculations of this thesis as with the standard VMD calculations.

For the decays of pseudoscalar mesons into two dileptons, one has to distinguish between decays into two different kinds of dileptons and into two identical dileptons. In the first case, the integral defining the partial decay width can be simplified to a two-dimensional integral (see section 5.1). In the second case, the partial decay width consists of a part which can be simplified in the same way, $\Gamma^{(13)}$, and a part which can only be simplified to a five-dimensional integral, $\Gamma^{(24)}$ (see section 5.2). This part has to be integrated numerically and was not fully stable for all calculations performed for this thesis. Furthermore, the calculations showed that only for the decays of pseudoscalar mesons into two dielectrons the full partial decay widths could be approximated as $\Gamma^{(13)}$ whereas the part $\Gamma^{(24)}$ was too important for such an approximation for the decays into dimuons. The calculated partial decay width for the decay of a neutral pion into two dielectrons agrees with the experimental value; for the decays of an η-meson into either two di-

electrons or two dimuons, the experimental upper bounds were fulfilled. All calculated partial decay widths are listed in Tab. 6.3.

Table 6.3: Partial decay widths for the decays of pseudoscalar mesons into two dileptons compared to the experimental values given in [A+08].

decay	calculated value [GeV]	experimental value [GeV]
$\pi^0 \to 2e^+2e^-$	$(2.28 \pm 0.04) \cdot 10^{-13}$	$(2.62 \pm 0.31) \cdot 10^{-13}$
$\eta \to \mu^+\mu^- e^+e^-$	$(3.92 \pm 0.07) \cdot 10^{-12}$	$< 2.08 \cdot 10^{-10}$
$\eta \to 2\mu^+2\mu^-$	$(7.35 \pm 0.13) \cdot 10^{-15}$	$< 4.68 \cdot 10^{-10}$
$\eta \to 2e^+2e^-$	$(3.04 \pm 0.05) \cdot 10^{-11}$	$< 8.97 \cdot 10^{-11}$
$\eta' \to \mu^+\mu^- e^+e^-$	$(1.50 \pm 0.04) \cdot 10^{-10}$	not available
$\eta' \to 2\mu^+2\mu^-$	$(4.40 \pm 0.28) \cdot 10^{-12}$	not available
$\eta' \to 2e^+2e^-$	$(3.72 \pm 0.18) \cdot 10^{-10}$	not available

The counting scheme [LL08] used in this thesis is proposed as the basis of an effective field theory. This is supported by this thesis because the leading-order calculations describe the experimental data well and the intrinsic error estimated roughly by the calculations including the particular next-to-leading-order term is small. Nevertheless, to show that it is a reasonable basis of an effective field theory instead of a hadronic tree-level model full next-to-leading-order calculations have to be performed.

7 Deutsche Zusammenfassung

In theoretischer Physik sollen physikalische Prozesse mit mathematischen Hilfsmitteln beschrieben werden. Außerdem soll gewährleistet werden, dass die so beschriebenen Observablen oder Annäherungen an sie in endlicher Zeit berechenbar sind. Im Niedrig-Energie-Bereich der starken Wechselwirkung werden hierfür u.a. effektive Quantenfeldtheorien verwendet. Hierbei werden statt Quarks Hadronen als Freiheitsgrade der Theorie gewählt und es werden bespielsweise Lagrangedichten als Reihe über kleine Energien und Impulse geschrieben. Der Vorteil solcher Theorien ist, dass endliche Rechnungen mit kontrollierbarem intrinsischen Fehler druchgeführt werden können und es möglich ist, diesen Fehler systematisch zu verringern.

Grundlage dieser Diplomarbeit ist ein Zählschema [LL08], das im Energiebereich der hadronischen Resonanzen K^*-, ρ-, ω- und ϕ-Mesonen diese leichten Vektormesonen und die pseudoskalaren Goldstonebosonen gleich behandelt, d.h. die Massen dieser Teilchen werden gleichermaßen als klein bewertet. Mittels dieses Zählschemas kann die erste Ordnung der Lagrangedichte für den Zerfall von Vektormesonen in ein pseudoskalares Meson und ein reelles Photon bzw. ein Dilepton[1] bestimmt werden. Aus dieser Lagrangedichte können dann (ebenfalls in erster Ordnung) Übergangsmatrixelemente und -formfaktoren sowie partielle Zerfallsbreiten für die Zerfälle von Vektormesonen berechnet werden.
Es stellt sich nun die Frage, ob und wie gut die auf Grundlage dieses Zählschemas berechneten Werte mit vorhandenen experimentellen Werten übereinstimmen und ob diese Übereinstimmung genauso gut oder besser ist als die Übereinstimmung mit dem phänomenlogischen Modell für diesen Energiebereich, dem Standard-Vektormesondominanz-Modell (Standard-VMD-Modell). Die in [LL08] und [LL09] berechneten Werte für radiative 2- und hadronische 3-Körper-Zerfälle leichter Vektormesonen stimmten gut mit den experimentellen überein. Weiter ist zu klären, ob das Zählschema die Basis einer effektiven Quantenfeldtheorie für den Bereich der hadronischen Resonanzen bildet oder ob es ein Model ist ohne Möglichkeit, den intrinsischen Fehler zu kontrollieren. Dafür wird in dieser Arbeit ein Term der Lagrangedichte von nächst höherer Ordnung bestimmt. Damit lässt sich der intrinsische Fehler einer berechneten Größe sehr grob als Unterschied zwischen dem Ergebnis der Rechnung in führender Ordnung und dem der Rechnung mit diesem zusätzlichen Term höherer Ordnung abschätzen.

In dieser Arbeit werden folgende Zerfälle von leichten Vektormesonen behandelt, $\omega \to \pi^0\gamma/\pi^0 l^+l^-$, $\omega \to \eta\gamma/\eta l^+l^-$ und $\phi \to \eta\gamma/\eta l^+l^-$, wobei l^+l^- ein Dilepton bezeichnet. Für alle Zerfälle stimmen die berechneten Breiten gut mit den vorhandenen experimentellen überein. Dabei werden die am SPS durch die NA60-Kollaboration gemessenen Daten für den $\omega \to \pi^0$ Formfaktor [A$^+$09] mit diesen Berechnungen sehr viel besser beschrieben als mit den Berechnungen aufgrund des Standard-VMD-Modells.

Die Lagrangedichte für die Zerfälle der leichten Vektormesonen kann außerdem als Test

[1] Aufgrund der geringen Masse der leichten Vektormesonen sind nur Zerfälle in Dielektronen oder Dimyonen möglich; ein Zerfall in ein Ditauon ist nicht möglich. Im Weitern bezieht sich der Ausdruck Dilepton immer auf Dielektronen oder Dimyonen.

für die Effektivität des Zählschemas bei Zerfällen von pseudoskalaren Mesonen in ein Vektormeson und reelles oder virtuelles Photon bzw. in zwei reelle oder virtuelle Photonen genutzt werden. Dabei enthält diese Lagrangedichte jedoch nicht alle Terme führender Ordnung, die für den Zerfall pseudoskalarer Mesonen erforderlich wären. Ein Term, der in dieser Diplomarbeit hinzugenommen wurde, ist der Wess-Zumino-Witten-Term in führender Ordnung, der den direkten Zerfall eines pseudoskalaren Mesons in zwei Photonen ermöglicht.
Bei den Zerfällen $\pi^0 \to \gamma\gamma/\gamma l^+l^-$, $\eta \to \gamma\gamma/\gamma l^+l^-$, $\eta' \to \gamma\gamma/\gamma l^+l^-$ und $\eta' \to \omega\gamma/\omega l^+l^-$ von pseudoskalaren Mesonen stimmen die berechneten Breiten immer noch hinreichend mit den experimentellen überein, jedoch nicht mehr so gut wie bei den Zerfällen der Vektormesonen. Weiter konnten die von NA60 gemessen Daten für den $\eta \to \gamma$ Formfaktor [A$^+$09] sehr gut beschrieben werden, wobei es jedoch kaum Abweichungen von den Berechnungen mit dem Standard-VMD-Modell gab.
Zusätzlich wurden die Zerfälle der pseudoskalen Mesonen π^0, η und η' in zwei Dieleptonen von unterschiedlicher oder gleicher Art berechnet. Hierbei stimmt die Zerfallsbreite für den Zerfall des neutralen Pions in zwei Dielektronen mit dem experimentellen Wert überein; die Breiten für die Zerfälle der Mesonen η und η' erfüllen die experimentellen Schranken.

Außerdem konnte bei allen Berechnungen festgestellt werden, dass der Einfluss des Terms von nächst höherer Ordnung auf die berechneten Werte, also die grobe Abschätzung des intrinsischen Fehlers, klein war. Somit wurde die These unterstützt, dass das hier verwendete Zählschema Basis einer effektiven Theorie ist. Um diese These weiter zu untermauern, müssen jedoch in Zukunft vollständige Rechnungen in der nächst höheren Ordnung durchgeführt werden.

A Appendix

A.1 Transformation Properties of the Goldstone Bosons

The aim of this section is to describe all Goldstone bosons corresponding to the spontaneous symmetry breaking in QCD as one hermitian and traceless matrix. Within the approach of Goldstone's theorem, they are described as eight independent fields ϕ_a on the Minkowski space M^4, so they are continuous real functions on M^4.
The section follows the explanations given in [Sch03].

First step:

All Goldstone boson fields are collected into one eight-component vector Φ which is an element of the space

$$M_1 := \left\{ \Phi : M^4 \to \mathbb{R}^8 \,\middle|\, \phi_a : M^4 \to \mathbb{R} \text{ continuous} \right\}. \tag{A.1}$$

It is possible to define an operation φ of G on M_1, i.e. φ is a mapping of $G \times M_1$ into M_1 fulfilling:

- $\forall\, \Phi \in M_1 : \varphi(1_G, \Phi) = \Phi,$ (A.2)
- $\forall\, g_1,\, g_2 \in G,\, \Phi \in M_1 : \varphi(g_1, \phi(g_2, \Phi)) = \varphi(g_1 g_2, \Phi).$ (A.3)

If $\Phi = 0$ denotes the "origin" of M_1, which is the state corresponding to the ground state configuration, and the subgroup H of G is the symmetry group of the ground state, the operation φ will have to satisfy the additional property

$$\forall\, h \in H : \varphi(h, 0) = 0. \tag{A.4}$$

Second step:

A (well defined) mapping $\hat{\varphi}$ of the set of all left cosets $G/H := \{gH | g \in G\}$ into M_1 is defined by

$$\forall\, g \in G,\, h \in H : \hat{\varphi}(gH) := \varphi(gh, 0) = \varphi(g, \varphi(h, 0)) = \varphi(g, 0). \tag{A.5}$$

Since all left cosets are either equal or disjoint, the mapping $\hat{\varphi} : G/H \to M_1$ is injective and therefore an isomorphism between G/H and the Goldstone bosons. Thus, there exists a $g \in G$ for every Goldstone boson Φ with $\Phi = \hat{\varphi}(gH)$. Therewith, the transformation behaviour of the Goldstone bosons under an element $g' \in G$ can be described as

$$\Phi \overset{g'}{\mapsto} \Phi' = \hat{\varphi}(g' \cdot gH, 0) = \varphi(g'g, 0) = \varphi(g', \varphi(g, 0)) = \varphi(g', \Phi). \tag{A.6}$$

In QCD, the symmetry groups are equal to

$$G = \mathrm{SU}(3)_\mathrm{L} \times \mathrm{SU}(3)_\mathrm{R} = \{(L,R)\,|L,\, R \in \mathrm{SU}(3)\}\,, \tag{A.7}$$
$$H = \{(V,V)\,|\,V \in \mathrm{SU}(3)\}\,. \tag{A.8}$$

For every $g = (L,R) \in G$ the left coset $gH = \left\{(LV,RV) = (1,RL^\dagger)(V,V)\,|\,V \in \mathrm{SU}(3)\right\}$ is determined by $U = RL^\dagger \in \mathrm{SU}(3)$. Thus, the set of these U is isomorphic to the Goldstone bosons. Therefore, every U has to be a function on the Minkowski space M^4 and transforms as:

$$\forall\, x \in M^4 : U(x) \overset{\tilde{g}=(\tilde{R},\tilde{L})}{\mapsto} U'(x) = \tilde{R}U(x)\tilde{L}^\dagger. \tag{A.9}$$

Third step:

Define the real vector space (with respect to addition of matrices) of all hermitian and traceless 3×3 matrices as

$$\tilde{\mathcal{H}} := \{A \in \mathrm{gl}(3,\mathbb{C})\,|\,A^\dagger = A,\, \mathrm{tr}(A) = 0\} \tag{A.10}$$

and the real vector space

$$M_2 := \{\Phi : M^4 \to \tilde{\mathcal{H}}\,|\,\Phi \text{ continuous}\}. \tag{A.11}$$

The elements of M_1 and M_2 are related via

$$M_2 \ni \Phi(x) = \sum_{a=1}^{8} \lambda_a \phi_a(x) = \begin{pmatrix} \phi_3 + \frac{1}{\sqrt{3}}\phi_8 & \phi_1 - i\phi_2 & \phi_4 - i\phi_5 \\ \phi_1 + i\phi_2 & -\phi_3 + \frac{1}{\sqrt{3}}\phi_8 & \phi_6 - i\phi_7 \\ \phi_4 + i\phi_5 & \phi_6 + i\phi_7 & -\frac{2}{\sqrt{3}}\phi_8 \end{pmatrix}$$
$$=: \begin{pmatrix} \pi^0 + \frac{1}{\sqrt{3}}\eta & \sqrt{2}\pi^+ & \sqrt{2}K^+ \\ \sqrt{2}\pi^- & -\pi^0 + \frac{1}{\sqrt{3}}\eta & \sqrt{2}K^0 \\ \sqrt{2}K^- & \sqrt{2}\bar{K}^0 & -\frac{2}{\sqrt{3}}\eta \end{pmatrix} \tag{A.12}$$

with $\phi_a \in M_1$, $a = 1,\ldots,8$. This is the wanted description of the Goldstone-boson fields as one hermitian and traceless matrix. For further calculation, the additional set

$$M_3 := \left\{ U : M^4 \to \mathrm{SU}(3) \;\middle|\; U(x) = \exp\left(i\frac{\Phi(x)}{f}\right),\, \Phi \in M_2 \right\} \tag{A.13}$$

is defined with the origin $U_0 = \exp\left(i\frac{0}{f}\right) = 1$. Defining the operation

$$\tilde{\varphi} : G \times M_3 \ni ((L,R),U(x)) \longmapsto RU(x)L^\dagger \in M_3 \tag{A.14}$$

shows that U_0 is invariant under H but not invariant under axial transformation $(A,A^\dagger) \notin H$ which rotates left-handed quarks by A and right-handed ones by $A^\dagger$. Therefore, the new fields are consistent with the assumed symmetry breaking.

A.2 Derivation of Feynman Diagrams and Rules

In this section, a derivation of Feynman diagrams and rules for the ϕ^4 theory described by the Lagrangian

$$\mathcal{L} = \frac{1}{2}(\partial_\mu \phi)^2 - \frac{1}{2}m^2\phi^2 - \frac{\lambda}{4!}\phi^4 \tag{A.15}$$

is given. Thereby, the explanations given in [PS95] are followed.

A.2.1 Perturbation Expansion of Correlation Functions

As a first step, the two-point correlation function

$$\langle \Omega | T\phi(x)\phi(y) | \Omega \rangle \tag{A.16}$$

with the ground state $|\Omega\rangle$ of the interacting ϕ^4 theory shall be calculated. This correlation function can be interpreted physically as the amplitude for the propagation of a particle between the two time-space points y and x. The capital T denotes the time-ordering function, i.e.

$$T\phi(x)\phi(y) = \theta(x_0 - y_0)\phi(x)\phi(y) + \theta(y_0 - x_0)\phi(y)\phi(x). \tag{A.17}$$

In the free theory where $\lambda = 0$, the correlation function can be determined easily as

$$\langle 0 | T\phi(x)\phi(y) | 0 \rangle_{\text{free}} = \int \frac{\mathrm{d}^4 p}{(2\pi)^4} \frac{i e^{-ip\cdot(x-y)}}{p^2 - m^2 + i\varepsilon} =: D_F(x-y) \tag{A.18}$$

with ε being infinitesimally small.

The solutions of the free theory are known (as solutions of a Klein-Gordon equation). Therefore, the unknown ground state and fields of the interacting theory with $\lambda \neq 0$ should be described by the free fields using the splitting of the Hamiltonian into a free and an interacting part:

$$H = H_0 + H_{\text{int}} = H_{\text{Klein-Gordon}} + \int \mathrm{d}^3 x \frac{\lambda}{4!}\phi^4(x). \tag{A.19}$$

In the Heisenberg picture the free field is equal to

$$\begin{aligned} \phi_I(t,\vec{x}) &= \phi(t,\vec{x})|_{\lambda=0} = e^{iH_0(t-t_0)}\phi(t_0,\vec{x})e^{-iH_0(t-t_0)} \\ &= \int \frac{\mathrm{d}^3 p}{(2\pi)^3} \frac{1}{\sqrt{2E_p}} \left(a_p e^{-ipx} + a_p^\dagger e^{+ipx} \right)\Big|_{x^0 = t - t_0} \end{aligned} \tag{A.20}$$

with annihilation and creation operators a_p and $a_p^\dagger$, respectively. Thus, the interacting field in the Heisenberg picture can be written as

$$\begin{aligned}\phi(t,\vec{x}) &= e^{iH(t-t_0)}\phi(t_0,\vec{x})e^{-iH(t-t_0)} \\ &= e^{iH(t-t_0)}e^{-iH_0(t-t_0)}\underbrace{e^{iH_0(t-t_0)}\phi(t,\vec{x})e^{-iH_0(t-t_0)}}_{=\phi_I(t,\vec{x})}e^{iH_0(t-t_0)}e^{-iH(t-t_0)} \\ &=: U^\dagger(t,t_0)\phi_I(t,\vec{x})U(t,t_0). \end{aligned} \tag{A.21}$$

$U(t,t_0)$ can be described in terms of ϕ_I because it is the unique solution of the differential Eq.

$$i\frac{\partial}{\partial t}\xi(t) = H_I(t)\xi(t) \tag{A.22}$$

with the interaction Hamiltonian

$$H_I(t) := e^{iH_0(t-t_0)}H_{\text{int}}e^{-iH_0(t-t_0)} = \int \mathrm{d}^3x \frac{\lambda}{4!}\phi_I^4(x) \tag{A.23}$$

for the initial condition $\xi(t_0) = 1$. Thus, the following identity holds:

$$\begin{aligned} U(t_f,t_i) &= T\left\{\exp\left[-i\int_{t_i}^{t_f}\mathrm{d}t\, H_I(t)\right]\right\} \\ &= \sum_{n=0}^{\infty}\frac{(-i)^n}{n!}\int_{t_i}^{t_f}\mathrm{d}t_1\ldots\mathrm{d}t_n\, T\left\{H_I(t_1)\ldots H_I(t_n)\right\} \\ &= 1 + (-i)\int_{t_i}^{t_f}\mathrm{d}t_1\, H_I(t_1) + \frac{(-i)^2}{2!}\int_{t_i}^{t_f}\mathrm{d}t_1\mathrm{d}t_2\, T\left\{H_I(t_1)H_I(t_2)\right\}. \end{aligned} \tag{A.24}$$

Inserting this formula for $t_i = t_0$ and $t_f = t$ into Eq. (A.21) yields the field ϕ for the interacting theory being described in terms of the field ϕ_I. As ϕ_I is the free field in the Heisenberg picture and hence controllable, the interacting field is controllable.

To be able to calculate the two-point correlation function (A.16), the ground state of the interaction theory $|\Omega\rangle$ has to be expressed in variables of the free theory. Considering only interactions which are small perturbations of the free theory, the overlap between $|\Omega\rangle$ and the free ground state $|0\rangle$ is unequal zero. With the eigenvalues E_n of the Hamiltonian H the free ground state can therefore be evolved through time as

$$e^{-iHT}|0\rangle = \sum_{n\in\mathbb{N}_0} e^{-iE_nT}|n\rangle\langle n|0\rangle = e^{-iE_0T}|\Omega\rangle\langle\Omega|0\rangle + \sum_{n\in\mathbb{N}} e^{-iE_nT}|n\rangle\langle n|0\rangle \tag{A.25}$$

with the minimal energy $E_0 := \langle\Omega|H|\Omega\rangle < E_n$ for all $n \in \mathbb{N}$. The last term involves the (unknown) eigenvalues and eigenfunctions of the interaction Hamiltonian H. They can

be set equal to zero if T is sent to $\infty(1-i\varepsilon)$ with a infinitesimal $\varepsilon > 0$ because the term e^{-iE_nT} dies slowest for $n = 0$. Rewriting Eq. (A.25) then yields

$$\begin{aligned}
|\Omega\rangle &= \lim_{T\to\infty(1-i\varepsilon)} \left(e^{-iE_0T}\langle\Omega|0\rangle\right)^{-1} e^{-iHT}|0\rangle \\
&= \lim_{T\to\infty(1-i\varepsilon)} \left(e^{-iE_0(T+t_0)}\langle\Omega|0\rangle\right)^{-1} e^{-iH(T+t_0)}|0\rangle \\
&= \lim_{T\to\infty(1-i\varepsilon)} \left(e^{-iE_0(t_0-(-T))}\langle\Omega|0\rangle\right)^{-1} \underbrace{e^{-iH(t_0-(-T))}e^{iH_0(t_0-(-T))}}_{=U(t_0,-T)}|0\rangle
\end{aligned} \tag{A.26}$$

since $H_0|0\rangle = 0$. A formula for $\langle\Omega|$ can be derived analogically:

$$\langle\Omega| = \lim_{T\to\infty(1-i\varepsilon)} \langle 0|U(T,t_0)\left(e^{-iE_0(T-t_0)}\langle 0|\Omega\rangle\right)^{-1}. \tag{A.27}$$

Thus, the two-point correlation function in terms of ϕ_I equals

$$\langle\Omega|T\phi(x)\phi(y)|\Omega\rangle = \lim_{T\to\infty(1-i\varepsilon)} \frac{\langle 0\left|T\left\{\phi_I(x)\phi_I(y)\exp\left[-i\int_{-T}^{+T}\mathrm{d}t\, H_I(t)\right]\right\}\right|0\rangle}{\left\langle 0\left|T\left\{\exp\left[-i\int_{-T}^{+T}\mathrm{d}t\, H_I(t)\right]\right\}\right|0\right\rangle}. \tag{A.28}$$

In real applications, a finite number of terms of the Taylor series expansion is taken instead of the whole exponential function.

The higher-order correlation function involving more fields can be derived in the same way: For each additional factor of ϕ on the left-hand side there has to be an additional factor of ϕ_I on the right-hand side. This yields the time-ordered product of m fields which can be evaluated using "Wick's theorem":

$$T\left\{\phi_I(x_1)\dots\phi_I(x_m)\right\} = N\left\{\phi_I(x_1)\dots\phi_I(x_m) + \begin{pmatrix}\text{all possible}\\ \text{contractions}\end{pmatrix}\right\}. \tag{A.29}$$

Hereby, the function N denotes the normal-ordered product[1]. The contraction of two field $\phi_I = \phi_I^+ + \phi_I^-$ with

$$\phi_I^+ \sim \int \mathrm{d}^3p\, a_p e^{-ipx},\ \phi_I^- \sim \int \mathrm{d}^3p\, a_p^\dagger e^{+ipx} \tag{A.30}$$

is defined as

$$[\phi_I(x)\phi_I(y)]^* = \begin{Bmatrix}[\phi_I^+(x),\phi_I^-(y)] & ,\text{ if } x^0 > y^0\\ [\phi_I^+(y),\phi_I^-(x)] & ,\text{ if } x^0 < y^0\end{Bmatrix} = D_F(x-y). \tag{A.31}$$

[1] A normal-ordered product has all annihilators on the right-hand side and all creators on the left-hand side. Therefore, the vacuum expectation value of any normal-ordered product which is not proportional to 1 is zero.

Then "all possible contractions" is an abbreviation for the sum of all possible terms with contractions of the m fields with each other. For, e.g., $m = 4$ and $\phi_I(x_i) =: \phi_i$ for $i = 1, \ldots, 4$, all possible contractions are

$$[\phi_1\phi_2]^*\phi_3\phi_4 + [\phi_1\phi_3]^*\phi_2\phi_4 + [\phi_1\phi_4]^*\phi_2\phi_3 + [\phi_2\phi_3]^*\phi_1\phi_4 + [\phi_2\phi_4]^*\phi_1\phi_3 + [\phi_3\phi_4]^*\phi_1\phi_2 + [\phi_1\phi_2]^*\,[\phi_3\phi_4]^* + [\phi_1\phi_3]^*\,[\phi_2\phi_4]^* + [\phi_1\phi_4]^*\,[\phi_2\phi_3]^*. \tag{A.32}$$

Due to the normal-ordering all terms which still include uncontracted operators have the vacuum expectation value zero. So, the vacuum expectation value of Eq. (A.29) equals

$$\langle 0|T\{\phi_I(x_1)\ldots\phi_I(x_m)\}|0\rangle = \left\langle 0 \middle| \begin{pmatrix}\text{sum of all totally}\\ \text{contracted terms}\end{pmatrix} \middle| 0 \right\rangle = \begin{pmatrix}\text{sum of all totally}\\ \text{contracted terms}\end{pmatrix}. \tag{A.33}$$

In the case of $m = 4$, that expectation value thus equals

$$\begin{aligned}\langle 0|T\{\phi_1\ldots\phi_4\}|0\rangle &= [\phi_1\phi_2]^*\,[\phi_3\phi_4]^* + [\phi_1\phi_3]^*\,[\phi_2\phi_4]^* + [\phi_1\phi_4]^*\,[\phi_2\phi_3]^* \\ &= D_F(x_1-x_2)\,D_F(x_3-x_4) + D_F(x_1-x_3)\,D_F(x_2-x_4) \\ &\quad + D_F(x_1-x_4)\,D_F(x_2-x_3).\end{aligned} \tag{A.34}$$

A.2.2 Feynman Diagrams

If the numerator of the correlation function (A.28) is expanded in terms of ϕ_I, it can be calculated using the derivations from Wick's Theorem (A.33). To make sure one does not forget one of the summands, each of them is represented by "Feynman diagrams": Every point $x_1, \ldots, x_m$ is represented by a dot and the contractions $D_F(x_i - x_j)$ $(i, j = 1, \ldots, m)$ by a straight line. E.g.,

$\langle 0|T\{\phi_1\ldots\phi_4\}|0\rangle =$ 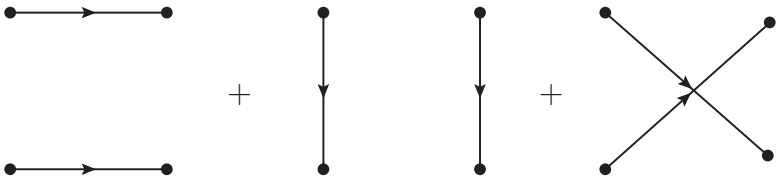 $+$ $+$

In general, the numerator of the correlation function for m fields equals[2]

$$\left\langle 0 \middle| T\left\{\phi_I(x_1)\ldots\phi_I(x_m)\exp\left[-i\int \mathrm{d}t H_I(t)\right]\right\} \middle| 0\right\rangle = \begin{pmatrix}\text{sum of all possible diagrams}\\ \text{with } m \text{ external points}\end{pmatrix}. \tag{A.35}$$

[2]The equivalence is based on the superposition principle of quantum mechanics: If a process can happen in alternative ways, the amplitude of the process will be equal to the sum of the amplitudes of each way.

As an additional simplification, each part of a diagram is associated with an analytical expression so that the value of the term according to a particular diagram can be read off from the diagram by multiplying these expressions. In the ϕ^4 theory this analytical expressions ("Feynman rules") are

- $D_F(x-y)$ in momentum-space for each line between two points x and y ("propagator"),
- $-i\lambda \int \mathrm{d}^4 z$ for each vertex,
- 1 for each external point.

Additionally, one has to divide by the symmetry factor, i.e. the number of diagrams which one gets out of one be interchanging same parts. The Feynman rules used in this thesis are given in section 2.6.1.

Consider again the two-point correlation function. A typical diagram with two external points x and y consists of a piece which is connected to x and y and several parts which are disconnected from these external points. Let $\{\tilde{V}_i\}$ describe the set of all possible disconnected pieces and V_i be the value of the disconnected diagram $\tilde{V}_i \in \{\tilde{V}_i\}$. If a typical diagram has n_i disconnected diagrams of the type $\tilde{V}_i \in \{\tilde{V}_i\}$, its value will be

$$\Big(\text{value of the connected part}\Big) \cdot \prod_i \frac{1}{n_i!} (V_i)^{n_i} \tag{A.36}$$

with the symmetry factor $\frac{1}{n_i!}$ arising from the possibility to interchange the n_i copies of the disconnected diagram $\tilde{V}_i$. Thus,

$$\begin{aligned}
&\left\langle 0 \left| T\left\{ \phi_I(x)\phi_I(y) \exp\left[-i \int \mathrm{d}t H_I(t) \right] \right\} \right| 0 \right\rangle \\
&= \sum_{\substack{\text{all possible} \\ \text{connected pieces}}} \sum_{\substack{\text{all ordered} \\ \text{sets } \{n_i\}}} \begin{pmatrix} \text{value of} \\ \text{connected piece} \end{pmatrix} \cdot \prod_i \frac{1}{n_i!} (V_i)^{n_i} \\
&= \left(\sum_{\substack{\text{all possible} \\ \text{connected pieces}}} \begin{pmatrix} \text{value of} \\ \text{connected piece} \end{pmatrix} \right) \cdot \underbrace{\sum_{\text{all } \{n_i\}} \prod_i \frac{1}{n_i!} (V_i)^{n_i}}_{= \exp\left[\sum_i V_i\right]} .
\end{aligned} \tag{A.37}$$

With an identical argument the denominator equals

$$\left\langle 0 \left| T\left\{ \exp\left[-i \int_{-T}^{+T} \mathrm{d}t H_I(t) \right] \right\} \right| 0 \right\rangle = \exp\left[\sum_i V_i \right] . \tag{A.38}$$

As the argumentation is the same for the numerator and denominator of the correlation functions with $m > 2$ fields, it equals

$$\langle \Omega \left| T\left\{ \phi_I(x_1) \dots \phi_I(x_m) \right\} \right| \Omega \rangle = \begin{pmatrix} \text{sum of diagrams connected} \\ \text{to all } n \text{ external points} \end{pmatrix} . \tag{A.39}$$

B Bibliography

[A+01] M. N. Achasov et al. Study of conversion decays phi –> eta e+ e- and eta –> gamma e+ e- in the experiment with SND detector at the VEPP-2M collider. *Phys. Lett.*, B504:275–281, 2001.

[A+08] C. Amsler et al. Review of particle physics. *Phys. Lett.*, B667:1, 2008.

[A+09] R. Arnaldi et al. Study of the electromagnetic transition form-factors in $\eta \to \mu^+\mu^-\gamma$ and $\omega \to \mu^+\mu^-\pi^0$ decays with NA60. *Phys. Lett.*, B677:260–266, 2009.

[ABBC92] L. Ametller, J. Bijnens, A. Bramon, and F. Cornet. Transition form-factors in pi0, eta and eta and eta-prime couplings to gamma gamma. *Phys. Rev.*, D45:986–989, 1992.

[BW01] O. Bar and U. J. Wiese. Can one see the number of colors? *Nucl. Phys.*, B609:225–246, 2001.

[EGPdR89] G. Ecker, J. Gasser, A. Pich, and E. de Rafael. The role of resonances in chiral perturbation theory. *Nucl. Phys.*, B321:311, 1989.

[Gio10] S. Giovannella. Talk presented at the PrimeNet workshop on conversion decays of vector mesons. Frascati, Italy, June 18, 2010. http://www.fz-juelich.de/ikp//primenet/2010_Meeting_Frascati/giovannella.pdf.

[GL84] J. Gasser and H. Leutwyler. Chiral perturbation theory to one loop. *Ann. Phys.*, 158:142, 1984.

[GL85a] J. Gasser and H. Leutwyler. Chiral perturbation theory: Expansions in the mass of the strange quark. *Nucl. Phys.*, B250:465, 1985.

[GL85b] J. Gasser and H. Leutwyler. eta —> 3 pi to one loop. *Nucl. Phys.*, B250:539–560, 1985.

[Iiz66] J. Iizuka. Systematics and phenomenology of meson family. *Prog. Theor. Phys. Suppl.*, 37:21–34, 1966.

[Kup10] A. Kupsc. Private communication. 2010.

[Lan85] L. G. Landsberg. Electromagnetic decays of light mesons. *Phys. Rept.*, 128:301–376, 1985.

[LK04] M. F. M. Lutz and E. E. Kolomeitsev. On meson resonances and chiral symmetry. *Nucl. Phys.*, A730:392–416, 2004.

[LL08] M. F. M. Lutz and S. Leupold. On the radiative decays of light vector and axial-vector mesons. *Nucl. Phys.*, A813:96–170, 2008.

[LL09] S. Leupold and M. F. M. Lutz. Hadronic three-body decays of light vector mesons. *Eur. Phys. J.*, A39:205–212, 2009.

[LS08] M.F.M. Lutz and M. Soyeur. Radiative and isospin-violating decays of D(s)-mesons in the hadrogenesis conjecture. *Nucl. Phys.*, A813:14–95, 2008.

[Mos99] U. Mosel. *Fields, symmetries, and quarks*. Springer Verlag, Berlin Heidelberg, Germany, 1999.

[Oku63] S. Okubo. Phi meson and unitary symmetry model. *Phys. Lett.*, 5:165–168, 1963.

[PS95] M. E. Peskin and D. V. Schroeder. *An introduction to quantum field theory*. Addison-Wesley, Reading, USA, 1995.

[Sak69] J. J. Sakurai. *Currents and mesons*. University of Chicago Press, Chicago, USA, 1969.

[Sam61] N. P. Samios. Dynamics of internally converted electron-positron pairs. *Phys. Rev.*, 121:275–281, 1961.

[Sch03] S. Scherer. Introduction to chiral perturbation theory. *Adv. Nucl. Phys.*, 27:277, 2003.

[TL10] C. Terschlüsen and S. Leupold. Electromagnetic transition form factors of light vector mesons. *Phys. Lett.*, B691:191–201, 2010.

[Wei79] S. Weinberg. Phenomenological Lagrangians. *Physica*, A96:327, 1979.

[Zwe64] G. Zweig. An SU(3) model for strong interaction symmetry and its breaking. CERN-TH-401, 1964.

C Danksagungen

Ich möchte Herrn Professor Ulrich Mosel für die Aufnahme in sein Institut danken und für die Möglichkeit, diese Diplomarbeit zu erstellen. Seine Anregungen haben mir immer geholfen, Probleme aus anderen Blickwinkeln zu betrachten.
Professor Stefan Leupold möchte ich für das interessante Thema und die exzellente Betreuung danken. Bei allen Arten von Problemen konnte ich mich an ihn wenden. Außerdem konnte ich mich immer an Fabian Eichstädt wenden, auch ihm gilt mein Dank.

Weiter möchte ich Elke Jung danken, die mich bei allen administrativen Fragen unterstützt hat, und bei den Computer-Administratoren Janus Weil und Fabian Eichstädt. Auch allen anderen Mitgliedern des Institutes für Theoretische Physik danke ich für physikalische und technische Unterstützung und angenehme Mensa- und Pausenzeiten.

Ferner möchte ich meiner Familie und meinen Freunden danken für ihre Unterstützung während meines gesamten Studiums.

D Eidesstattliche Erklärung

Hiermit erkläre ich, dass ich diese Arbeit selbständig verfasst und keine anderen als die angegebenen Quellen und Hilfsmittel benutzt habe und dass die Arbeit in gleicher oder ähnlicher Fassung noch nicht Bestandteil einer Studien- oder Prüfungsleistung war.

Uppsala, den 16. November 2010

Carla Terschlüsen